2013

Molecular Considerations In The Design Of Novel Alpha/Beta Hydrolase Inhibitors

Shana Victoria Stoddard
University of Mississippi

MOLECULAR CONSIDERATIONS IN THE DESIGN OF NOVEL ALPHA/BETA HYDROLASE INHIBITORS

A Dissertation
presented in partial fullfilment of requirements
for the degree of Doctoral Philosophy
in the Department of Chemistry and Biochemistry
The University of Mississippi

by

SHANA STODDARD

August 2013

ABSTRACT

Alpha/beta hydrolases (ABHs) are a superfamily of hydrolytic enzymes that process a wide variety of substrates. A subfamily of ABHs called carboxylesterases (CEs) are important enzymes that catalyze biological detoxification, hydrolysis of certain pesticides, and metabolism of many esterified drugs. The chemotherapy drug irinotecan used for treatment of colorectal cancer is metabolized to SN-38, the active drug metabolite, by two CE isozymes CES1 (localized in the liver) and CES2 (localized in the small intestines). CES2's ability to activate irinotecan at a faster rate than CES1 creates a localization of activated SN-38 in the gut epithelium, resulting in the dose limiting side effect of delayed diarrhea. Development of inhibitors for the CE subfamily of ABHs could assist in ameliorating the toxic side effects associated with some esterified prodrugs such as irinotecan, and enhance the distribution of prodrugs *in vivo*. Hence, our research targets CES2 for inhibitor design with the goal of amelioration of intestinal cytotoxicity associated with irinotecan chemotherapy. In this work we (*i*) utilized QSAR technology to design and optimize novel sulfonamide CES2 inhibitors; (*ii*) combined QSAR with *in silico* design to generate new CE inhibitor scaffolds that maintained the potency of previous CE inhibitor generations, yet had improved water solubility; and (*iii*) investigated the contribution of the loop 7 in CEs to sensitizing the enzyme to inhibition by sulfonamides through docking analysis. Our QSAR model, developed using 57 sulfonamide analogs, identified several features of this class of CE inhibitor that confer their potency. Using a QSAR model, constructed using 4 classes of CE inhibitors (benzils, benzoins, isatins, and sulfonamides), as a pocket site to

perform *in silico* design we generated several new scaffolds predicted to have good solubility and potency. This work suggests that the inner loop 7 on CE plays a role in inhibitor selectivity, and interactions with this loop should be considered in the development of selective CE inhibitors. The contributions from this work will be applicable to the design of novel ABH inhibitors, help to increase the likelihood of these drugs entering in clinical use, and ameliorate the dose-limiting side effect associated with irinotecan.

DEDICATION

This work is dedicated to the one and only true God.

> Each one of you should use whatever gift he has received to serve others, faithfully administering God's grace in its various forms. If anyone speaks, he should do it as one speaking the very words of God. If anyone serves, he should do it with the strength God provides, so that in all things God may be praised through Jesus Christ. To him be the glory and the power for ever and ever. Amen.
>
> **1 Peter 4:10-11**

The Lord tells every Christian that we should use our gifts to build his kingdom. Being blessed with the gift to teach, and called to serve as chemistry professor I owe it to him to always yield my career, my research, and my classroom to him. I hope that this work, which serves as my entry point into this field, will not only help alleviate the suffering of some undergoing therapy for their ailments, but also fulfill the intended purposes of the Lord.

LIST OF ABBREVIATIONS

ABBREVIATIONS	NAME
ABH	alpha/beta hydrolases
ABUS	alpha/beta unsaturated sulfoxide
ACh	acetylcholine
AChE	acetylcholinesterase
AD	Alzheimer's disease
ALOGpS	calculated solubility
AM1	Austin model 1
Arg	arginine
BChE	butrylcholinesterase
CAS	chemical abstract service
CBs	carbamates
CE	carboxylesterase
CEs	carboxylesterases
CES1	human liver carboxylesterase
CES2	human intestinal carboxylesterase
CM2	charge model 2
COX-1	cyclooxygenase 1
CoMFA	comparative molecular field analysis

CoMSIA	comparative molecular similarity index analysis
clogP	calculated Log P
CPT-11	7-ethyl-10-[4-(1-piperidino)-1-piperidino]carbonyloxycamptothecin
Cys	cysteine
DFI	dual function inhibitor
DMSO	dimethylsufoxide
DNA	deoxyribonucleic acid
DTT	dithiothreitol
Glu	glutamate
Gly	glycine
hAChE	human acetylcholinesterase
hBChE,	human butrylcholinesterase
HEPES	(4-(2-hydroxyethyl)-1-piperazineethanesulfonic acid
hiCE	human intestinal carboxylesterase
hCE1	human liver carboxylesterase
His	histidine
HOMO	higest occupied molecular orbital
IPTG	isopropyl β-D-1-thiogalactopyranoside
LogS	log of Solubility
LUMO	lowest occupied molecular orbital

Lys	lysine
MCPBA	*meta*-chloroperoxybenzoic acid
MD	molecular dynamics
MM	marine metabolite
MM2	molecular mechanics 2
MOL2	tripos mol2 file
NDDO	neglect of diatomic differential overlap
NEB	New England Biolabs
NMA	normal mode analysis
o-NP	ortho nitrophenol
o-NPA	ortho nitrophenyl acetate
OPs	organophosphates
PAGE	poly acrylamide gel electrophoresis
PAS	peripheral anionic site
PCR	polymerase chain reaction
PCR	principle components regression
PDB	protein data bank
p*I*	isoelectric point
PLS	partial least squares
PM3	parametric model 3

pNB	para nitrobenzyl
pnbCE	para nitrobenzyl carboxylesterase
pNV	para nitrovalerate
PZT	psuedozoanthoxathin like
QSAR	quantitative structure activity relationships
rCE	rabbit carboxylesterase
RE	restriction enzyme
RNA	ribonucleic acid
RMSD	root mean square deviation
RTB	rotational-translational block
SCF	self consistent field
SDS	sodium dodecyl sulfate
Ser	serine
SN-38	7-ethyl-10-hydroxy-camptothecin
TAE	tris-acetate-ethylenediaminetetraacetic acid
TBE	tris-borate-ethylenediaminetetraacetic acid
TCP	tetrazacyclopentazulene compounds
TFK	tri-fluoroketone
TRAP	target related affinity profiling
Tyr	tyrosine

UV	ultraviolet

ACKNOWLEDGMENTS

I will be forever grateful for the throng of people who supported my journey to becoming a scientist, and aided me in the completion of this work.

To start off I would like to thank my Advisor Dr. Wadkins. I am truly happy that he came to Prairie View A&M University five years ago to recruit, and did so with such enthusiasm that it sparked my interest in the University of Mississippi. He has been a dynamic support of my talents, and abilities, and as a result I have been afforded opportunities. It was his leadership and direction that has guided me to be the researcher I am today. I only hope that I will one day become the researcher he knows I can be.

I would like to thank my former professors at Prairie View A&M University. The support, recommendations and training I received at PV catapulted me into a successful graduate school career.

Next, I would like to thank my committee members, Dr. Doerksen, Dr. Mattern, Dr. Pedigo, and Dr. Tschumper. My committee members have challenged me to dig deeper into my work, have helped to guide my project to completion and have answered my many unannounced questions when I dropped by their offices, or saw them in the hallway.

I would like to thank Dr. Godfrey for his encouragement and willingness to help me in any endeavor as I went through this program. I would like to give a big thank you to Dr.

Mossing for his willingness to answer my many questions, as I was frequent visitor to his office with the words “I have a quick question.”

I would like to thank my lab members and colleagues in the department for their support of my work, teaching me, and challenging me to be the best I could be. Yogini and Samantha, thank you for your editing, constructive criticism, and help in preparing presentations, manuscripts and whatever else I needed.

I would like to also thank the University of Mississippi office of Student Disabilities, for the work they did to get me the accommodations I needed for completing my coursework. Years ago I was told I should not have graduated from high school because of the severity of my disorder. And was then told that typically if people like me do graduate from high school they usually just take a job somewhere. However, I will soon be Dr. Shana Stoddard, and I hope that my success will encourage others like me, with severe cases of ADHD, to pursue higher-level degrees.

I would like to thank my family and friends. I especially wish to thank my parents who have not only supported my decision to pursue a Ph.D. (actually expected, as a terminal degree is required in my family), but also have contributed to my many needs while I was here in Oxford. I want to give a special thank you to my brother Damian Stoddard, who is currently a Ph.D. student here at the University of Mississippi in the Department of Mechanical Engingeering. Mrs. Watkins, my mentor Dr. Eyerce, Armstrong–Polston, and my friend Gia I also want to thank for their many phone calls and prayers.

I want to thank my Clear Creek Missionary Baptist Church members, and the children I teach Bible study and Sunday school to. It would have been extremely difficult for me to pursue this kind of degree without having a surrogate family. It was my church family who enabled me to create the balance necessary for me to be able to focus on my work in school and not on seeking people.

Lastly, I want to thank Garry Brown, Jr. Garry entered the Ph.D. program here at the University of Mississippi with me in 2008. Together we have studied for our classes, cumulative exams, practice presentations, analyzed our work, completed our dissertations and just relaxed to vent of the frustrations of graduate work. If it was not for Garry, I would not have even participated in my own commencement ceremony, because the process of graduating was so frustrating that I became bitter. But with Garry pulling me along in the end I did, and it gave me part of the final thrust I needed to finish this work.

Thank you everybody!

TABLE OF CONTENTS

LIST OF TABLES

LIST OF FIGURES

CHAPTER 1 INTRODUCTION

1.1 ALPHA/BETA HYDROLASES

Alpha/Beta hydrolases (ABHs) are a superfamily of proteins that share a similar canonical structure but vary in function. In 1992, the α/β hydrolase fold was identified from the five proteins acetylcholinesterase (*Torpedo*), carboxylpeptidase II (Latin), dienelactone hydrolase (*Pseuodomonas*), dehydrogenase (*Xanthobacter*), and lipase (*Geotrichum*) [1]. Since then, this family of proteins has grown from 5 to over 600 proteins, comprising 89 subgroups, and containing proteins with a wide range of amino acids. As examples, the 194 residue human retinoblastoma binding protein 9 [2] and the dipeptidyl aminopeptidase X [3] which has 723 residues are both ABHs [4]. In addition to varying sizes, these proteins process a wide variety of substrates [4]. Some examples of the hydrolytic variety of these enzymes can be found in these examples: acetylcholinesterase, which degrades the neurotransmitter acetylcholine; [4] carboxylesterases (CE), which hydrolyze xenobiotics such as organophosphate and carbamate pesticides [5] and also illicit drugs such as heroin [6] and cocaine [7]; thioesterases, which degrades thioester bonds [4]; halokane dehydrogenase, which hydrolyzes alkyl chlorides [4]; cutinase, which degrades, cutin, a triacylglycerol [4, 8]; and epoxide hydrolases, which hydrolyze epoxides [4]. These enzymes possess very little sequence similarity; however they do have several conserved features [9, 10] and the same overall fold.

The first characteristic feature of this family is an alpha/beta fold; a string of β sheets sandwiched in between 2 sets of α helices. The canonical fold contains 8 mostly parallel β sheets (β2 is antiparallel) and 6 α helices. Strand order is 12435678, and has a connection of +1, +2, -1x, +2x, +1x, +1x, +1x. The beta sheets twist in a left-handed superhelical twist fashion, such that first and last strand are at 90º to one another. The helices αA and αF are found on the convex side of the enzyme while the helices αB through αE are located on the concave side of the fold [1, 4, 9, 10]. Figure 1-1 shows a schematic of the canonical fold of ABHs, using human carboxylesterase 1 (CES1).

The second feature of this fold is a histidine residue in the catalytic triad consisting of a nucleophile, acid, and histidine. The only residue of the triad that is identical in all ABHs is the histidine [10]. Serine, cysteine and aspartate can be nucleophiles, while the acid residue can be either glutamate or aspartate [1, 9]. The use of the glutamate as an acid in the triad is novel to the ABH family [9]. The histidine residue is positioned after the last beta sheet, [10] nucleophiles are located after β5, and the acid residue is typically positioned after β7 on a loop having one or two reverse turns [1, 4, 10].

A third feature of this fold is a sharp γ turn that houses the nucleophile at its apex, and is called a "nucleophilic elbow," which maintains the hydrolytic function. The "nucleophilic elbow" can be identified by the consensus sequence as S-X-N-X-S, where S is any small residue like a glycine, X is any residue, and N is the nucleophile. This "nucleophilic elbow" is positioned in such a way to allow easy access of substrate and water molecules to the nucleophile [10].

The presence of an "oxy-anion hole," which stabilizes the negatively charged intermediate generated during catalysis, is the last feature of this fold. A minimum of two

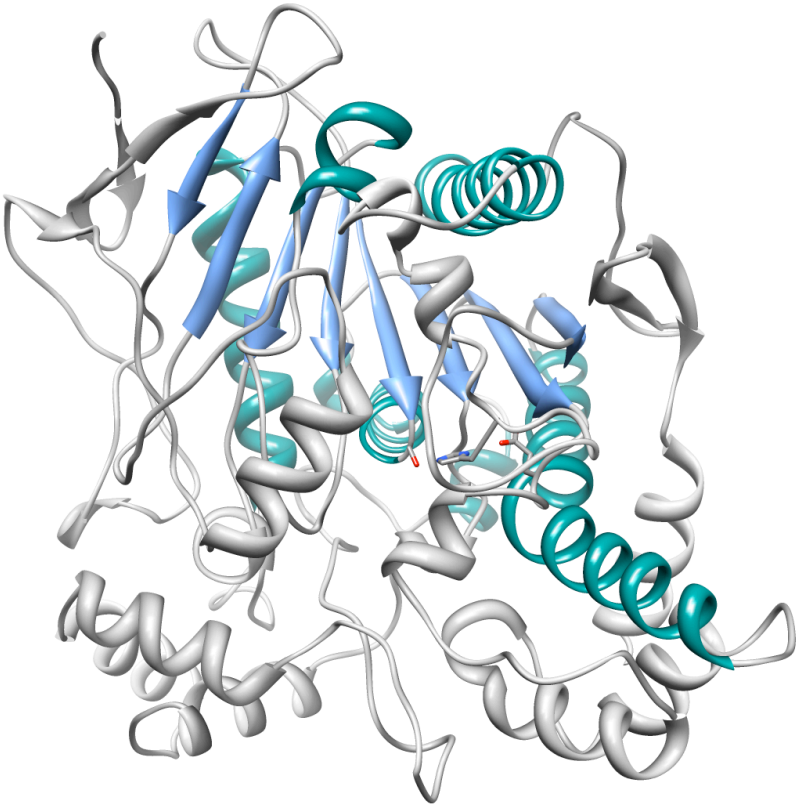

Figure 1-1. The canonical fold of alpha/beta hydrolases using human liver carboxylesterase 1 (hCE1). Depicted in blue are the 8 mostly parallel beta sheets. The helices highlighted in green represent the 6 helices common to this fold.

backbone nitrogen atoms create the "oxy-anion hole." The first is located on a residue immediately following the nucleophile and the second nitrogen atom is typically located on a residue between the β3 sheet and the αA helix. With the exception of a few members of the ABH family, like the lipases, the "oxy-anion hole" is present in the substrate-free enzyme. In lipases, one residue creating the "oxy-anion" hole resides on a mobile loop, preventing the "oxy-anion hole" from forming until substrate binds and the loop becomes orientated in the active conformation.

1.2 CARBOXYLESTERASE SUBFAMILY

Carboxylesterases are one of the subfamilies of ABH enzymes. These enzymes are ubiquitous, and found in all kingdoms of life. This family of enzymes hydrolyzes carboxylate esters into their corresponding alcohol and carboxylic acid derivatives. The residues in the catalytic triad responsible for metabolism are serine, histidine, and glutamate. The mechanism begins when glutamic acid is ionized and then removes a proton from histidine. The lone pair on the histidine then abstracts a proton from serine resulting in the nucleophilic species serine Oγ. Initiation of substrate hydrolysis is then performed by nucleophilic attack of the serine Oγ residue [5]. The serine Oγ attacks the carbonyl carbon of the carboxylate ester substrate, creating a tetrahedral intermediate. The reformation of the carbonyl moiety causes the release of the OR group, which receives a proton from glutamate. A H_2O molecule then attacks the carbonyl carbon, generating another tetrahedral intermediate. Finally, the release of the carboxylic acid is performed when the carbonyl bond reforms and releases the serine residue. This mechanism, "ester hydrolysis," is the primary mechanism, which is employed in most CE inhibition reactions (Figure 1-2).

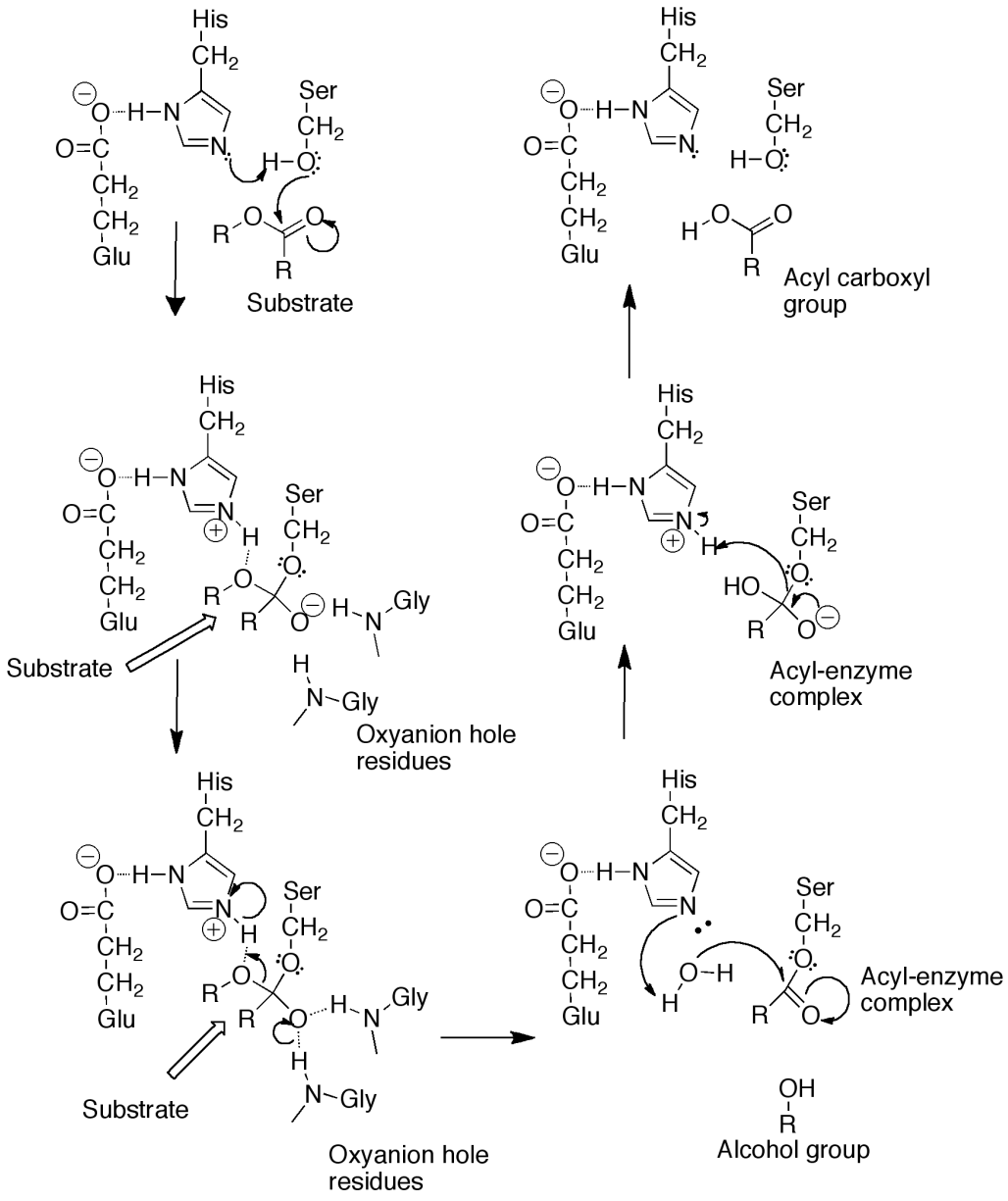

Figure 1-2. The catalytic mechanism of carboxylesterases

The cytotoxicity to the intestinal epithelium by SN-38 is the dose-limiting toxicity. Development of selective CE inhibitors has been pursued to ameliorate this mechanism of dose-limiting toxicity of irinotecan. Carboxylesterase inhibitors could be given as adjuvunct therapy for toxicity modulation of irinotecan, allowing for higher dosing and hence more effective treatment of colorectal cancer.

In mammals, CEs can be found in numerous tissues types [11]. The hydrolytic activity is based on tissue type; however, the liver isozyme is known to be the most active of all isozymes studied. The hydrolytic abilities of these enzymes are employed in the roles of drug metabolism, protection against xenobiotics, and pesticide detoxification. They are responsible for, hydrolyzing clinically useful drugs such as capecitabine [12] and irinotecan [13], [12] illicit drugs such as heroin [6]; and detoxifying pesticides such as pyrethoids [14].

Therapeutically, CEs have many uses due to their broad substrate specificity. For example, CEs have the potential to be used for protein-based therapies for pesticide detoxification. Organophosphates and carbamates, when used as insecticides, have the potential to cause poisoning to humans since they also act on acetylcholinesterase. However, the reversible or irreversible binding of organophosphate and carbamate insecticides to CEs can reduce toxicity to humans. Two reaction pathways are involved in this successful alleviation of pesticide poisoning: metabolism of the insecticide by CEs or irreversible inhibition of CEs by the insecticides [15], [16].

Carboxylesterases are also important to the use of pro-drugs. Irinotecan is an anticancer pro-drug currently used to treat colorectal cancer. In humans several carboxylesterases exist in different tissues, namely liver carboxylesterase 1 (hCE1; CES1), and liver carboxylesterase 2 (hCE2) both localized in the liver, and human intestinal carboxylesterase (hiCE; CES2) localized primarily in the small intestinal epithelial. Irinotecan is a substrate for hCE1, hCE2, and hiCE. Human liver carboxylesterase is the desired enzyme for irinotecan activation. The enzyme hiCE is present in greater concentrations in the small intestine, thus hiCE is much more efficient at hydrolyzing irinotecan to the active metabolite SN-38 [12], [17]. The resulting over-production

of SN-38 results in damage to the lining of the small intestine, causing delayed diarrhea and often requiring hospitalization [12].

1.3 BACTERIAL CARBOXYLESTERASE

One CE receptor, bacterial p-nitrobenzyl carboxylesterase (pnbCE), is approximately 489 amino acids, contains 13 β-sheets and 15 α-helices, and is structurally homologous to the mammalian CEs. The catalytic residues are Ser-189, His-399 and Glu-310 [18]. It can hydrolyze irinotecan and is simple to express and purify. The crystal structure of pnbCE, like CES1, has been solved. For these reasons it has been used as a model system to study the mammalian carboxylesterases by the Potter and Wadkins labs [19].

Several loops on pnbCE have been shown to be important. In 2011, using molecular dynamics and normal mode analysis, it was calculated that the active site loops, loop 5 and loop 21, had an anticorrelated motion [20]. This motion was found to hold the substrate into place during the catalytic reaction. Gwaltney's lab performed a molecular dynamics simulation on pnbCE to determine which loop the substrate interacted with. The substrate was found to actually interact with loop 7. Loop 7 is an internal loop surrounding the active site, which contains the oxyanion hole.

1.4 CHALLENGES IN INHIBITOR DESIGN FOR CARBXOYLETERASES

The Potter and Wadkins labs have collaborated for several years, with the goal of developing CES2 specific inhibitors to ameliorate the dose limiting side-effect. Currently, five major classes of selective CE inhibitors have been developed, the 1,2 diones (subclasses: isatins, benzils, 1-phenyl-2-pyridyl-ethane-1,2-dione, and indole alkaloid marine natural products),

fluorobenzoins, sulfonamides (benzene- and fluorenesulfonamide subclasses), triflouroketones, and other miscellaneous inhibitors (loperamide, cholesterol analogs, bis(4-nitrophenyl)phosphate, benzodioxaphosphorines), all of which show no inhibition of acetylcholinesterase [21]. In this work we will focus on the isatins, sulfonamides, benzils, and fluorobenzoins (Figure 1-3). We will not explore the trifluoroketones since they do not have a similar mechanism of inhibition compared to the rest of the CE inhibitors, the miscellaneous inhibitors since they are not candidates for drug design, or the 1-phenyl-2-pyridyl-ethane-1,2-diones and indole alkaloid marine natural products, since they were discovered after development of our QSAR models. Most of the CE inhibitors developed have K_i values in the nanomolar range. Two issues, however, plague these compounds: isotyope selectivity and low aqueous solubility.

Of the classes of CE inhibitors developed, three classes are water insoluble (benzils, fluorobenzoins, and sulfonamides), and three classes are generally not isozyme specific (benzils, fluorobenzoins and isatins). The benzils are selective inhibitors for human carboxylesterases, discovered in 2005 [22]. The isatins, which are water-soluble, do not show great potency against hiCE or specificity between hCE1 and hiCE. The sulfonamides, which show isozyme specificity, have great potency against hiCE but suffer from very poor water solubility. Evaluation of over 50 sulfonamides [23] revealed an inverse correlation of clog P (calculated Log P value) and log K_i. Hence, the least soluble compounds were the best inhibitors of the enzyme. These characteristics made these families of inhibitors poor candidates for clinical therapies. In order for hiCE inhibitors to be more effective, new scaffolds, which have more favorable chemical properties, must be developed.

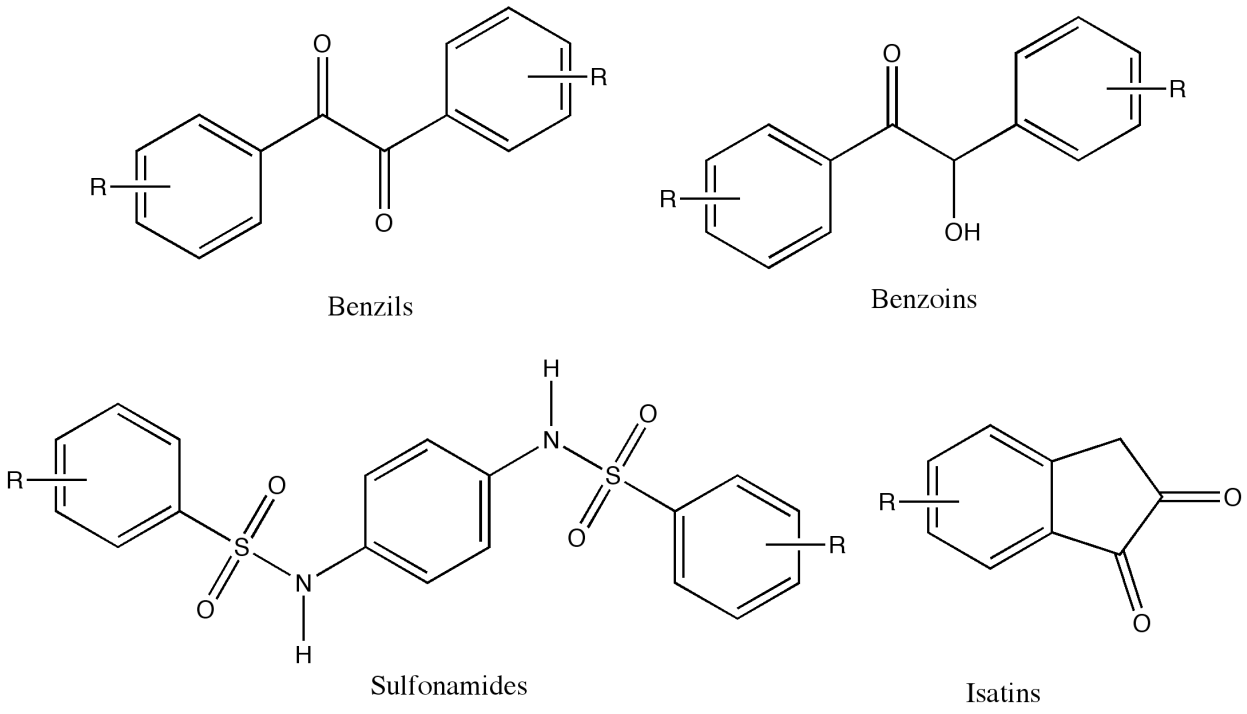

Figure 1-3. Major scaffolds of mammalian selective carboxylesterase inhibitors used in this work

1.5 DISSERTATION FOCUS

The big idea of my dissertation work is controlling the dose limiting side-effect of irinotecan. This would decrease the toxicity of irinotecan, allow clinicians to give higher doses of irinotecan, and in turn provide a more effective, and less taxing therapy for patients. Our approach to preventing the dose limiting side-effect is through development of CES2-selective inhibitiors. Although we have made some progress in developing selective inhibitors for this family of enzymes, a more rational way of developing drugs is needed. What we need to understand to design effective CES2 selective inhibitors is three things. Firstly, we need to understand how to make CES2 inhibitors potent, a more potent drug means less needs to be administered to achieve the desired medicinal effect. Secondly, we must understand how to make a CES2 inhibitor soluble, an insoluble drug is not typically feasible for clinical use. Lastly, we should understand how to make a CES2 inhibitor selective. A CES2 inhibitor shouldn't prevent CES1 and other critical ABH enzymes such as AChE from functioning. Therefore the emphasis of my project is defining contributions that control these features: potency, solubility, and selectivity.

We have used computational work and kinetics to probe specificity. Our computational analysis has helped us understand the requirements for inhibitor potency and generate new inhibitor scaffolds with enhanced drug-like properties. Docking and kinetic analysis was used to explain the molecular interactions that control isozyme specificity. By studying both the inhibitors, through ligand-based methods such as quantitative structure activity relationships, *in silico* design and kinetics, ways to develop potent, water soluble and selective inhibitors have been delineated.

CHAPTER 2 BACKGROUND OF METHODS

2.1 QUANTITATIVE STRUCTURE ACTIVITY RELATIONSHIP (QSAR)

Quantitative structure activity relationship (QSAR) is a mathematical and statistical model where the structures of a series of compounds are correlated to their biological activities. The development of the QSAR modeling technique is credited to Hansch, who used a series of descriptors to correlate a series of steroids to their biological activity [24-26]. QSAR models can be used for a number of applications. One such use is determination of structural properties that increase the potency of a series of inhibitors. An example of this application can be seen in the 2009 study performed by Hicks et al., wherein they developed a series of 57 sulfonamide inhibitors based on their prior three dimensional quantitative structure activity relationship (3D-QSAR) results indicating that halogenation of the phenyl ring would increase the potency of the sulfonamide inhibitors [27, 28]. A second applicaton of QSAR modeling is predicting the activities of a series of compounds that have not been experimentally tested. Numerous research groups have successfully used QSAR to predict activities of potential drug compounds [19, 29-34]. QSAR may tell the researcher what properties are important for increasing potency against a target, but it does not tell specific moieties that should be introduced, although this can sometimes be inferred from the experiment.

The advantage of QSAR is that it can speed up the identification of lead drug targets by successfully weeding out inactives (compounds not having the desired biological activity). This

technique is also ligand-based, thus, unlike docking, is not limited to targets that have an experimentally derived 3D structure. Because of these qualities, QSAR is well suited for drug design and optimization. In our study, we used it to optimize existing sulfonamide CE inhibitors, and as a hypothetical pocket site for *in silico* design (will be discussed in later chapters).

A typical QSAR experiment has three main components: (1) a dataset of compounds, (2) a set of descriptors, (3) and an algorithm to correlate the descriptors to the compound's activity. The QSAR dataset usually consists of a least 10 compounds usually having a common scaffold, with only variances in substituents and/or substitution pattern. The dataset should have a broad range of activities, typically at least 3 orders of magnitude. Descriptors are properties that are derived from the structure of a compound, and can be expressed in a numerical form. There are several types of descriptors varying from zero dimensional to six dimensional. With increasing dimensionality comes a more complex description of a series of compounds (atom count, 1D descriptor; versus HOMO, 3D descriptor). All descriptors 3 dimensional (3D) and higher are dependent on the 3D structure of the compound. The descriptors used are correlated to the structures in the compound series by some algorithm. Examples of algorithms that can be used are simple linear regression analysis, multiple linear regression, principle components regression (PCR), partial least squares (PLS), principle component analysis (PCA), comparative molecular field analysis (CoMFA), neural networks, or genetic algorithms (GA).

We used a GA for all modeling experiments. A genetic algorithm functions by initially developing a population of models. Subsequently, crossing-over events and random mutations of properties describing the model are performed to develop a new population of models. The number of generations can be designated by the user. Typically, this iterative processs is continued until a certain q^2 valued is reached. Q^2 is the cross-validated correlation coefficient.

This value represents the goodness of predictability for the generated model. In a biological system anything abouve 0.4 is considered statistically significant. Many programs have been developed to generate QSAR models, such as SYBYL, CoMFA, and Quasar. In this work, multidimensional QSAR was used employing the program Quasar to develop our multidimensional QSAR models.

The QSAR model is developed and validated using a training set and a test set. A training set consists of a series of compounds with experimentally derived properties. These compounds are used develop the QSAR equation. Typically a range of three orders of magnitude, in the biological property being studied, is needed to develop a decent model. The model can be validated using two types of test sets to determine the robustness of the model. The first, is called an internal test set, and is a group of compounds that have known experimental values, while the second, is an external test set, and does not have experimentally derived values for the property you are developing your model for. The more accurately your model is at correctly predicting the values of these compounds in the internal or external test set the higher the q^2 value.

2.2 AMSOL 7

The AMSOL program calculates solvation energies and class IV partial atomic charges [35]. It is an SCF program that uses solvation models based on the NDDO semi-empirical molecular orbital theory. The SM5.42R model within the AMSOL program was used to calculate both the free energy of solvation and the partial atomic charges. This model used the CM2 charges and calculates the partial atomic charges in both the gas phase and solution phase. The NDDO, AM1, or PM3 semi-empirical Hamiltonians may be used with this solvation model. The

parameter we used was the PM3 to match the charge models of molecular mechanics used in Chem3D software.

The SM5.42R is a rigid gas phase model; thus, it does not take into account the geometry relaxation in solution [36]. The compounds are, however, optimized in the gas phase and these parameters are used for the solvent phase as well. For this experiment the gas phase CM2 charges were used. Therefore, a solvent phase optimization was unnecessary and the SM5.42R proved sufficient.

2.3 LIGBUILDER

In silico drug design is a structure based drug design technique that relies on the 3-dimensional structure of a target to develop a novel drug candidate. This technique has been used to develop several drugs that are currently in clinical trials [37]. Several programs exist to perform *in silico* design such as Concerts [38], Grid [39], LeapFrog [40], LigBuilder [37], Ludi, SPROUT [41, 42], and Synopsis [43]. In general these types of program build a drug candidate inside the crystal structure of a target receptor by adding either atoms or molecular fragments such as benzene or sulfonamide groups.

The active site of a target receptor is termed a "pocket" in this *in silico* process. Identification of a pocket site for an enzyme is simple when a 3D structure is available. This however is not the case for enzymes that have no experimentally solved structure. One option to getting around this is quantitative structure activity relationships (QSAR). QSAR can be used to develop a pseudo-receptor site, in which known ligands are used to develop a model that represents features of the active site. These pseudo-receptor sites can be 3-dimensionally represented and used as a hypothetical pocket site for an enzyme target when there is no

experimentally solved structure. In using these models in *in silico* design processes, new lead compounds for various drug targets can be generated.

In this work we used LigBuilder 1.2v [37] for all of our *in silico* design. LigBuilder uses a genetic algorithm to develop the best candidates. A total 20 generations of models are created. LigBuilder has two options for building structures, GROW and LINK. The link method allows the user to position several moieties in the receptor site; then subsequently LigBuilder builds linkages to connect these groups. The GROW module requires positioning a seed structure in the receptor site. Then, fragments and atoms are incrementally added to the structure to develop an initial population of candidates. We used the GROW module for all design performed here.

LigBuilder uses a series of three input files to dictate the parameters of the run; the first is pocket.index that contains parameters to generate the pocket site key interactions map. The second is grow.index that contains files to generate populations of compounds. The third is process.index, which contains filters to pool the best 200 compounds in a final dataset. Default parameters were used for both pocket.index and process.index. During the GROW process several parameters can be modified. Our modifications to the GROW input files are described in the appropriate chapters where they were used. Examples of some typical pocket.index, grow.index, and process.index input file are contained in the appendix.

2.4 ALOGPS

Solubility of compounds is an important variable that affects the efficacy, potency, and clinical usefulness of drugs *in vivo.* Because humans are 70 to 80% water, a water-insoluble drug will never be active in patients, due to the drug's inability to dissolve. To assist in the development of water-soluble drugs, their solubilities can be tested (for synthesized compounds)

or predicted to rule out unfavorable candidates that have yet to be synthesized. The Online Lipophilicity/Aqueous Solubility Calculation software, ALOGPS 2.1, is an online lipophilicity server that can predict LogS (Log of solubility) of compounds using their structures [44, 45]. The url for this program is http://www.vcclab.org/lab/alogps/. This program was developed using a neural network algorithm and a data set of 1400+ compounds. We used ALOGPS to predict the solubilities of all compounds generated. Compounds were converted to SMILES string then appended into one file. The libraries were uploaded to the ALOGPS website; then the output file was saved. For all calculations, the ALOGpS (calculated solubility) value was used. To calculate the actual solubility in grams per liter the following equation was used.

$$\text{Solubility} = (\text{antilog}(\text{LogS}))*\text{MW} \qquad \text{(Equation 2-1)}$$

$$\text{Solubility} = S * \text{MW} \qquad \text{(Equation 2-2)}$$

where, LogS is ALOGpS value, and MW is the molecular weight of the compound.

2.5 MOLECULAR DOCKING

Molecular docking is the process of predicting the binding orientation of a ligand in its target receptor. This computational method is used heavily in virtual screening to determine interactions that are present between a receptor and ligand [46-49]. Typically, a target receptor is a macromolecule like RNA, DNA or a protein. Identification of molecular interactions to binding of the ligand to the receptor can contribute the development of novel drugs, and help to define molecular pathway analysis. Docking works by first searching for ligand poses (possible receptor-ligand conformation), and then scoring of poses to determine the most likely bioactive

conformation.

Several methods exist to explore active site space, and to score poses in docking. In rigid docking, the simplest algorithms treat both the receptor and the ligand as rigid bodies. Thus, in these cases, only translational and rotational degrees of freedom are considered. Examples of algorithms that allow for a researcher to consider the conformational degrees of freedom of the ligand are Monte Carlo [50], incremental construction [50-52], and genetic algorithms[53]. Monte Carlo methods change the ligand conformation either randomly or through bond rotation after each iteration. Incremental construction builds a ligand up in the active site of the receptor step-wise. Genetic algorithms evolve a population of ligand conformations and orientations in the receptor. After ligand conformations are generated the poses are scored or ranked using a scoring algorithm.

Several docking programs exist today: DOCK [54], FRED [55], Autodock [56], Glide [57], GOLD [58], Surflex [59]. In this work we used DOCK program which was developed by Kuntz et al., which uses the incremental construction method to explore the active site space, and find a receptor-ligand conformation with a high degree of shape compementarity [60].

2.6 MODELLER

Protein homology modeling is a process that generates the most probable 3-dimensional structure of a protein using its amino acid sequence and a template protein structure. A template protein is any structure that is highly homologous in sequence to the input sequence and has a solved 3-dimensional structure. The protein input is then structurally aligned to the template. This process is valuable due to the large number of unsolved protein sequences. A homology model can allow a researcher to evaluate structural features even in the absence of a crystal

structure

MODELLER is a homology-modeling program that we used to generate a 3D structure of our mutant proteins. The MODELLER BLAST analysis is used to find protein sequences that are highly homologous to the input protein sequence. The wild-type pnbCE structure was used as our template structure. The modeling process produced five candidates for each mutant. We performed further analysis on the model that had the lowest ZDOPE score (a measure of the quality of the model). The lower the ZDOPE score, the better the model. Models with positive scores are not likely to be native-like, while models with scores less than -1 are strongly suggestive of the native protein structure.

CHAPTER 3 IMPROVED, SELECTIVE, HUMAN INTESTINAL CARBOXYLESTERASE (CES2) INHIBITORS DESIGNED TO MODULATE 7-ETHYL-10-[4-(1-PIPERIDINO)-1-PIPERIDINO]CARBONYLOXYCAMPTOTHECIN (IRINOTECAN; CPT-11) TOXICITY

3.1 ABSTRACT

CPT-11 is an antitumor prodrug that is hydrolyzed by carboxylesterases (CE) to SN-38, a potent topoisomerase I poison. However, the dose limiting toxicity, delayed diarrhea, is thought to arise, in part, from activation of the prodrug by a human intestinal CE (hiCE). Therefore, we have sought to identify selective inhibitors of hiCE that may have utility in modulating drug toxicity. We have evaluated one such class of molecules (benzene sulfonamides) and developed QSAR models for the inhibition of this protein. Using these predictive models, we have synthesized a panel of fluorene analogues that are selective for hiCE, demonstrating no cross reactivity to the human liver CE, hCE1, or toward human cholinesterases, and have K_i values as low as 14 nM. These compounds prevented hiCE-mediated hydrolysis of the drug and the potency of enzyme inhibition correlated with the clogP of the molecules. These studies will allow the development and application of hiCE-specific inhibitors designed to selectively modulate drug hydrolysis in vivo.

3.2 INTRODUCTION

Carboxylesterases (CEs) are ubiquitously expressed enzymes that are thought to be responsible for the hydrolysis of xenobiotics [61]. They catalyze the conversion of esters to their corresponding alcohols and carboxylic acids. Because numerous clinically used compounds are esterified, an approach used by the pharmaceutical industry to improve the water solubility of molecules, they are substrates for these enzymes. Hence, drugs such as heroin, cocaine, **1** (irinotecan; CPT-11; [62] Figure 3-1), capecitabine, oseltamivir, lidocaine, and meperidine are all hydrolyzed by CEs [12, 13, 17, 63-73]. Therefore, identifying compounds that modulate the hydrolysis of these agents may be useful in either altering the half-life and/or toxicities associated with these drugs. For example, the β-blocker flestolol, is rapidly hydrolyzed by CEs to an inactive metabolite and hence its biological activity is rapidly lost [74]. Inhibition of the enzyme responsible for this hydrolysis would increase the in vivo stability of the molecule and likely improve its therapeutic utility. In contrast, the delayed diarrhea that is associated with **1** treatment is thought to arise, in part, from hydrolysis of the drug in the intestine by the human intestinal CE (hiCE, CES2) [12, 17, 75] to yield **2** (7-ethyl-10-hydroxycamptothecin SN-38; Figure 3-1). Because this is the dose limiting toxicity for this highly effective anticancer agent, approaches that ameliorate this side effect would improve patient quality of care and potentially allow drug dose intensification. This could potentially be achieved by an inhibitor that targets hiCE within the gut.

In 2004 the Potter lab discovered the sulfonamide class of CES2 inhibitors using Telik's target related affinity profiling [76, 27]. The sulfonamide compounds are very potent CES2 specific inhibitors, having no cross reactivity to the cholinesterases human acetyl- or butyrylcholinesterase (hAChE and hBChE, respectively). The Wadkins lab developed a QSAR model for

these sulfonamides to determine what features of these compounds contributed towards thier potency. This study indicated that halogenation of the benzene rings would increase potency of sulfonamide inhibitors. We also demonstrated the usefulness of computational research in the design of CES2 inhibitors. However, these studies were based on a series of 9 compounds (4-12 in Table 3-1) with a disparate set of different chemotypes. Here we have considerably expanded these analyses and have now assayed and analyzed 57 benzene sulfonamides for their ability to inhibit hiCE, hCE1, hAChE, or hBChE. We developed a new QSAR model with this expanded dataset of sulfonamides to further delineate any relevant features important for CES2 inhibition of the sulfonamides. Using detailed QSAR models, we have designed a series of novel fluorene analogues that are highly potent hiCE inhibitors and can modulate **1** metabolism. Potentially, these molecules would be lead compounds for subsequent drug design.

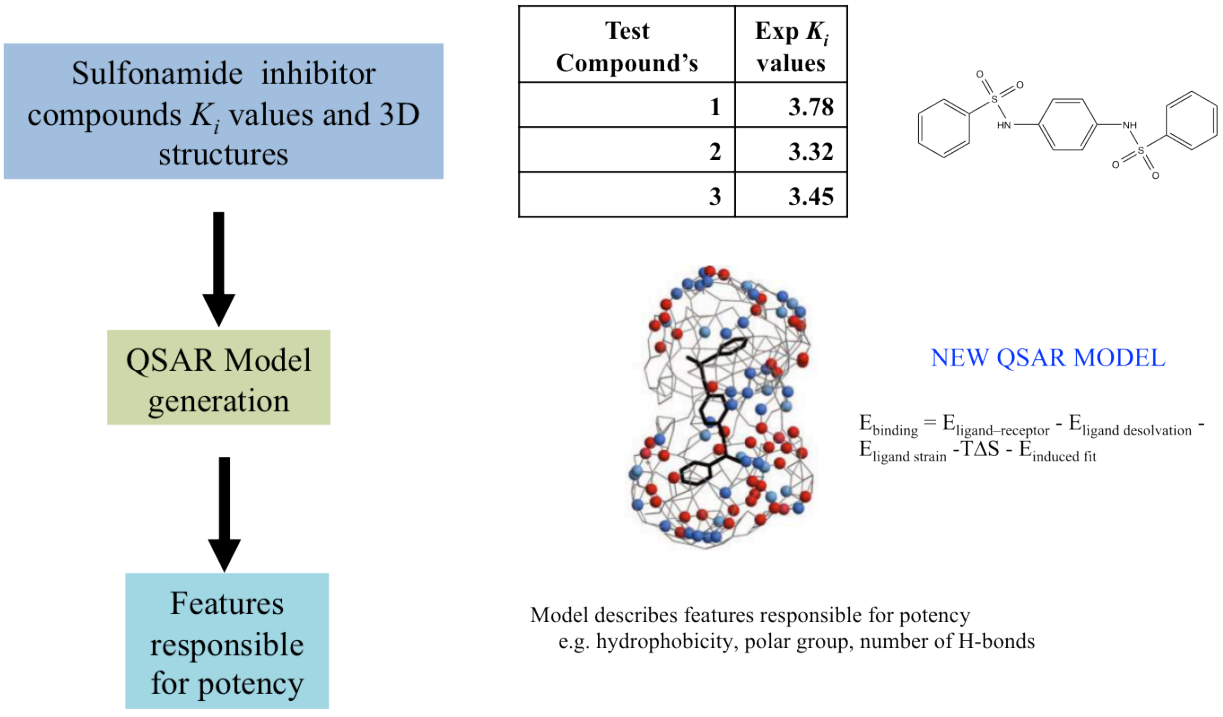

Figure 3-1 Flow chart of QSAR inhibitor design process

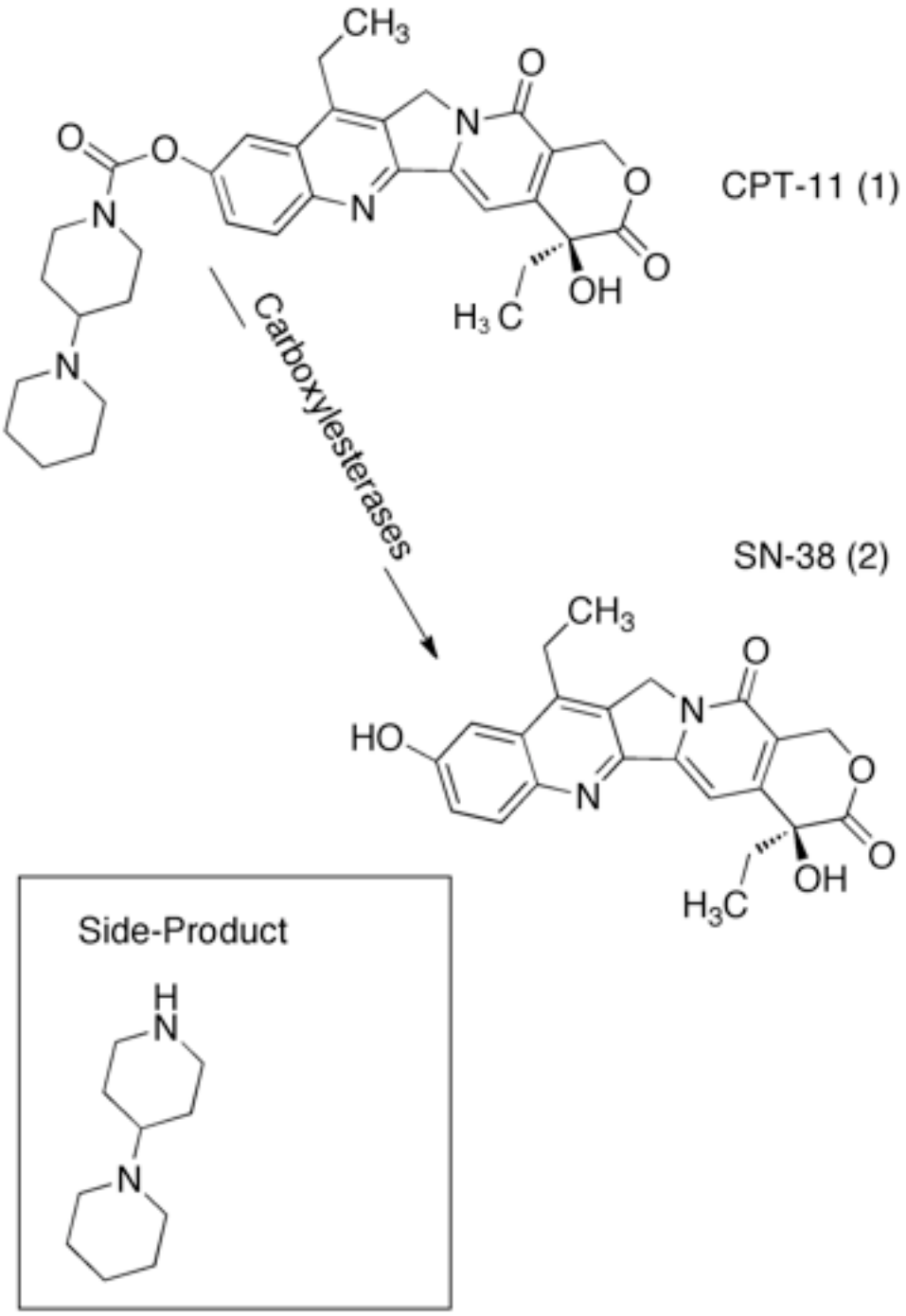

Figure 3-2 Hydrolysis of CPT-11 By Carboxylesterases

ID	compound	R_1	R_2	R_3	clog P	hiCE $K_i \pm SE$ (nM)	hCE1 $K_i \pm SE$ (nM)
4	4,6-dimethyl-N1,N3-diphenylbenzene-1,3-disulfonamide	Bz[a]	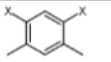	Bz	2.75	218 ± 45[b]	>100,000
5	4-chloro-N-(4 ethoxyphenyl) benzene sulfonamide	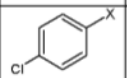	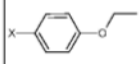	None	3.46	1,310 ± 176[b]	>100,000
6	4-bromo-N-(4-phenoxyphenyl)benzene sulfonamide	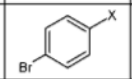	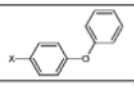	None	5.03	165 ± 33[b]	>100,000
7	N,N'-(4,4'-disulfanediylbis(4,1-phenylene)) dimethane sulfonamide	H	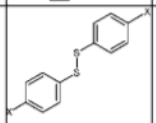	H	2.39	767 ± 285[b]	>100,000
8	N,N'-(1,4-phenylene)benzene sulfonamide	Bz	Bz	Bz	3.63	1,060 ± 133[b]	>100,000
9	N,N'-(2-methyl-1,4-phenylene)benzene sulfonamide	Bz	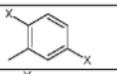	Bz	3.36	365 ± 87[b]	>100,000
10	N,N'-(naphthalene-1,4-diyl)bis(4-chloro benzene sulfonamide)	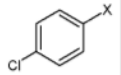	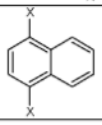	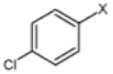	5.08	194 ± 23[b]	>100,000
11	N,N'-(1,4-phenylene)bis(4-chlorobenzene sulfonamide)	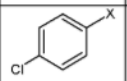	Bz	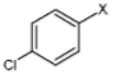	4.40	53.2 ± 5.5[b]	13,700 ± 4,870[a]
12	N,N'-(perchloro-1,4-phenylene)dibenzene sulfonamide	Bz	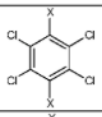	Bz	4.63	451 ± 39[b]	>100,000
13	N,N'-(2,3,5,6-fluoro-1,4-phenylene) bis(4-chlorobenzene sulfonamide)	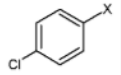	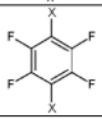	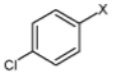	4.33	41.5 ± 6.5[b]	>100,000
14	N,N'-(1,4-phenylene)bis(2-fluoro benzene sulfonamide)	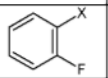	Bz	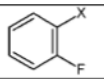	3.02	1,450 ± 154	>100,000
15	N,N'-(1,4-phenylene)bis(3-fluorobenzene sulfonamide)	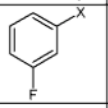	Bz	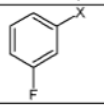	3.61	248 ± 26	>100,000
16	N,N'-(1,4-phenylene)bis(4-fluorobenzene sulfonamide)	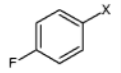	Bz	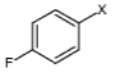	3.72	355 ± 70	>100,000
17	N,N'-(1,4-phenylene)bis(3-chlorobenzene sulfonamide)	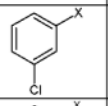	Bz	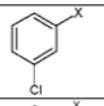	4.31	74.0 ± 5.5	>100,000
18	N,N'-(1,4-phenylene)bis(3-bromobenzene sulfonamide)	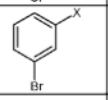	Bz	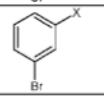	4.55	67.0 ± 9.6[b]	>100,000
19	N,N'-(1,4-phenylene)bis(4-bromobenzene sulfonamide)	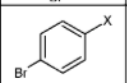	Bz	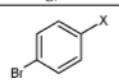	4.70	85.2 ± 10.1	>100,000
20	N,N'-(1,4-phenylene)bis(2,6-difluoro benzene sulfonamide)	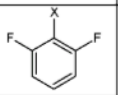	Bz	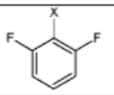	2.78	5,260 ± 620	>100,000
21	N,N'-(1,4-phenylene)bis(3,4-difluoro benzene sulfonamide)	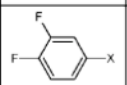	Bz	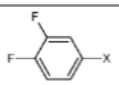	3.81	160 ± 7.5	>100,000

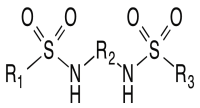

Sulfonamide Scaffold

ID	compound	R_1	R_2	R_3	clog P	hiCE K_i ± SE (nM)	hCE1 K_i ± SE (nM)
22	N,N'-(1,4-phenylene)bis(3,5-difluoro benzene sulfonamide)	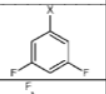	Bz	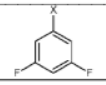	3.76	246 ± 34	>100,000
23	N,N'-(1,4-phenylene)bis(3,4,5-trifluorobenzene sulfonamide)	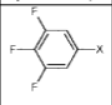	Bz	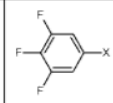	3.81	210 ± 33	>100,000
24	N,N'-(1,4-phenylene)bis(2,3-dichlorobenzene sulfonamide)	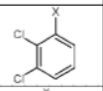	Bz	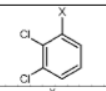	4.63	268 ± 137	>100,000
25	N,N'-(1,4-phenylene)bis(2,5-dichloro benzene sulfonamide)	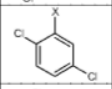	Bz	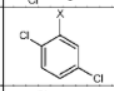	4.60	119 ± 15	>100,000
26	N,N'-(1,4-phenylene)bis(3,4-dichloro benzene sulfonamide)	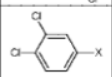	Bz	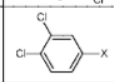	4.63	91.5 ± 23	>100,000
27	N,N'-(1,4-phenylene)bis(3,5-dichloro benzene sulfonamide)	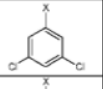	Bz	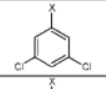	4.87	385 ± 80	>100,000
28	N,N'-(1,4-phenylene)bis(2,4,5-trichlorobenzene sulfonamide)	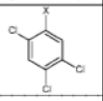	Bz	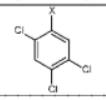	4.74	>100,000	>100,000
29	4-chloro-N-(4-(4-fluorophenylsulfonamido) phenyl)benzene sulfonamide		Bz	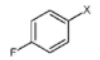	4.06	200 ± 11	>100,000
30	3,4-difluoro-N-(4-(phenylsulfonamido) phenyl)benzene sulfonamide	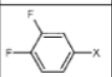	Bz	Bz	3.64	488 ± 30	>100,000
31	4-chloro-N-(4-(4-methylphenyl sulfonamido)phenyl) benzene sulfonamide		Bz	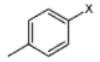	4.40	161 ± 9.3	>100,000
32	4-fluoro-N-(4-(4-methylphenyl sulfonamido)phenyl) benzene sulfonamide		Bz	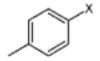	4.02	281 ± 38	>100,000
33	2,4-difluoro-N-(4-(4-methylphenyl sulfonamido)phenyl) benzene sulfonamide	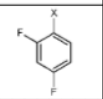	Bz	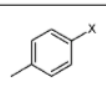	3.69	385 ± 50	>100,000
34	2,5-difluoro-N-(4-(4-methylphenyl sulfonamido)phenyl)benz ene sulfonamide	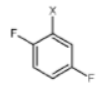	Bz	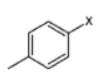	3.67	467 ± 38	>100,000
35	3,4-difluoro-N-(4-(4-methylphenyl sulfonamido)phenyl)benz ene sulfonamide	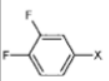	Bz	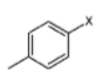	4.15	194 ± 18	>100,000
36	N,N'-(1,4-phenylene)bis(4-fluoro-2-methyl benzene sulfonamide)	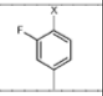	Bz	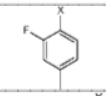	3.35	273 ± 33	>100,000
37	4-fluoro-N-(4-(4-methyoxy phenyl sulfonamido)phenyl)benz ene sulfonamide	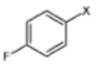	Bz	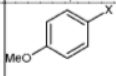	4.10	568 ± 76	>100,000
38	N-(4-(4-fluorophenylsulfonamido) phenyl)-2,5-dimethylbenzene sulfonamide	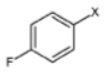	Bz	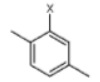	3.62	240 ± 30	>100,000
39	4-(N-(4-(4-fluorophenylsulfonamido) phenyl)sulfamoyl) benzoic acid	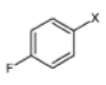	Bz	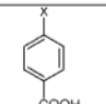	3.06	>100,000	>100,000
40	3-(N-(4-(4-fluorophenylsulfonamido) phenyl)sulfamoyl)-4-methyl benzoic acid	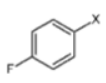	Bz	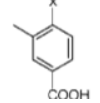	3.06	693 ± 187	>100,000

ID	compound	R_1	R_2	R_3	clog P	hiCE $K_i \pm SE$ (nM)	hCE1 $K_i \pm SE$ (nM)
41	4-(N-(4-(4-fluorophenyl sulfonamido) phenyl)sulfamoyl)-N-methyl benzamide	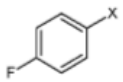	Bz	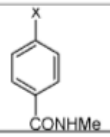	3.77	>100,000	>100,000
42	N,N'-(2-chloro-1,4-phenylene) dibenzene sulfonamide	Bz	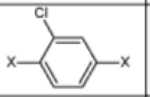	Bz	4.25	696 ± 28	>100,000
43	N,N'-(2,5-dichloro-1,4-phenylene) bis(4-chlorobenzene sulfonamide)	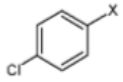	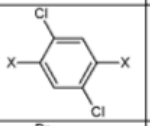	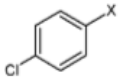	4.72	455 ± 79	>100,000
44	N,N'-(2,5-dibromo-1,4-phenylene) bisbenzene sulfonamide	Bz	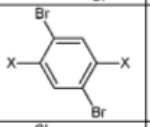	Bz	4.24	>100,000	>100,000
45	N,N'-(2,5-dibromo-1,4-phenylene) bis(4-chlorobenzene sulfonamide	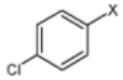	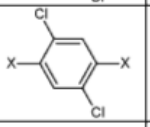	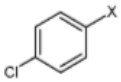	4.82	>100,000	>100,000
46	N,N'-(2,3,5,6-tetramethyl-1,4-phenylene) bis(4-fluorobenzene sulfonamide)	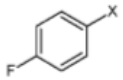	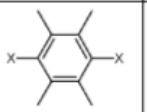	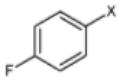	2.82	>100,000	>100,000
47	N,N'-(2,3,5,6-tetramethyl-1,4-phenylene) bis(3-chlorobenzene sulfonamide)	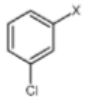	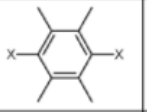	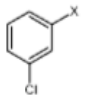	3.16	2,060 ± 750	>100,000
48	N,N'-(2,3,5,6-tetramethyl-1,4-phenylene) bis(4-chlorobenzene sulfonamide	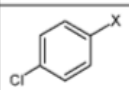	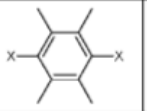	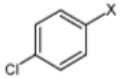	3.21	2,010 ± 710	>100,000
49	N,N'-(2,3,5,6-tetramethyl-1,4-phenylene) bis(3-bromobenzene sulfonamide)	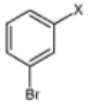	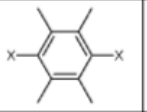	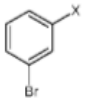	3.12	1,570 ± 480	>100,000
50	N,N'-(2,3,5,6-tetramethyl-1,4-phenylene) bis(4-bromobenzene sulfonamide)	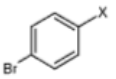	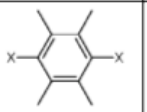	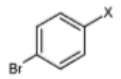	3.22	3,240 ± 1,780	>100,000
51	N,N'-(2,3,5,6-tetramethyl-1,4-phenylene) bis(3,4-dichlorobenzene sulfonamide)	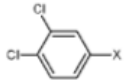	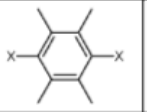	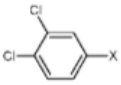	3.99	344 ± 57	>100,000
52	N,N'-(2,3,5,6-tetramethyl-1,4-phenylene) bis(3,5-dichlorobenzene sulfonamide)	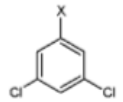	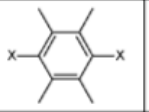	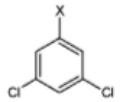	4.13	2,600 ± 1,010	>100,000
53	N,N'-(2,3,5,6-tetrafluoro-1,4-phenylene) bis(4-fluorobenzene sulfonamide)	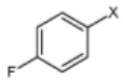	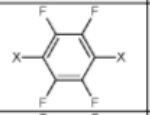	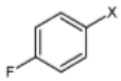	4.03	314 ± 46	>100,000
54	N,N'-(2,3,5,6-tetrafluoro-1,4-phenylene) bis(4-bromobenzene sulfonamide)	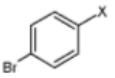	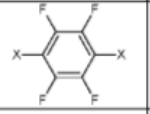	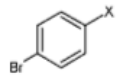	4.75	23.4 ± 2.7[b]	>100,000
55	N,N'-1,4-phenylenebis-2-naphthalene sulfonamide	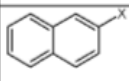	Bz	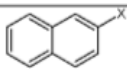	4.87	1,580 ± 730	>100,000

Table 3-1 Compound database for sulfonamide inhibitors and K_i values

a C_6H_4 represents benzene ring. b Data taken from Wadkins et al.[27] c Data taken from Hatfield et al. (manuscript submitted). d For the CEs, 3 was used as a substrate and the respective thiocholines were used for hAChE and hBChE. The general structure of the sulfonamides is indicated. The X in the subfragment represents the point of attachment to the sulfonamide moiety.

3.3 RESULTS

3.3.1 SELECTIVE INHIBITION OF CES2 BY BENZENE SULFONAMIDES

Based on our previous work, the Potter lab identified benzene sulfonamides as selective inhibitors of hiCE [27]. The 3D-QSAR analysis presented in this chapter indicated that (i) halogenation of the phenyl rings resulted in more potent compounds, and (ii) the central region of the inhibitor-enzyme complex was hydrophobic and could accommodate a large aromatic structure. Therefore, the Potter lab synthesized or acquired a total of 57 sulfonamide analogues, mostly containing halogen atoms appended to the benzene rings, and assessed their inhibitory potency toward the CEs hiCE and hCE1, as well as hAChE and hBChE. These assays used o-nitrophenyl acetate (*o*NPA) as a substrate for CEs and acetylthiocholine and butyrylthiocholine for the respective cholinesterases.

The majority of the compounds were shown to be excellent inhibitors having K_i values ranging from 41 to 3240 nM. The vast majority of the sulfonamides were selective for hiCE, with only one molecule showing weak activity toward hCE1 (compound 11). Compound, 11 was still over 250-fold more potent against hiCE (K_i values were 53 vs 13700 nM for hiCE and hCE1, respectively). None of the sulfonamides inhibited either hAChE or hBChE (data not shown), consistent with Wadkins et al. previous reports of these types of compounds [27]. The specificity of the sulfonamides for hiCE is though to be due to unique interactions with amino acids within the active site of this protein since, both CEs and cholinesterases demonstrate very similar crystal structures, [63, 77].

Six compounds were inactive toward all enzymes (28, 39, 41, and 44-46). The majority of these compounds contained large bulky atoms or moieties present within either the terminal benzene rings (28, 39, 41) or the central domain of the molecule (44-46). These groups would

likely impede access of the inhibitor to that active site gorge, thereby mitigating their biological activity.

The mode of enzyme inhibition by the sulfonamide inhibitors was partially competitive, indicating that while their structure resembled the substrate molecule, they were unable to completely inhibit substrate hydrolysis [78]. For this series of compounds, therefore, the inhibitory potency will be partially dependent upon the structure of the substrate. To confirm that these molecules could indeed inhibit the hydrolysis of other substrates, the Potter lab also assessed their effect on the metabolism of irinotecan.

3.3.2 3D-QSAR ANALYSES

We undertook detailed 3D-QSAR analyses with the goal of identifying specific domains within the molecules that might improve (or ablate) inhibitory potency. We have previously performed similar studies, and the pseudoreceptor site models that have been generated have significantly enhanced subsequent inhibitor design. Therefore, compounds 5, 8, 8-11, 14-31, 35-37, 47-56, and 60 were used as a training set for the development of the QSAR model. This was then validated using molecules (the test set). As can be seen from Table 3-2 and Figure 3-2, the linear correlation coefficients (r^2) for the observed versus predicted K_i values for the training set were ~0.9, with similar values for the cross correlation coefficients (q^2). Because q^2 values greater than 0.4 are considered statistically significant for biological systems [79], these models are likely to have excellent predictive value in the design of novel sulfonamide-based hiCE inhibitors. In addition, the q^2/r^2 values were close to unity, confirming the validity of the models.

Substrate	r^2	q^2	q^2/r^2
Irinotecan	0.89	0.83	0.93
*o*NPA	0.91	0.88	0.96

Table 3-2. QSAR validation parameters obtained from Quasar software when using the K_i values for hiCE inhibition with either irinotecan or *o*NPA as a substrate

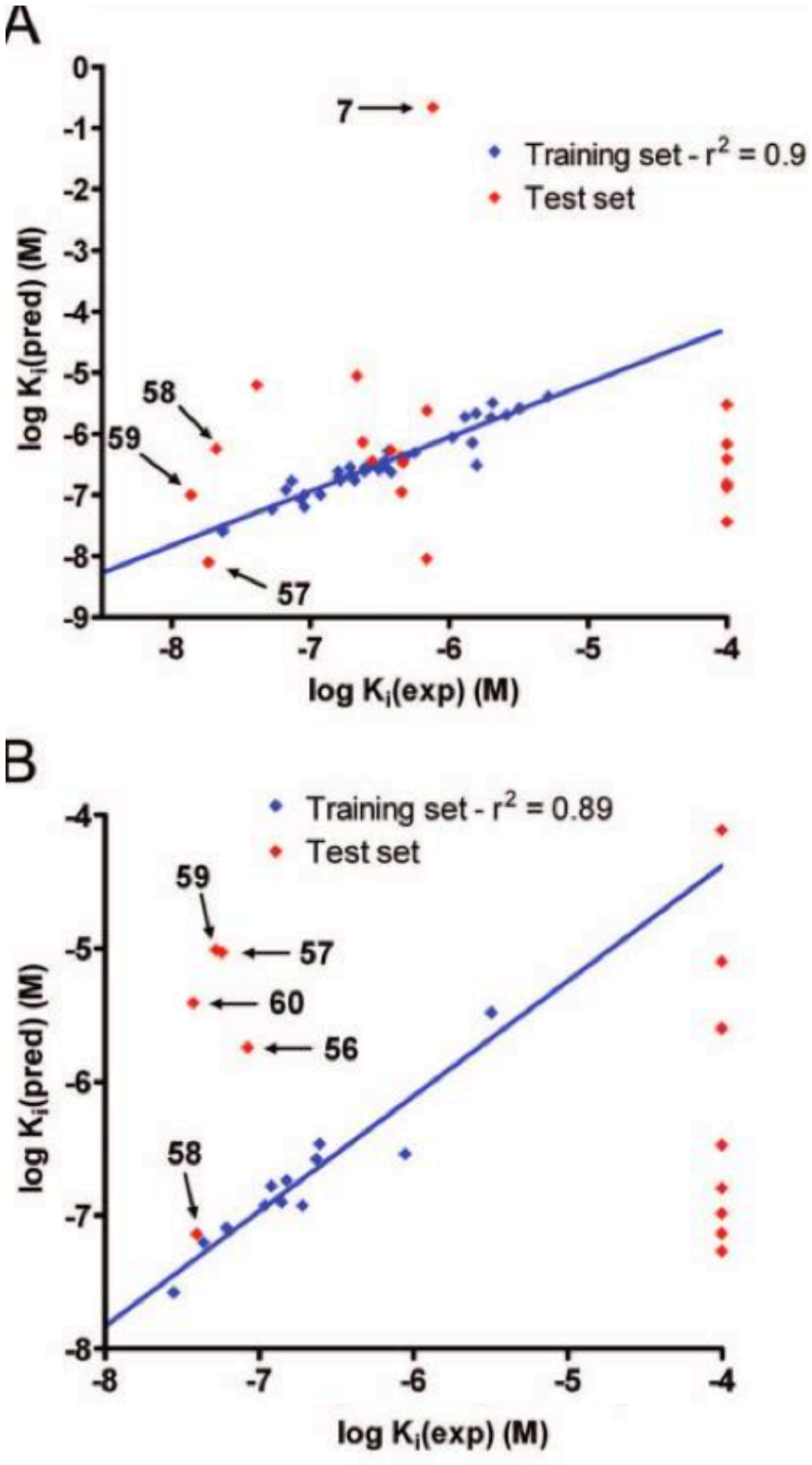
A
Training set - r2 = 0.9
Test set
7
58
59
57
log Ki(pred) (M)
log Ki(exp) (M)
B
Training set - r2 = 0.89
Test set
59
57
60
56
58
log Ki(pred) (M)
log Ki(exp) (M)

Figure 3-3.Graphs demonstrating the correlation between the predicted and the observed K_i values obtained from the QSAR models. (A) Graph when using *o*NPA as a substrate, and (B) when using irinotecan. Linear correlation coefficients for the line fits (r^2) are indicated on the graphs.

The QSAR models were reasonable at predicting the K_i values for the fluorene analogues 56-60, with all compounds except 58 being considered excellent inhibitors of hiCE (<100 nM) when using *o*NPA as a substrate. Interestingly, the latter molecule had the highest clogP value (5.69), suggesting that for these models, this parameter is not a major determinant of biological potency. Significantly, while the fluorene moiety increased the length of the molecule by 4-5 Å as compared to the benzene derivative, this did not significantly impact enzyme inhibition. Also it should be noted (see Figure 3-2) that the model was very poor at predicting the efficacy of 7. This is potentially due to the fact that this compound contains a
disulfide chemotype (unlike all of the other molecules that were assayed) and can potentially adopt alternate conformations that would not be accurately predicted by the model.

The QSAR predicted K_i values for the inhibition of hiCE mediated irinotecan metabolism were not as good as though seen for *o*NPA. Indeed, while the fluorene compounds were considered good inhibitors of hiCE (K_i values in the low μM range), only 58 was predicted with any great accuracy (Figure 3-2b). This is likely due to the fact that only 12 compounds were used as the training set for this model, and this did not include any of the fluorene analogues. However, these QSAR models will allow for rapid screening of analogues for inhibitor potency prior to the initiation of chemical synthesis.

		clogP	pred K_i **3** (nM)	exp K_i **3** (± SE, nM)	pred K_i **1** (nM)	exp K_i **1** (± SE, nM)	hCE1 K_i **3** (± SE, nM)
56	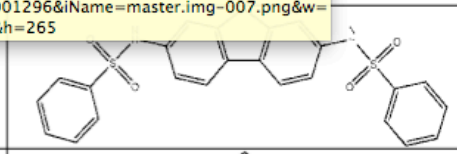	4.83	98.4 (Train)	90.8 ± 1.1	1,820	84.7 ± 14.0	>100,000
57	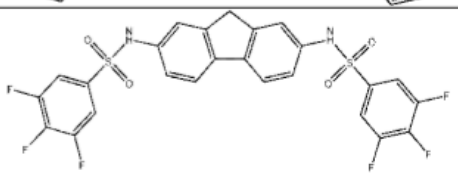	4.10	7.9	18.6 ± 5.3	9,350	58.1 ± 12.3	>100,000
58	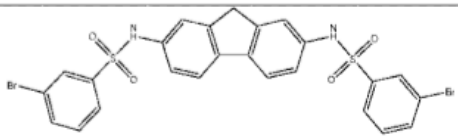	5.69	570	21.2 ± 2.5	72.8	39.7 ± 7.9	>100,000
59	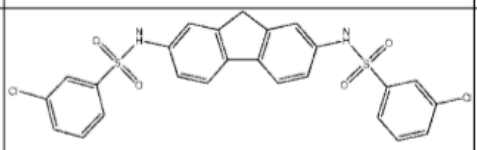	5.52	100	13.9 ± 2.5	9,780	52.8 ± 20.7	>100,000
60	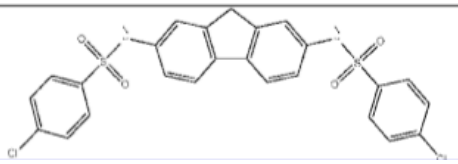	5.55	25.2 (Train)	23.5 ± 5.7	3,930	37.7 ± 7.0	>100,000

Table 3-3: Predicted and observed *K*i Values for hiCE with five fluorene analogues (Compounds **56**-**60**) that were postulated from the QSAR analyses to be excellent CE inhibitors

3.3.3 PSEUDORECEPTOR SITE QSAR MODELS

To provide a graphical representation of the QSAR results, we developed a pseudoreceptor model for hiCE with data sets derived from the inhibition of hydrolysis of *o*NPA (Figure 3-3A). This figure outlines the interactions that describe receptor-ligand binding in the enzyme. The model has primarily anionic (red areas) regions of charge located in a cluster at the base of the model and a weakly cationic (blue spheres) domain located at the top. This is consistent with all our previous analysis of hiCE inhibitors, where charge asymmetry was observed both in the QSAR models 20, 21, 24, 27-29 and in the enzyme structure determined from homology modeling [27]. We also present an electrostatic potential map of the model (Figure 3-3B) oriented to emphasize the charge asymmetry. While the origin of this charge distribution is not completely understood, at least for homology structures of hiCE, it maps well onto the position of charged amino acids present within the active site [27]. It should be remembered that these figures represent a description of the interior surface of the active site and not the combined surfaces of the inhibitor molecules. However, in general, the electrostatic potential inside the active site was negative [80] and hence it is not clear whether the positive areas required to fit the inhibition data reflect interactions within the active site alone, or represent potential interactions with positively charged residues near the active site opening. The interpretation of these models will be greatly enhanced if a crystal structure of hiCE becomes available.

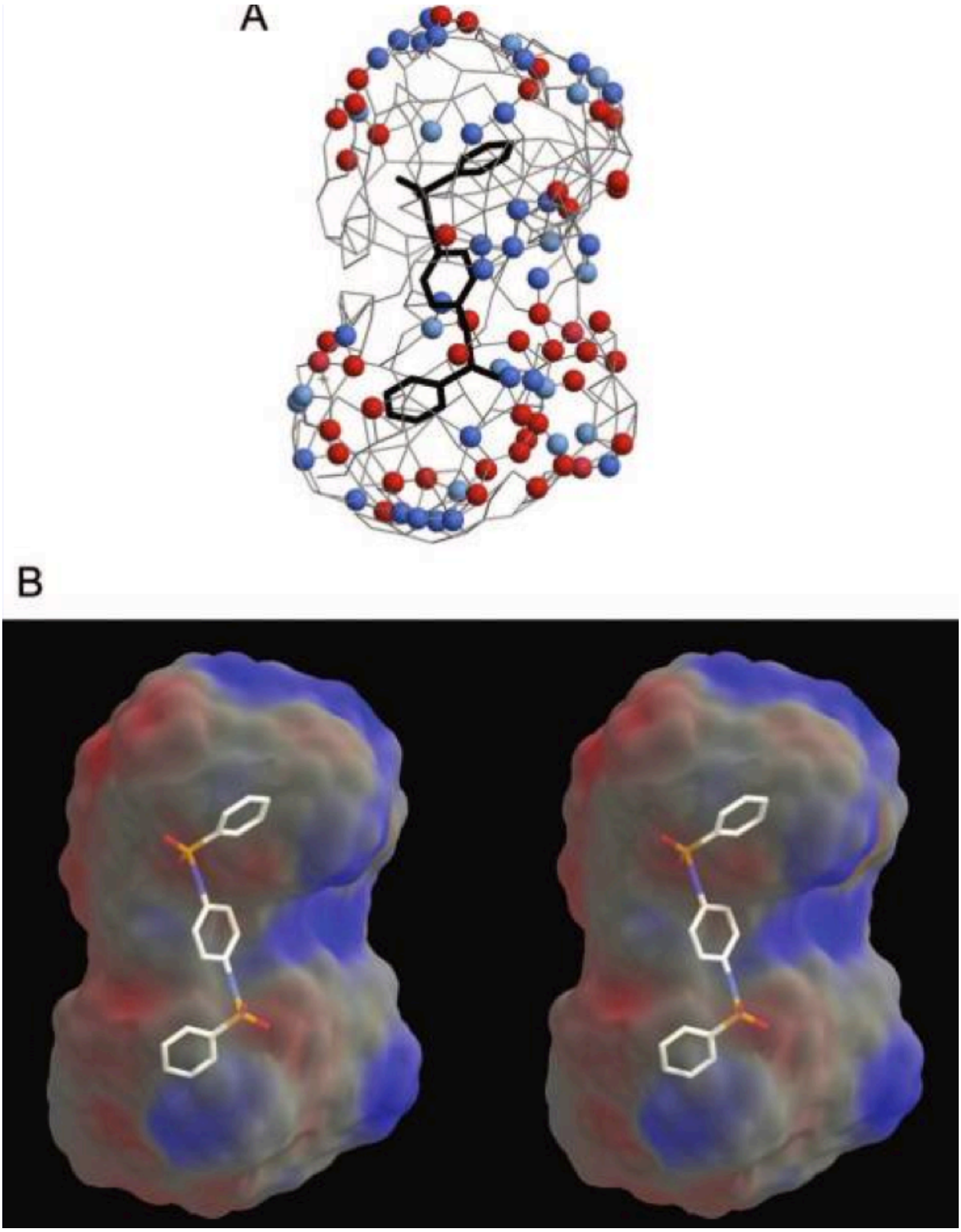
A
B

Figure 3-4. 3D-QSAR pseudoreceptor site models generated from the enzyme inhibition data for hiCE using the benzene sulfonamides with 3 as a substrate. These models were generated using results obtained from all 57 sulfonamides and include compound 8 for reference. Both figures were generated using Raster3D4 [81] and Molscript 44. (A) The model is depicted as colored spheres on a hydrophobic gray grid. Areas that are hydrophobic are indicated in gray, where dark-blue spheres represent regions that are positively charged (+0.25e) and light-blue spheres correspond to reduced charge (+0.1e). Dark-red spheres indicate domains that are negatively charged (-0.25e), and light-red spheres represent areas of reduced negative charge (-0.1e). In all cases, e is the charge of the proton. (B) Stereo view of a 3D-QSAR pseudoreceptor site model that describes sulfonamide binding as a molecular surface upon which the electrostatic potential is mapped. The electrostatic potential is calculated from the Quasar software partial charges, which were defined as -0.25e, -0.1e, +0.1e, and +0.25e for negative salt bridge, hydrophobic negative, hydrophobic positive, and positive salt bridge characteristics, respectively. As above, e is the charge of the proton. The figure is oriented to emphasize the charge asymmetry that appears in all QSAR models that we have observed in previous analyses [27, 82-86].

3.4 DISCUSSION

In this chapter, we have demonstrated that potent, selective inhibitors of hiCE based upon the benzene sulfonamide scaffold can be developed. This has resulted in the development of a series of fluorene analogues that have K_i values in the low nM range for both the inhibition of hydrolysis of irinotecan and *o*NPA. These compounds (56-60) were designed and synthesized based upon prior 3D-QSAR pseudoreceptor site models that indicated that a bulky, hydrophobic central domain within the inhibitors improved their potency.

The benzene sulfonamide analogues that we assayed fell into four broad classes. Compounds 4-13 were originally identified in a small scale library screen, [27] and they essentially contained three domains. This included terminal and central phenyl rings bonded via sulfonamide chemotypes and substitutions within the rings that altered the chemical properties of the compounds. Because compound 13 demonstrated the lowest K_i for hiCE inhibition, this molecule was used as a scaffold for the design and synthesis of analogues 14-55. Due to the fact that the most potent compounds tended to be halogen substituted, [27] we concentrated our efforts on the generation of inhibitors containing these atoms, principally in the terminal benzene rings (molecules 14-41). Among this latter series of compounds, we noted that substitution in either the 3-(meta-) or 4-(para-) position with chlorine or bromine (compounds 17-19; K_i values ranging from 67-85 nM) resulted in significantly lower inhibition constants as compared to that of the unsubstituted molecule (8; K_i) 1060 nM). Indeed, 17-19 were the most potent of the molecules containing substitutions within the terminal benzene rings. These halogens increase the hydrophobicity of the molecules (clog P for 17-19 range from 4.3-4.7, ~1 log greater than compound 8), and therefore these analogues would be more likely to localize within the hydrophobic active site gorge of the protein.

In contrast, substitution with multiple larger atoms (e.g., compound 28) resulted in loss of biological activity and is likely due to the fact that this molecule is too large to fit within the active site of hiCE. Furthermore, molecules containing a carboxylic acid or amide group at the 4-position (39 and 41) were inactive. Whether this loss of enzyme inhibition is due to electronic effects on the other atoms within the sulfonamide, or a steric interaction that forces the inhibitor into a conformation such that it can no longer interact with amino acids that line the active site, or a combination of both, is unclear. However, it is apparent that introducing substitutions that increase the clogP without dramatically increasing the size of the molecules can improve the potency of these analogues.

Compounds 42-54 contained substitutions within the central benzene ring coupled with halogens appended in the terminal phenyl groups. In general, these modifications resulted in reduced potency toward hiCE inhibition. This is exemplified by compounds 44-46, which are inactive in this assay. However, 54, which contains the 2,3,5,6-tetrafluoro substitution, resulted in increased activity as compared to the unsubstituted molecule (19). Because these compounds demonstrate very similar clogP values, the increase in biological activity is likely due to a change in the electron distribution afforded by the very electronegative fluorine atoms. As we have not yet obtained the X-ray structure of hiCE, it has not been possible to identify the specific amino acids with which these sulfonamides interact. Hence, it is unclear how these small molecules demonstrate specificity for hiCE. However, based on previous observations that sulfonamides can inhibit thrombin, we presume that a similar mechanism of enzyme inhibition occurs [87-89]. These studies demonstrated that the oxygen atoms within the sulfonamide group can hydrogen bond with amino acids present within the active site of this protein. Therefore, we believe that the unique arrangement of residues present within the hiCE catalytic gorge and their ability to

form hydrogen bonds with the sulfonamides, represent the key interactions responsible for selective CE inhibition.

Consistent with our previous reports describing CE inhibitors, [82, 83, 86] molecules that contained substitutions that increased the bulkiness or width of the compound were generally poor inhibitors. This was exemplified in this series of analogues by 28, 39, 41, and 44-46. All of these sulfonamides contained groups or atoms that significantly increased either the width or length of the molecule that would preclude facile access of the inhibitor to the CE active site. Because the hydrolysis of compounds by CEs is dramatically influenced by their ability to interact with the catalytic amino acids, [72, 80] it is highly likely that the same holds true for inhibitor molecules. Therefore, compounds that exceed the dimensions of the active site gorge in these proteins would not be inhibitors of these proteins. Molecules 28, 39, 41, and 44-46 are much larger and bulkier than the other compounds described here and therefore do not inhibit hiCE.

On the basis of the results of the QSAR analyses, we hypothesized that introducing a larger, planar, aromatic core domain within the center of the molecule should increase its potency. This was due to the fact that this moiety would increase the clogP (hydrophobicity) of the compound, without impeding the ability of the sulfonyl groups to interact with the amino acids present within the active site. This is consistent with the 3D-QSAR model depicted in Figure 3-3. This data set was generated using both compounds 56 and 60 in the training set. Excluding these compounds resulted in QSAR relationships that predicted 56-60 to be good inhibitors, but the experimental data revealed them to be excellent inhibitors: much better than predicted and some of the most potent compounds we have examined to date. One difficulty with any QSAR analysis is that the fewer members of a class of molecules in the training set, the less

likelihood of correct prediction of that series of compounds. Hence, we rebuilt the models, including 56 and 60, to determine whether this would result in improved prediction of the K_i values for 57-59. As expected, the predictive properties of the data were improved by at least 1 order of magnitude by including 56 and 60, suggesting that as we synthesize and test more fluorene-containing molecules, we should be able to produce a more accurate QSAR relationship for other classes of molecules beyond those used in this study.

In general, halogen substitution of the distal phenyl rings slightly decreased the K_i value as compared to that of the unsubstituted analogue 11, whereas methyl groups added to the central phenyl ring did not much affect the binding of the analogues. This was somewhat surprising, as the 3D-QSAR pseudoreceptor model (Figure 3-3) is highly hydrophobic in the central ring area, as indicated by gray lines. However, replacement of the central phenyl ring with a naphthyl or fluorene chemotype greatly reduced the inhibition constants of the compounds, i.e., making them more potent hiCE inhibitors. We attribute this to π-π interactions of the small molecules with the tryptophan and phenylalanine rings that are known to line the active site gorge of hiCE [5]. Similarly, this would explain the potent inhibitory power of the indole-containing isatins that we have previously characterized [83].

3.5 CONCLUSIONS

In summary, the active site contains a large area of hydrophobicity in the central ring area, and the active site has a charge separation. Our QSAR model suggests that potency of the sulfonamide inhibitors can be increased by (*i.*) the addition of a larger hydrophobic core region of the sulfonamides, (*ii.*) substitution of the distal benzene rings with halogens and placing those electronegative groups in the para or meta position, (*iii.*) removal of moderately EWG groups

from the para position, (*iv.*) removal of bulky groups from the core region of the sulfonamides. Dr. Potter's Lab is currently determining the ability of these compounds to inhibit hiCE intracellularly and evaluating whether any of these molecules represent valid lead compounds for in vivo use. If so, they may allow the design of clinical candidates, suitable for the modulation of irinotecan induced toxicity, in patients treated with this drug.

3.6 EXPERIMENTAL

3.6.1 THREE DIMENSIONAL QSAR MODELING OF INHIBITORS

Multidimensional-QSAR modeling of carboxylesterase inhibitors was performed using Quasar 5 software [90-92] running on a Macintosh G5. The structure for each compound was built using Chem 3D, and each structure was minimized with MM2 and PM3 formalisms. The solvation energies and charges were calculated using the AMSOL 7.1 program [35] using the SM5.42R solvation method. The gas phase charges obtained were used for all QSAR analyses. A resulting receptor surface was then generated using Quasar 5.0 and analyzed to yield over 200 independent models and subsequently refined to generate ~ 7000 pseudoreceptor site models. Repeated analyses of the data sets were then performed until the cross correlation coefficients (q^2) were greater than 0.7 for the experimentally determined versus the predicted K_i values. Routinely, this yielded correlation coefficients (r^2) of > 0.8.

Two independent QSAR models were constructed using two different training sets. The first was constructed using 37 sulfonamides as inhibitors of hiCE using *o*NPA as a substrate. The second was obtained using the K_i values of 12 inhibitors of irinotecan hydrolysis. In all cases, a range of K_i values spanning 3 orders of magnitude were used to ensure a reasonable model. We then included the structures of a number of potential inhibitors of hiCE in the test set to identify

novel chemical scaffolds that might be potential selective inhibitors of hiCE. These included the fluorene-containing compounds 56-60.

PUBLICATION NOTICE

This work was published in the Journal of Medicinal Chemistry in 2009.

Improved, Selective, Human Intestinal Carboxylesterase Inhibitors Designed to Modulate CPT-11 Toxicity, Latorya D. Hicks, Janice L. Hyatt, **Shana Stoddard**, Lyudmila Tsurkan, Carol C. Edward, Monika Wierdl, Randy M. Wadkins, Philip M. Potter. *Journal of Medicinal Chemistry* 52 (2009) 3742-3752

CHAPTER 4 IN SILICO DESIGN AND EVALUATION OF CARBOXYLESTERASE INHIBITORS

4.1 ABSTRACT

Carboxylesterases (CEs) are important enzymes that catalyze biological detoxification, hydrolysis of certain pesticides, and metabolism of many esterified drugs. The development of inhibitors for CE has many potential uses, including increasing drug lifetime and altering biodistrubution; reducing or abrogating toxicity of metabolized drugs; and reducing pest resistance to insecticides. In this chapter, we discuss the major classes of known mammalian CE inhibitors and describe our computational efforts to design new scaffolds for development of novel, selective inhibitors. We discuss several strategies for *in silico* inhibitor development, including structure docking, database searching, multidimensional quantitative structure activity analysis (QSAR), and a newly-used approach that uses QSAR combined with *de novo* drug design. While our research is focused on design of specific inhibitors for human intestinal carboxylesterase (hiCE), the methods described are generally applicable to inhibitors of other enzymes, including CE from other tissues and organisms.

4.2 INTRODUCTION

Carboxylesterases are enzymes that convert esters into the corresponding alcohol and carboxylic acid. Carboxylesterases are members of the larger α/β-hydrolase fold family that

includes a wide variety of enzymes such as lipases, cholinesterases, haloalkane dehydrogenases, and epoxide hydrolases [9, 93, 94]. The catalytic machinery of the CE is an amino acid triad consisting of the residues serine, histidine, and glutamate that sit in a nucleophilic elbow, making these enzymes members of the even larger family of serine hydrolases.

Carboxylesterases are ubiquitous in nature. In mammals, they are expressed in numerous tissues [11, 95]. The hydrolytic activity will vary based on tissue type, with the liver isozyme being one of the most active of all isozymes studied. The hydrolytic activity of these enzymes are important in drug metabolism, protection against xenobiotics, and detoxifying pesticides such as pyrethoids [14]. CE's are also responsible for hydrolyzing clinically useful drug such as capecitabine and irinotecan [12, 13], as well as illicit drugs such as heroin [6].

CEs have potential as therapy for pesticide overexposure. Organophosphate and carbamate insecticides have the potential to poison humans by acting on acetylcholinesterase (AChE). CEs can bind organophosphate and carbamate insecticides and reduce toxicity by two pathways: metabolism of the insecticide by CEs and irreversible binding by the insecticides [15, 16].

Carboxylesterases are also important in the activation of prodrugs. One such clinically important prodrug is irinotecan (7-ethyl-10-[4-(1-piperidino)-1-piperidino]carbonyloxycamptothecin), an anticancer agent used as front-line therapy for colorectal cancer (Figure 3-1). In humans, several CEs have been well characterized, particularly liver carboxylesterase 1 (hCE1) and human intestinal carboxylesterase (hiCE), the latter of which is localized to the small intestinal epithelia. Both hCE1 and hiCE are known to convert irinotecan into its active form, SN-38 (7-ethyl-10-hydroxycamptothecin; Figure. 3-1). However, hiCE is expressed at high levels in the small intestine and is much more efficient at converting irinotecan

than hCE1 [12, 17]. Thus, overproduction of SN-38 occurs in the small intestine during irinotecan therapy, and tissue damage to this organ contributes to delayed diarrhea in patients, a side-effect that often requires hospitalization [96]. This is the dose-limiting toxicity of irinotecan. Development of hiCE-selective CE inhibitors to reduce or eliminate unwanted toxicity of irinotecan has been the recent goal of our laboratories. Selective hiCE inhibitors are envisioned as adjuvant therapy for the modulation of diarrhea, potentially allowing for higher dosing of the drug and more effective treatment of colorectal cancer.

Several molecular structural scaffolds of CE inhibitors exist (Figure 1-3), which include, sulfonamides, benzils, benzoins, carbamates, isatins, organophosphates, oxysterols, pyrethoids, acridines, trazines, trifluromethylketones, piperidines, serine specific agents, and inorganic compounds. In general, most of these inhibitors show limited selectivity or specificity among isozymes or across species.

Over the last several years, we have developed a number of specific or semi-specific hiCE inhibitors. However, one difficulty that has persisted among these inhibitors is poor water solubility. This chapter gives a brief overview of previously described molecular scaffolds of CE inhibitors, followed by a description of recent developments in the *in silico* methodologies we are using to design new selective and specific inhibitors with greater water solubility and overall "drugability" of their chemical properties. Detailed reviews of CE inhibitors have appeared recently [5, 97]. Here, our focus is on computer-based development of selective inhibitors of hiCE with the specific purpose of modulating irinotecan activation in the small intestine. However, the methodology used is general enough that it could be applied to the development of inhibitors of any enzyme

In the last chapter we developed a QSAR model using an expanded dataset of sulfonamide inhibitors. This was performed to further dileneate features, which contributed toward this class of CE inhibitors potency. Understanding the details that confer potency to these inhibitors is important, however, we also have a need to develop soluble compounds. In this chapter we demonstrate that we can generate soluble CE inhibitor compounds using a dual QSAR, de novo design method approach.

4.3 CARBOXYLESTERASE INHIBITORS: SCAFFOLDS, SELECTIVITY, SPECIFICITY AND MECHANISM OF INHIBITION

4.3.1 ACETYLCHOLINESTERASE INHIBITORS AND THEIR CE INHIBITION

We begin this chapter by looking at selectivity for CEs by several known groups of AChE inhibitors, starting with the alkylphosphonic esters, also known as organophosphate (OPs), which may be the most well known class of CE inhibitors. OPs are commonly used as insecticides (e.g., malathion (diethyl dimethoxythiophosphorylthiosuccinate) and paraxon (diethyl 4-nitrophenyl phosphate). Organophosphates are toxic due to their inhibition of AChE activity, which allows the muscarinic receptors to be continually activated by acetylcholine. The result of this AChE inhibition is the cholinergic effect, with symptoms of salivation, lacrimation, urination, defecation, gastrointestinal distress, vomiting, muscle spasms and ultimately death if the reaction is severe enough. Hence, sarin (O-isopropylmethylphosphonofluoridate), soman (O-pinacolylmethylphosphonofluoridate) and tabun (ethyl dimethylamidocyanophosphate), which demonstrate high affinity for human AChE, have been used as chemical warfare agents.

Carboxylesterases can also be irreversibly inhibited by organophosphates. The mechanism of inhibition involves the attack from the enzyme's serine Oγ on the phosphate atom

of the organophosphate. This creates a covalent bond ending the mechanism at an acyl–enzyme intermediate. Strategies to develop CEs to combat chemical warfare compounds have been pursued by the military. Essentially, CEs could be used as "bioscavengers", which work by sequestering or hydrolyzing a toxic substrate [98]. Recent work shows that hCE1 shows a preference for binding the P_R enatiomers of soman and cyclosarin analogues (1700-, 2900-fold respectively) and a slight preference for the P_S enantiomer of sarin analogues (5-fold) [99]. However, only one group of OPs has been found to be semi-selective for CEs: the benzodioxaphosphorines (Bomins; attributed to Patent USSR 06.22.1985. No. 1187444). Their selectivity however is only about 10-fold greater than for AChE, and hence the problematic toxicity of OPs make them an unlikely scaffold for development of clinically useful compounds. The carbamates (CBs) contain a central amide ester group and two alkyl or aryl substituents located on the nitrogen atom. CBs are not as toxic as the OPs but they still induce the same cholinergic effect. The CBs are reversible inhibitors of AChE and, like the OPs, have been used as insecticides (e.g., Carbaryl (1-naphthyl methylcarbamate)). The carbamates are also used in many clinical applications. For example rivastigmine (S)-N-ethyl-N-methyl-3-[1-(dimethylamino)ethyl]-phenyl carbamate is used to treat Alzheimer's disease. Rivastigmine is a selective, reversible brain AChE inhibitor [100].

Irinotecan also contains a carbamate moiety, which is primarily responsible for its initial cholinergic activity [80, 101]. Carbamates for CE inhibition have been explored by the Potter and Danks groups, who showed that four nitrophenyl derivatives with carbamate-linked side chains could selectively inhibit hiCE and rCE [102]. These derivatives were the first attempt at developing specific hiCE inhibitors. However, inhibition by these compounds is also confounded

by their AChE inhibition, and hence has the potential problems associated with all cholinergic drugs.

Trifluoromethylketones (TFKs), like the OPs and CBs, will also inhibit AChE; the carbonyl carbon of the TFK can form a covalent bond to the serine residue of the catalytic triad. Thus they are non-specific inhibitors of CEs. Although these CE inhibitors are some of the most potent known, they exhibit both partially competitive and partially noncompetitive modes of inhibition. Their mode of binding is somewhat unique compared to the rest of the CE inhibitors, in that they take time to reach equilibrium before maximum inhibitor potency can be reached [85]. TFKs inhibit a range of mammalian CEs. Hence, selectivity toward hiCE is problematic. Acridine inhibitors of AChE include tacrine, which is used to treat Alzheimer's disease. Tacrine itself is not an inhibitor of hCE1, but 6,9-diamino-2-ethoxyacridine and 9-amino-6-chloro-2-methoxyacridine does inhibit hCE1 selectively over hiCE. These derivatives are low μM inhibitors of hCE1 [77].

4.3.2 MORE SPECIFIC CE INHIBITORS

The AChE/CE cross inhibitors listed above came primarily from studies that emphasized the similar catalytic activity of the members of the α/β-hydrolase fold family. Indeed, the very first collaboration between the Potter and Wadkins laboratories was on molecular modeling of the interaction of irinotecan with AChE and the related butyrylcholinesterase[103]. In the subsequent decade, the quest for isozyme-specific CE inhibitors has produced several molecular scaffolds that do not possess anti-AChE activity. The design of many of the analogs was a combination of chemical library screens to isolate reasonably selective CE inhibitors, followed by chemical intuition and plausible synthetic schemes.

Telik's Target Related Affinity Profiling (TRAP) method was originally employed in the search for novel CE inhibitors. In this method, compounds were screened for their binding affinities toward a panel of protein targets. The binding affinities were subsequently used to create an "affinity fingerprint", which was subsequently used to identify novel inhibitors. Telik's methodology has the advantage of needing few initial compounds to generate several new scaffolds of inhibitors. The TRAP analysis had been utilized in the identification of novel inhibitors for cyclooxygenase-1 (COX-1) [104]. Hsu and coworkers used 19 known COX-1 inhibitors, all reversible competitive inhibitors of COX-1, comprising 8 structurally dissimilar classes, to create an affinity fingerprint for COX-1 inhibition. Using TRAP analysis, they derived 3 new COX-1 inhibitors. We used this method to identify novel CE inhibitors. The sulfonamides and benzils were both discovered through this methodology [27, 86].

4.3.3 SULFONAMIDES

The initial screening of a library of compounds isolated 9 sulfonamide derivatives as specific hiCE inhibitors vs. other human hydrolases [27]. Using a limited QSAR analysis of these 9 compounds, a number of other sulfonamides were synthesized or obtained from commercial sources. Examination of this larger group of sulfonamides determined that the ring at the central core moiety could accommodate either benzene or fluorene [27, 28]. The fluorene sulfonamides, in general, are more potent than the benzene sulfonamides with inhibition constants ranging from 41 nM to 3240 nM for benzene sulfonamides and from 14 nM to 91 nM for the fluorene sulfonamides. The majority of sulfonamides do not inhibit AChE or butyrylcholinesterase (BChE), and hence are highly selective CE inhibitors.

The mechanism of inhibition for the sulfonamides is partially competitive. However, unlike the majority of the CE inhibitors, there is no carbonyl carbon atom or electron deficient atom that would be susceptible to attack from the serine Oγ residue. Attack on the sulfur atom of the sulfonamide is an energetically disfavored process due to the stability of the sulfonamide. The sulfonamides could potentially hydrogen bond to the enzyme and lock it into a stable complex, or they may bind to the opening of the active site, blocking the entrance to the gorge.

The extended conformation of the sulfonamides matches the shape of the active site gorge of a homology model of hiCE, so it is entirely possible that they occupy the binding site of the enzyme, giving rise to isoform specificity. However, the sulfonamides as a whole suffer from very poor water solubility. Evaluation of over 50 sulfonamides [28] revealed an inverse correlation of clogP and log K_i. Hence, the least soluble compounds were the best inhibitors of the enzyme. This is the major difficulty with using sulfonamides as scaffolds for a potential drug application.

4.3.4 BENZILS

The diphenylethane-1,2-dione (benzil; Figure 1-3) analogues are another class of isotype-selective mammalian CE inhibitors that we have examined after the initial drug screening. Benzil itself is not a new compound (discovered in the late 1800s). However, it was not until 2005 that it was discovered to be a selective inhibitor for human carboxylesterases [86]. Inhibition constants (K_i) ranged from 4 nM to 18 μM for 31 benzil analogues that were evaluated, with no inhibition of AChE. The analogs were found to be competitive reversible inhibitors of the CEs The proposed mechanism of inhibition involves the inability of the enzyme to release the aldehyde as a leaving group. With no appropriate leaving group after the formation of the

tetrahedral intermediate, the initial carbonyl is reformed. The crystal structure of hCE1 has been solved with benzil in the active site, suggesting that cleavage of the dione moiety could occur, consequently generating a benzoic acid or benzaldehyde [105]. In contrast to the sulfonamides, there is no correlation between clogP values for these compounds and their K_i values, making them a much more interesting platform for drug development. Their selectivity appears to arise from the dihedral angle of the dione moiety. When the carbonyl oxygen atoms are cis-coplanar, greater selectivity for hCE1 occurs, while non-planarity results in selectivity for hiCE [106].

4.3.5 BENZOINS AND FLUOROBENZOINS

During the exploration of the benzil scaffold, compounds of similar structure were also tested for activity against the mammalian CEs. The compound 1,2-diphenyl-2-hydroxy ethanone (benzoin; Figure. 1-3) was found to be a weak but selective inhibitor of CEs, having a K_i of 2.7 μM for hiCE and 7.2 μM for hCE1. Subsequent addition of electron withdrawing groups to the benzene rings in both benzils and benzoins produced more potent, highly selective inhibitors. In particular, addition of fluorine significantly increased their ability to inhibit mammalian CEs without resulting in inhibition of AChE or BChE. The inhibition constants for the fluorinated analogues ranged from 8 nM to 1.3 μM [82].

4.4 *IN SILICO* METHODS AND DEVELOPMENT OF ISATINS

4.4.1 COMPUTATIONAL APPROACHES

One conceivable method of computationally deriving selective inhibitors for CEs might be to dock small molecule libraries into the active site of CEs in order to predict new inhibitors. However, in practice there are complications with that strategy that limit its effectiveness. The

substrate specificity of CEs is dependent on two structural features: the dimensions of their active site gorge and the external opening to the gorge. We have examined these important parameters using molecular dynamics calculations of CEs from rabbit, human liver, human intestine, and a bacterial CE (rCE, hCE1, hiCE, and pNB, respectively) [Shawn's-REF]. In addition, we have used normal mode calculations to examine low-frequency motions of the CEs (large conformational changes). Both the active site gorge diameter and the opening to the active site fluctuate significantly with time (Figure 4-1), so determining which structure the known inhibitors are binding to is complicated. The basic rationale for the need to include molecular dynamics in the development of enzyme inhibitors for the related AChE has been recently reviewed [107]. This rationale also applies to CEs. Briefly, enzymes are in constant motion at temperatures near 37°C and the understanding of the fluctuation is crucial for in silico docking or assembly of inhibitors. In the case of the α/β hydrolase fold family, the active site residues are at the bottom of a ~22 Å gorge, the walls of which are also fluctuating. The crystal structure of hiCE has not been determined, and so by necessity a homology model would need to be used for this enzyme (although it should be noted that earlier homology models of rCE [80] based on the folding of AChE were remarkably similar to the subsequently-determined crystal structure [108]; α carbon RMSD ~ 2Å). The crystal structures for the other 3 enzymes (rCE, hCE1, pNB) have been determined and hence MD calculations are easily accomplished. Even though the crystal structures exist, there is an additional reason MD is an important tool for docking ligands into these molecules. As with other enzymes, the crystal structures containing known substrates or inhibitors in the active site have an active site that is too small to accommodate other known, larger substrates. For example, the structure of hCE1 containing a product of benzil hydrolysis would be too close-packed to allow placement of CPT-11 in the same locale [105]. This can be

resolved by allowing the enzyme structure to fluctuate. An example of this is shown in Figure. 4-1, where the active site gorge diameter size of the pNB CE is calculated throughout a lengthy 10 ns MD simulation. Note that access to the active site can fluctuate from as little as 3.0 Å to as wide as 7.5 Å over a relatively short period of 1 ns.

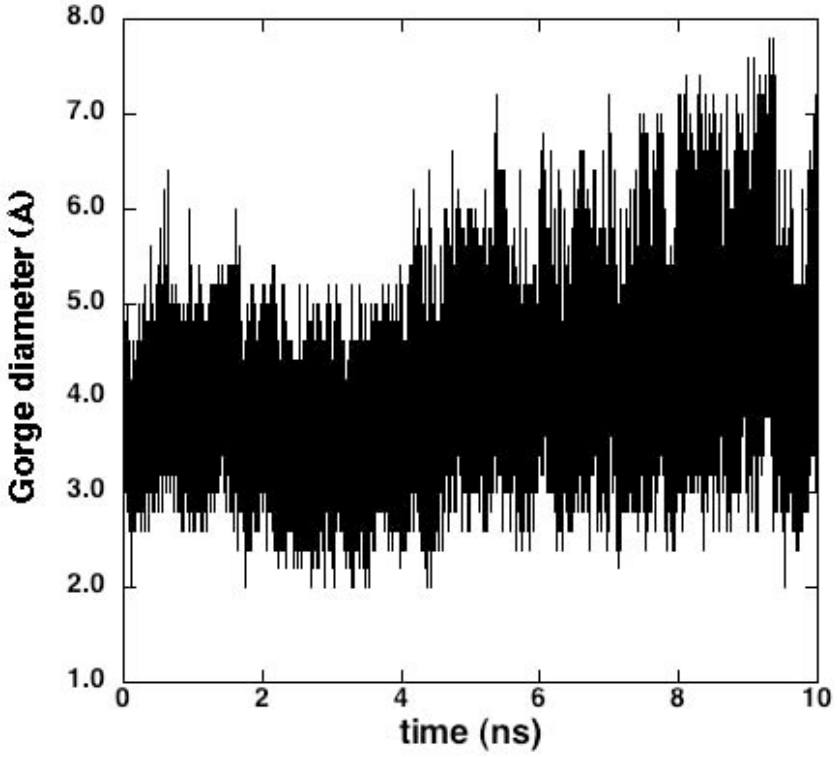

Figure 4-1. Fluctuation in the diameter of the active site gorge of a carboxylesterase from *B. subtilis*. The analysis was performed with a procedure modified from the work of McCammon and colleagues [109]. The solvent-accessible surface was calculated with an increasing probe radius until it no longer made contact with the active site Ser and His residues. The structure was taken from PDB code 1QE3 [18].

Other regions of structural fluctuation in CEs are the loops that form a putative lid over the entrance to the active site gorge. Normal mode analysis (NMA) of hCE1 and a homology model of hiCE (modeled using hCE1 as a template) was performed with the ElNémo web server [110], which is a web interface to the Elastic Network Model that implements the 'rotation-translation-block' (RTB) approximation. The lowest non-zero frequency mode for the enzymes having a high degree-of-collectivity (mode 7) are shown in Figure 4-2. It is this fluctuation that makes MD a critical component of inhibitor design by computer for the family of α/β hydrolases. However, these fluctuations are also a drawback to this type of computational design since computer docking to multiple enzyme structures must be performed.

The combination of MD and docking has been used for development of specific inhibitors of AChE vs. other serine hydrolase enzymes, and hence we expect this approach has the potential to work for CEs as well. Generic docking of known AChE inhibitors to a static AChE are generally not predictive for the relative magnitudes of the inhibition constants [107]. This has been attributed to the inability of static models to correctly calculate the entropy change upon inhibitor binding. A more successful approach taken by the McCammon laboratory involves using not just one static structure of CE for docking potential inhibitors, but rather numerous CE structures taken from a molecular dynamics simulation [111]. However, given the complications inherent in this approach, we developed a computationally-simpler multi-dimensional QSAR model as a reduced representation of the inhibitor binding site. This has the advantage over crystal structure docking approaches in that it does not require us to know the molecular details of the inhibitor binding site, just the chemical properties and K_i values for the inhibitors.

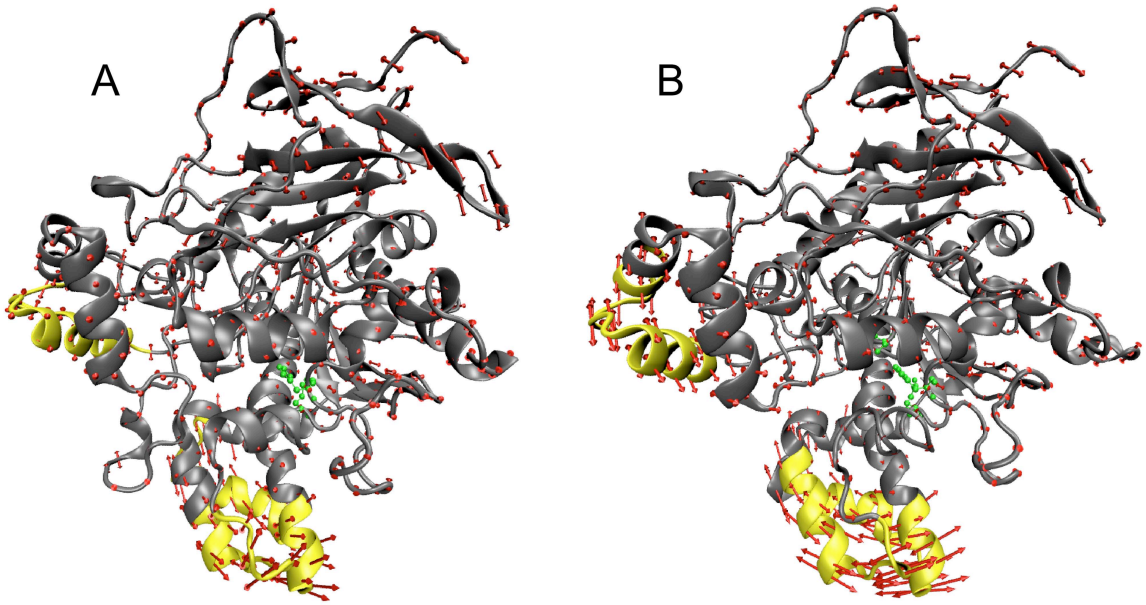

Figure 4-2. Fluctuation of the loop forming part of the "lid" over the active site in carboxylesterases (yellow residues) determined from normal mode calculations for (A) hCE1 and (B) hiCE homology model. The "lid" is oriented toward the bottom of each molecule. Arrows indicate the extent of motion for the entire enzyme for the lowest frequency mode (mode 7). The view is into the active site gorge. The active site residues Ser, Glu and His are shown in green. While the effect on catalysis of these loops is unknown, they may serve to bind substrate and guide it toward the active site gorge or to cover the active site to prevent diffusion of substrate out of the gorge before hydrolysis.

The idea for the indole-2,3-diones (isatin compounds; Figure. 1-3) was developed from this QSAR approach using biochemical data on the sulfonamide and benzil inhibitors. Our data suggested the presence of aromatic moieties were important for inhibition [86, 106]. Other earlier work found that there was a size constraint on the entrance to the active site gorge [80]. Using these two considerations as a parameter guide, a database search of commercially available compounds related to benzil was initiated, resulting in isatins as potential inhibitors of CEs. Simultaneously, a combination of QSAR and computerized model building using the sulfonamide data led to the prediction that indole-containing compounds would be CE inhibitors, and would also lead to selectivity for hiCE (Figure 4-3). This was ultimately borne out by analysis of 74 compounds related to isatin, and the discovery of several that were selective for hiCE [83], with inhibition constants as low as 6 nM. Below, we describe in detail the computational analysis that led to the predicted structures containing indole. Further, we describe the QSAR "grand model" that combines all compounds that we have evaluated for inhibition of CEs.

4.4.2 QUANTITATIVE STRUCTURE ACTIVITY RELATIONSHIPS (QSAR)

QSAR correlates the molecular structure and properties of a set of compounds with their activity. The parameters used for QSAR are molecular descriptors that can range from a simple count of atoms to HOMO and LUMO calculations; electronegativity; and other quantum molecular features. A QSAR model can also be modeled as a three-dimensional structure, which will show visually the nature of the relationship between the inhibitors and the receptor. QSAR has long been popular in assisting in the determination of essential interactions between the receptor and inhibitor. In our previous studies, almost all of the CE inhibitors have been

investigated through QSAR. These studies generated suggestions for improving the activities of inhibitor compounds (e.g., the addition of halogens, and inclusion of a larger aromatic moiety in the core of the inhibitor structure [27, 28, 112]).

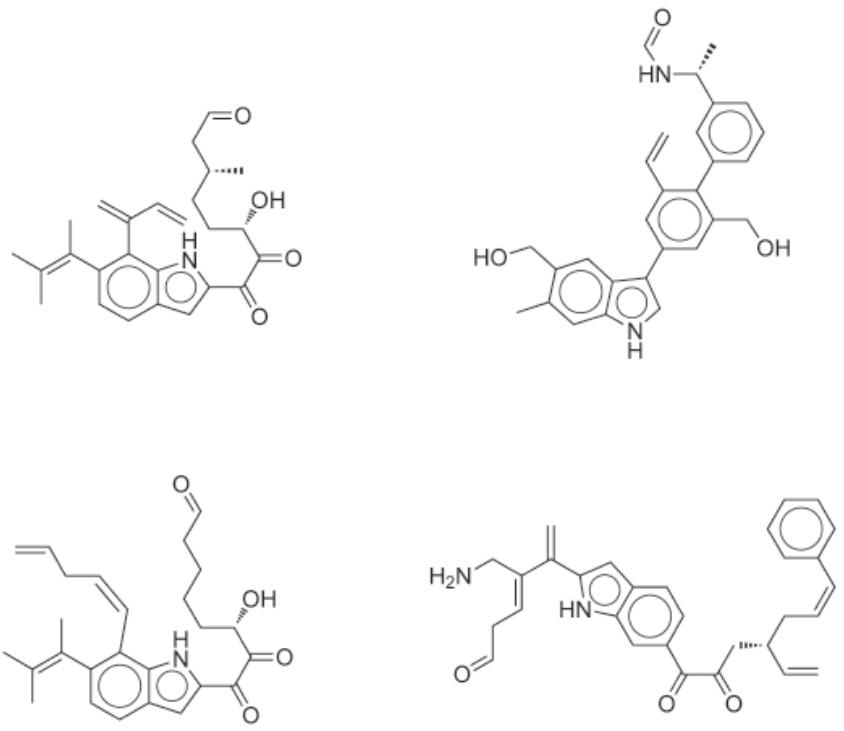

Figure 4-3. Selected indole-containing compounds originally predicted by the *de novo* design software LigBuilder to be good inhibitors of hiCE using a QSAR model based entirely on sulfonamides. The prediction led to discovery and evaluation of isatins [83].

QSAR reveals the important interactions between the ligands and the receptor site by using ligands that are known to be active inhibitors of the receptor of interest. The *de novo* design is an approach to structure-based drug discovery that utilizes a binding site pocket to build ligands specifically for the receptor [37, 113]. Common *de novo* design programs that are used today are GRID [39], SPROUT [41, 42], CONCERTS [38], SYNOPSIS [43], LeapFrog [40], and LigBuilder [37].

Using QSAR models as pocket sites for *de novo* design is an approach that can be utilized when no experimental receptor structure is available. Combining QSAR and *de novo* design has been used by several investigators [114-118]. For example, Gueto and coworkers [114] developed a CoMFA (Comparative Molecular Fields Analysis) model for aromatase inhibitors with 45 training set compounds and used a test set of 10 sulfonanilide compounds. This CoMFA model was used to generate new inhibitors *in silico* with the NEW module of LeapFrog, followed by calculation of their predicted activity. As another example, Kapou and coworkers [115] combined CoMFA and CoMSIA with LeapFrog to study and design steroidal mustard esters using a training set of 26 compounds and test set of 12 compounds. This model was then subsequently used to design new inhibitors using the OPTIMIZE module of LeapFrog.

CoMFA uses a grid-based approximation to develop 3D-QSAR models, and includes parameters such as steric and electrostatic effects by using both a Lennard-Jones and Coulombic potential. CoMSIA and LeapFrog also use a grid-based approximations to develop new compounds with good binding energies. In our laboratory, we have used the Quasar program [91, 92] to develop a 6D-QSAR model for hiCE inhibitors, and the *de novo* design program LigBuilder to generate new scaffolds of hiCE inhibitors (Table 4-1). The Quasar program is a grid-based technique as

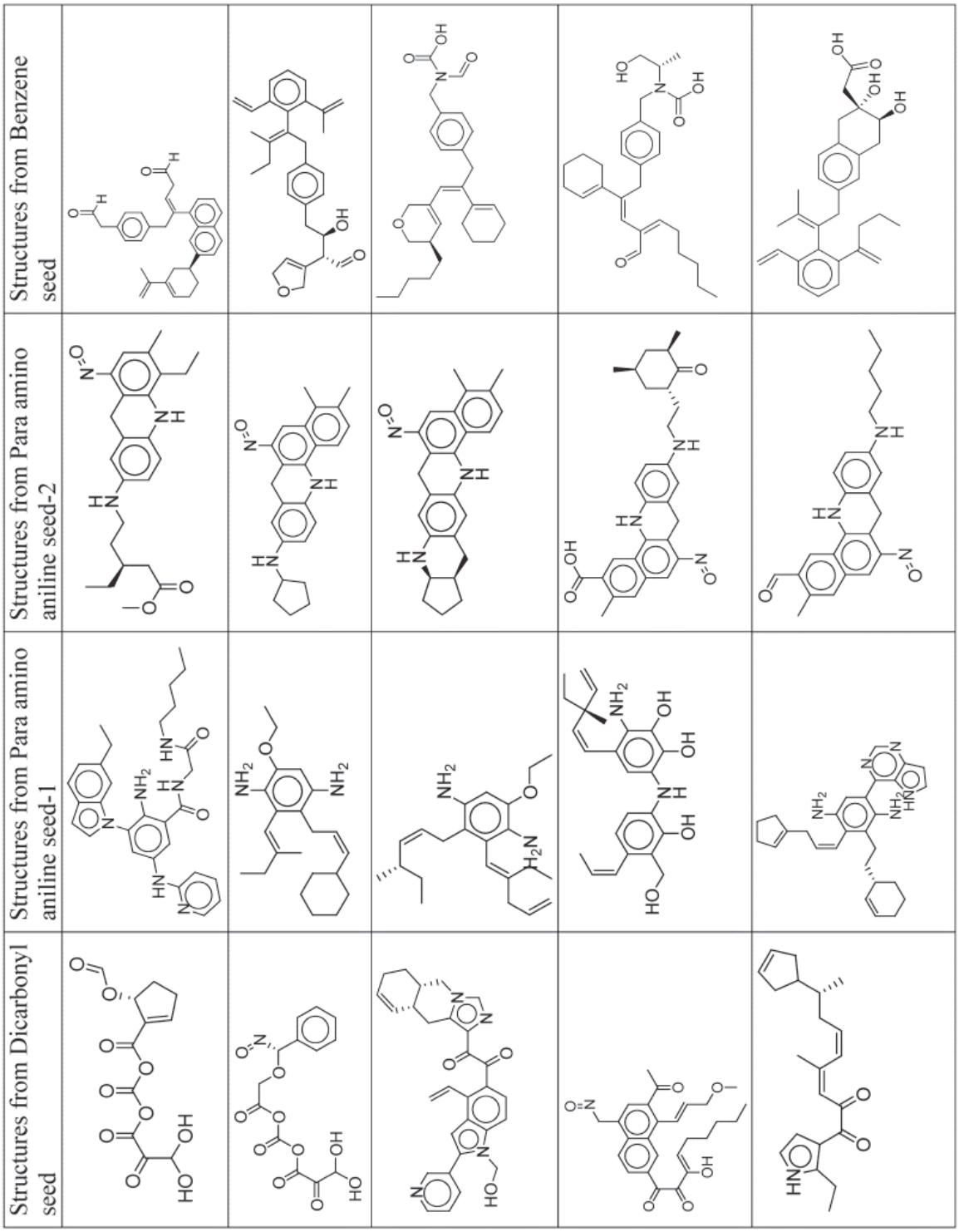

Table 4-1. Potential selective hiCE inhibitors output by LigBuilder using the QSAR structure shown in Figure 4-6. While many of these compounds are synthetically unfeasible, they do present a series of scaffolds that, combined with chemical intuition, may produce selective inhibitors in much the same way the isatins were discovered.

well, and it employs a genetic algorithm for model generation and induced fit. In addition of the 3 spatial dimensions of Quasar, the 4th dimension allows for analysis of different conformations of ligands (4D-QSAR), while the 5th dimension takes into account the potential for induced fit (5D-QSAR) [91]. The 6th dimension of Quasar added the ability to investigate different solvation effects (6D-QSAR) [119]. The following equation is used for calculation of binding affinity in Quasar.

$$E_{binding} = E_{ligand–receptor} - E_{ligand\ desolvation} + E_{ligand\ strain} - T\Delta S + E_{induced\ fit}$$

The term $E_{ligand–receptor}$ is calculated by the following equation,

$$E_{electrostatic} + E_{van\ der\ Waals} + E_{hydrogen\ bonding} + E_{polarization.}$$

Spreafico and coworkers have successfully used Quasar to develop models that include several classes of compounds [119]. Their data indicate that Quasar is effective when combining steroids, quinoline derivatives, fluorophenylindazole derivatives, and spirocyclic derivatives as inhibitors of glucocorticoid receptor.

The QSAR model developed in our study included sulfonamide, benzil, fluorobenzoin, and isatin inhibitors (Figure. 1-3). The TFKs were omitted because their mechanism of binding is different from the rest of these inhibitors, and requires a pre-incubation time to be most effective [85]. A more thorough investigation of TFK inhibition has recently appeared [112]. Our previous studies have used QSAR for development of pseudo-receptor site models in an effort to delineate pertinent information about the active site that could be useful in the design of new inhibitors [27, 28, 82, 83, 85, 86, 106]. However, these studies only somewhat used the pseudo-receptor site models for *de novo* design of potential inhibitors and were derived from limited data sets. Here we report our results on predicted structures using a "grand model" of CE inhibition based on data from 210 CE inhibitors comprising four inhibitor families. Our expectations were that

using this pseudo-receptor site as a hypothetical binding site might yield inhibitors other than indoles with improved drug-like properties (e.g., better water solubility).

The 6D-QSAR modeling of hiCE inhibitors was performed using Quasar 6.2 software running under Mac OS X. The 210 structures used included 4 diverse scaffolds; benzils, fluorobenzoins, isatins, and sulfonamides. Each analog had been previously drawn using Chemdraw, imported into Chem3D, and minimized first by using the MM2 molecular mechanics force field, followed by the PM3 semi-empirical method within MOPAC [90]. The solvation energies and charges were calculated using AMSOL and the SM5.42R solvation method [36]. SM5.42R is a rigid solvation model, which optimizes a compound's structure in the gas phase but optimizes only its electronic structure in the solvent phase. Gas phase charges were used for all QSAR analysis.

A training set of 133 compounds and a test set of 77 compounds were used to build the QSAR model. The K_i values that were used for these computations were those derived from the inhibition of o-nitrophenylacetate (*o*NPA) hydrolysis. As with any QSAR model that uses structurally divergent ligands, the complication in this process is the choice of how to align the structures with one another. We chose the central benzene ring of the sulfonamide inhibitors as the template to which all the other compounds would be aligned. The resulting 3D-pseudo-receptor site model describing the interactions between the active site and the ligands is shown in Figure 4-4, and is referred to as the "grand model" for hiCE inhibitors. The r^2 (squared correlation coefficient of model) and q^2 (predicted squared correlation coefficient, which describes the predictive quality of the model) generated were both 0.835, and the predicted vs. experimental $\Delta G°$ for inhibition constant values are shown in Figure 4-5. This QSAR model was

fairly robust in prediction of inhibitor binding, and therefore we used it as a template upon which to build new molecules.

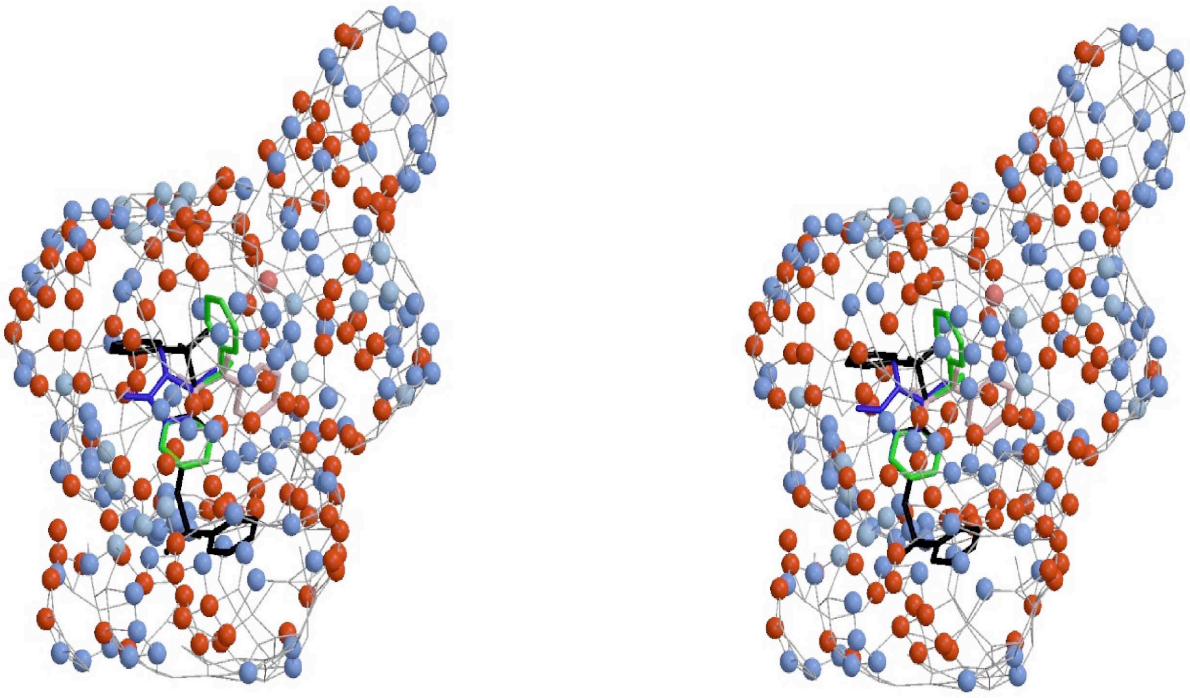

Figure 4-4. Stereo view of the 3-dimensional "grand model" for hiCE inhibitors is depicted as colored spheres on a hydrophobic gray grid. Areas that are hydrophobic are indicated in gray, whereas dark blue spheres represent areas that are positively charged (+0.25*e*) and light blue spheres correspond to lesser charge (+0.1*e*). Dark red spheres represent areas that are negatively charged (-0.25*e*), light red spheres indicate less negative charge (-0.1*e*). In all cases, *e* is the charge of the proton. The structure of representative sulfonamides (black), isatins (blue), benzils (green), and benzoins (pink) are shown. The Figure was generated using Molscript[120] and Raster3D [81] .

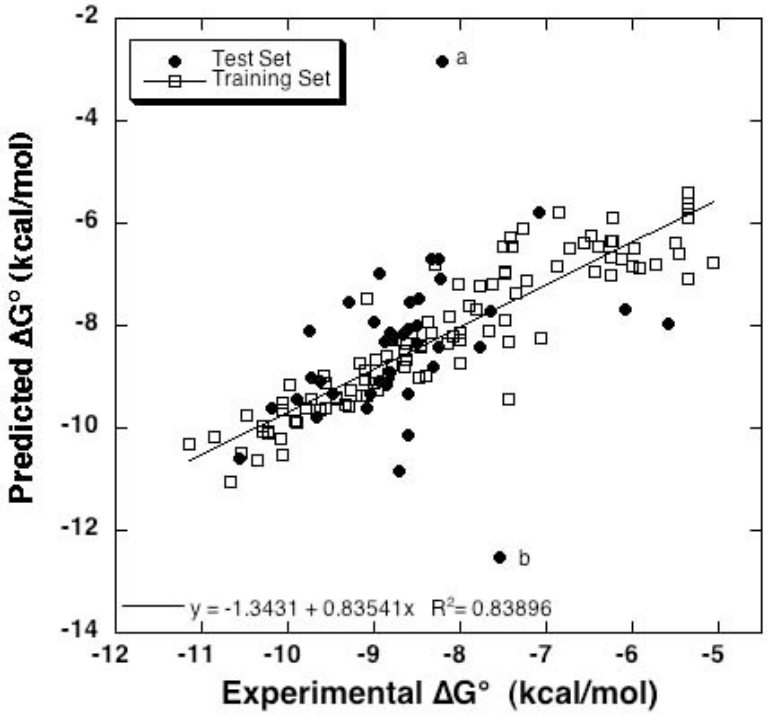

Figure 4-5. Predicted vs. experimental ΔG° values (in kcal/mol) for inhibition constants of 4 classes of molecules that inhibit the hiCE hydrolysis of o-nitrophenylacetate. K_i values were determined using a partially-competitive inhibitor model. The training set is indicated by the filled ovals, while the test set is represented by open boxes. The compound labeled "a" is a disulfide and is the lone member having this moiety. The compound labeled "b" is a 2,5-bis(trifluoromethyl) benzil analog. Its surprising lack of activity is under investigation. For clarity, compounds with K_i values > 100 μM are not included on this plot.

4.4.3 DE NOVO LIGAND DESIGN

The next step in the process was to have LigBuilder synthesize potential inhibitors based on the 3D-QSAR structure. LigBuilder begins with a user-defined seed structure that is the starting point for building new ligands by adding molecular fragments to the seed until the binding site is fully occupied. Each compound derived in this manner is evaluated via the Lipinski "rules" [121], and compounds violating these rules are rejected. LigBuilder uses an empirical scoring function to evaluate binding affinity, which is much different than that used by Quasar. LigBuilder alone has been combined with docking and pharmacophore modeling to design inhibitors for tyrosine kinase 2 [122], but to our knowledge has not been combined with QSAR models for lead compound development. To account for the other 3-dimensions of 6-D QSAR, the vertices of the model shown in Figure 4-4 were assigned pseudo-atomic properties within LigBuilder based on the corresponding property indicated in the legend of Figure 4-4. With this model as a hypothetical active site, potential inhibitors for hiCE were constructed from the seed structures 1,2-dione, p-aminoaniline, and benzene. For benzene, growth was allowed from all carbons in the ring. For p-aminoaniline, two seeds were used. The first allowed growth only from the amino group nitrogens, while the second allowed growth from both the amino groups and all unsubstituted ring carbons.

The results of this process are shown in Table 4-1 for the different starting seeds. Once the structures were generated, they were evaluated in the 6D-QSAR shown in Figure 4-4, and the top 5 ranked structures (lowest predicted K_i values) are shown. All of these computationally-derived structures were predicted to have good activities against hiCE, with free energy scores in the range of -10 to -13 kcal/mol (K_i from 46.7 nM to 0.3 nM). While only a select few compounds are shown in Table 4-1, over 40 new structural classes of inhibitors emerged from

this *in silico* process. These classes show new features such as large aromatic or planar groups attached to a long alkyl chain, the inclusion of a large part of the polar groups within cyclic ring systems, two aromatic groups joined together by a central alkyl group, and hybrid compounds that are a cross between two or more groups of inhibitors.

Table 1 also illustrates a problem with computer-generated ligands. Clearly, some of the predicted compounds are not feasible as biochemically active molecules, particularly the anhydrides that would be highly reactive with water. However, ignoring such unfeasible compounds, water solubility of most of the predicted structures using ALOGPS 2.1 indicated they have greater solubility than the sulfonamides, and many have solubility comparable to the anticancer drug irinotecan. This suggests that the solubility can be enhanced while maintaining or even improving the activity when a combined approach is used. Synthesis of a subset of these new classes of inhibitors is underway to verify the predicted results.

4.5 CONCLUSIONS

Over the last decade, QSAR has allowed a detailed analysis of known CE inhibitors and helped to generate CE inhibitors with greater specificity. As an example, tetrafluorine substituted sulfonamide analogs were synthesized when QSAR analysis of nine sulfonamides suggested the addition of halogens would increase potency [27]. The observed results concluded that this new inhibitor had greater selectivity for hiCE versus hCE1 than the previous nine. Another example is the fluorene sulfonamides [28], which were pursued because results from pseudo-receptor sites suggested that the active site of hiCE could accommodate a larger aromatic moiety. The fluorene sulfonamides proved to be much more potent than the structurally-similar benzene sulfonamide. The specificity was also not affected by inclusion of the fluorene moiety in the core. Hence,

QSAR (particularly, the 6D-QSAR methodology used by Quasar) is an invaluable tool for developing specific hiCE inhibitors.

While QSAR analysis has aided in the design to-date of more potent and specific inhibitors, it has not effectively addressed the issue that plagues most of the CE inhibitors designed theoretically: low aqueous solubility. The analysis and design described in this article suggest features of potential inhibitors that will increase their water solubility and yet retain or enhance potency. Further, our QSAR models are beneficial in understanding how the inhibitors are interacting within their binding site, which is presumed to be the enzyme active site. Such studies are useful in pointing toward optimization of lead compounds for structural scaffolds that may be discovered through means other than computer-generated structures.

PUBLICATION NOTICE

This work was published in the Journal of Pesticide Science in 2010

In Silico Design and Evaluation of Carboxylesterase Inhibitors, **Shana V. Stoddard**, Xiaozhen Yu, Philip M. Potter, Randy M. Wadkins. *Journal of Pesticide Science* 35 (2010) 240-249 – invited review

CHAPTER 5 COMBINING QUANTITATIVE STRUCTURE ACTIVITY ANALYSIS WITH *IN SILICO* DESIGN AND DOCKING TO DEVELOP NOVEL, SOLUBLE, SELECTIVE, AND SYNTHETICALLY ACCESSIBLE CARBOXYLESTERASE INHIBITOR SCAFFOLDS

5.1 ABSTRACT

Carboxylesterases (CEs) perform hydrolysis reactions, breaking down xenobiotics and metabolizing drugs. For example, the anticancer drug irinotecan is converted to its active form by the isozymes human carboxylesterase one (CES1, enriched in the liver) and human intestinal carboxylesterase (CES2, primarily enriched in the small intestine). CES2 converts CPT-11 to product 200 times faster than CES1, resulting in toxicity to the small intestinal epithelial. This cytotoxicity produces the dose-limiting side effect of delayed diarrhea. Selective inhibition of CES2 would promote better irinotecan distribution, increase irinotecan lifetime, and decrease its toxic side-effects. While in recent decades CES2 inhibitors have been developed, low water solubility has been an issue that prevents these potent inhibitors from use in the clinic. Many of these CEs also lack the appropriate selectivity. Therefore, we have used a triune approach to generate novel, potent, water-soluble, and selective CES2 inhibitors. We combined quantitative structure activity relationships with *in silico* design to generate new soluble inhibitors candidates

for CES2. Two of our previous QSAR models were used as hypothetical pocket sites for *de novo* design. Using the program LigBuilder1.2v, a library of 3100+ new compounds were generated *in silico* from 4 initial seed structures. The K_i score for each compound was predicted using the original multi-class QSAR model and the solubility predicted using the ALOGPS 2.1 program. We also developed a selectivity model to screen for selective CES2 inhibitors. In this chapter we present our experimental results for our top *in silico* generated scaffolds. Our results suggest that (*i.*) solubility can be increased while maintaining inhibitor potency, (*ii.*) inclusion of several classes of inhibitors aids in development of new drugable features, and (*iii.*) loop 7 plays a role in inhibitor selectivity.

5.2 INTRODUCTION

Carboxylesterases (CEs) are ubiquitous enzymes that carry out hydrolysis reactions of carboxylate ester functional groups. CEs play an important role in drug biodistribution of esterified drugs. In some cases they deactivate drugs, and subsequently decrease the amount of active metabolite *in vivo*; hydrolysis of flestolol is an example of this [74]. In other cases these enzymes activate pro-drugs *in vivo*; such as is the case with irinotecan, a front line chemotherapy drug for colorectal cancer [12, 17]. In the last decade, researchers have tried to develop selective CE inhibitors to abrogate the activity of the intestinal CE isozyme (CES2), which has been shown to produce the dose limiting side effect associated with irinotecan therapy [12, 17, 123]. Selective CES2 inhibitors would result in a myriad of benefits, namely, improving patient care through the reduction of intestinal cytotoxicity, reducing the dosage levels required to achieve the desired medicinal effect, increasing the lifetime of drugs deactivated by CES2, and improving biodistribution of drugs activated by CEs.

A variety of *in silico* methods have been shown to be useful in developing potent inhibitors for numerous biological targets, including CEs. Recently, Topai et al. used a pharmacophore model to screen the MoDa database for new gelatinase inhibitors [124]. In 2012 Qu et al. used docking to help create improved compstatin inhibitors and to explain experimental results [46]. Tanabe et al. also used docking to effectively design inhibitors for the α-glucosidase receptor [47]. From their docking insights, they generated novel compounds that introduced new interactions within α-glucosidase [47]. In 2004, Wadkins et al. reported the first class of CE isozyme specific compounds (the sulfonamides), and in 2005 reported the benzil scaffolds as mammalian specific CE inhibitors [27, 86]. Both the sulfonamides and benzils were originally identified using Telik's target related affinity profiling technique, then optimized using quantitative structure activity relationships (QSAR) studies. In 2007 Hyatt et al. identified a series of isatin compounds through database searching [83]. The sulfonamides and benzils were discovered to be potent CE inhibitors yet water insoluble (Table 5-1). The isatins possessed water solubility, but in general, had moderate potency and lacked appropriate CE selectivity (Table 5-1). We can see that there is a broad range of the average CES2 inFhibitor activity (range 34 nM to 15665 nM)

CE inhibitor class	**Average Solubility (mg/L)**	**Average K_i (nM)**
Sulfonamides	7	(Benzene Sulfonamides) 746 (Fluorene Sulfonamides) 34
Benzils	15	209
Isatins	1000	15665
Fluorobenzoins	9000	457

Table 5-1: CE Inhibitor Solubility and K_i

Poor water solubility is a persistent problem in drug development altogether [125, 126], resulting in many drug candidates not reaching the market. One problem that plagues selective CES2 inhibitor development is the fact that there is an inverse correlation of LogP with potency, rendering most selective potent compounds insoluble [28]. The solubility problem is often overcome by chemical intuition on the part of the researcher [127-130]. Guantai et al. used chemical intuition to develop enone- and chalcone-chloroquinoline hybrid analogs having antiplasmodial activity [129]. By replacing the triazole linker with an aminoalkyl- or piperazinyl-based linker, they improved the solubility by increasing the polarity of the compound. In 2009, Emmitte et al. designed thiophene inhibitors for polo-like kinase 1 with improved solubilities by introducing an amine polar group on the compound [130]. In 2010 Young et al. also used the addition of a polar functional group to enhance solubilities of a series of CE inhibitor compounds. They replaced one of the phenyl rings of benzil with a pyridine group enhancing the solubility relative to benzil [131]. Yoshizawa et al. improved the solubility of an angiogenesis inhibitor SU5416 by formulating the inhibitor in a pegylated O/W emulsion [132]. Ohashi et al. reduced the planarity of a pyrrolo[3,2-*c*]pyridine derivative (a hedghog signaling inhibitor) to improve the solubility compared with the parent compound [128]. While many individuals have successfully enhanced the solubility of a series of compounds, *in silico* methods are not typically employed to addresses this problem. Visentin et al. have attempted to use QSAR and chemical intuition to enhance solubility of existing 1,4-dihydropuridine scaffolds [127]; however, this model was not extremely successful. A computational method that could be employed to enhance solubility would greatly benefit the drug design society.

In the last chapter we hypothesized that the water insolubility of the CE inhibitors could be addressed by using a dual method approach of QSAR coupled with *in silico* design. We also

hypothesized that the inclusion of multiple classes of CE inhibitors in the development of the QSAR model would aid in the generation of scaffolds that had more drugable features. We were successful in proposing compounds that maintained predicted potency yet enhanced predicted solubility; however many compounds were synthetically inaccessible and experimental validation of the method was not performed. In this chapter we have generated several new CE scaffold candidates and experimentally tested 1 scaffold and 4 scaffold precursors. We have also compared the results of this approach using our multi-scaffold QSAR model against the results gathered using the singular class sulfonamide scaffold QSAR model.

In addition to developing soluble scaffolds, understanding the molecular details contributing to inhibitor specificity between CEs would also significantly improve our ability to rationally develop inhibitors and/or drug candidates. Computational modeling had been performed on many classes of CE inhibitors to describe their potency as inhibitors, but never to predict which isozyme receptor they would favor. The development of a predictive model for inhibitor selectivity would also aid in teasing out compounds with inappropriate selectivity. The residue composition of loop 7 varies between CES1 and CES2 (Table 5-2). We hypothesized that the structural variances of loop 7 between the CES1 and CES2 played a role in selection of inhibitors. In this chapter, we investigated the contribution of the loop 7 in CEs to sensitizing the enzyme to inhibition by sulfonamide inhibitors through a combination of homology modeling, docking and kinetics. Our results suggest that the inner loop 7 on CE plays a role in inhibitor selectivity, and interactions with this loop should be considered in the development of selective CE inhibitors.

Residue #	101	102	103	104	105	106	107	108	109	110	111	112	113	114	115	116	117	118	119
pnbCE	*Val*	*Trp*	*Ile*	*His*	*Gly*	*Gly*	*Ala*	*Phe*	*Tyr*	*Leu*	*Gly*	*Ala*	*Gly*	*Ser*	*Glu*	*Pro*	*Leu*	Tyr	Asp
CES1	Val	Trp	Ile	His	Gly	Gly	**Gly**	**Leu**	**Met**	**Val**	Gly	Ala	**Ala**	*Ser*	Thr	Tyr	Leu	Tyr	Asp
CES2	Val	Trp	Ile	His	Gly	Gly	Ala	**Leu**	**Val**	**Phe**	Gly	**Met**	**Ala**	Ser	Leu	Tyr	*Leu*	Tyr	Asp

Table 5-2: Loop 7 rsesidue variations between pnbCE, CES1, and CES2. Loop 7 residues are numbers 104 to 116.

5.3 RESULTS

5.3.1 SCAFFOLDS GENERATED FROM LIGBUILDER 1.2v DE NOVO GENERATION PROGRAM

We used both our 2009 sulfonamide QSAR model (SM) [28] and our 2010 grand model (GM) [133] developed from multiple classes of CE inhibitors as hypothetical pocket sites, to test our hypothesis that the predicted water insolubility of the CE inhibitors could be overcome by using a dual method approach of QSAR coupled with *in silico* design. The development and evaluation of these models can be found in chapters 3 (SM) and 4 (GM).

Scaffolds generated from the SM were compared to scaffolds generated from the GM, to test the hypothesis that the inclusion of multiple classes of CE inhibitors, in developing the QSAR model, aided in generation of more drugable features *in silico*. Compound generation was restricted to Lipinski rules (MW < 500; LogP < 5, Number of hydrogen donors < 5, and number of hydrogen acceptors < 10), a parameter not used in our previous 2010 study, to aid in solubility enhancement. A total of 3167 compounds were generated using LigBuilder 1.2v, consisting of 196 distinct scaffolds. We used the following criteria to narrow down our dataset.

Compounds with a solubility of > 50 mg/L, and having an activity (CES2 inhibitory potency) of less than -7.0 kcal/mol, were pooled into our hit database. Fifty milligrams per liter was chosen as the solubility cutoff because it is an improvement relative to the sulfonamide scaffold solubility of 7 mg/L. The activity score cutoff was chosen to generate compounds that also maintained CES2 potency. Figure 5-1 shows examples of the types of scaffolds generated. Of the 196 scaffolds outputted, scaffolds 112, and 126 were selected for further investigation.

5.3.2 COMPARISON OF COMPOUNDS GENERATED WITH THE SULFONAMIDE MODEL VERSUS COMPOUNDS GENERATED WITH THE GRAND MODEL

The solubility of each compound was calculated first using the ALOGPS program. We found that 136 compounds showed improved solubility compared to that of the sulfonamide inhibitors. The GM generated 66 compounds encompassing 13 different scaffold classes. The SM generated 70 compounds having 18 different scaffold classes.

The activity of each compound was predicted by using the initial QSAR "grand" model [133]. The grand model has a q^2 of 0.835; thus this model has goodness of predictability. Fifty-nine compounds either maintained activity or showed improved activity compared to the previous generations of CE inhibitors (determined by ΔG^o score < -7.00). From the grand model we generated 29 compounds consisting of 7 scaffolds having improved solubility and potency. The sulfonamide model outputted 30 compounds having improved solubility and potency consisting of 13 scaffolds of molecules.

Our goal was to identify scaffolds, which could be substituted easily, that already had inherent solubility themselves. We did not want to pursue compounds whose solubility was a property conferred to them by the addition of substituents. Thus the solubility of the remaining

Seed 1 Compounds		Seed 2 Compounds		Seed 3 Compounds		Seed 4 Compounds	
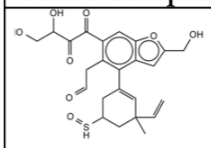		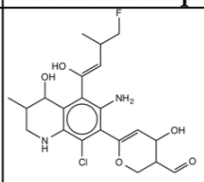		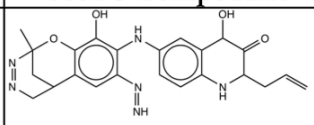		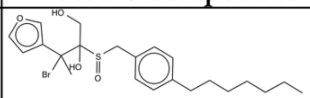	
70.1 mg/L	-6.335	277.6 mg/L	-7.903	87.4 mg/L	-8.745	100.7 mg/L	-8.807
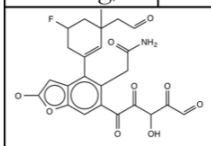		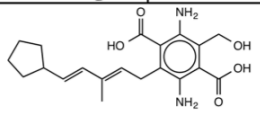		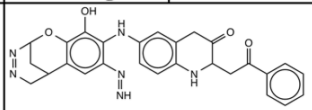		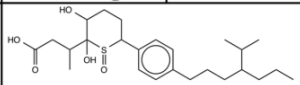	
53.3 mg/L	-6.136	56.6 mg/L	-8.921	61.0 mg/L	-8.974	139.7 mg/L	-7.172
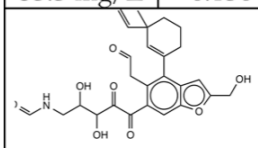		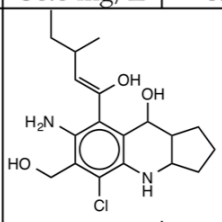		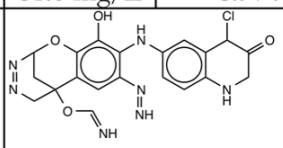		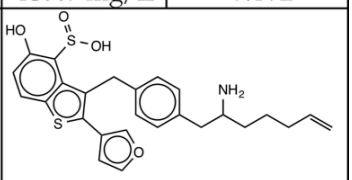	
50.5 mg/L	-3.262	167.3 mg/L	-7.349	97.3 mg/L	-5.776	51.6 mg/L	-5.056

Figure 5-1: Examples of compounds generated from grand model using LigBuilder 1.2v program. Corresponding solubility (given in mg/L) and ΔGº score (given in kJ/mol) for each compound are listed below the structure.

20 scaffolds was assessed to identify soluble scaffolds (Table 5-2 and Figures 5-2 and 5-3). Nine scaffolds produced had improved solubility (≥ 50 mg/L). Eight of these scaffolds had solubilities greater than 150 mg/L. Of these nine the SM produced 2 scaffolds having decent solubility, while all seven of the remaining scaffolds generated from the GM had improved solubility Table 5-2. Of the remaining 9 scaffolds, those having solubility < 490 mg/L and scaffolds not easily synthetically accessible were eliminated. This resulted in a final dataset of two scaffolds, 112 and 126, both generated from the GM. The rest of this chapter will discuss these scaffolds.

Table 5-2: Comparison of Scaffolds Solubilities from SM and GM		
Model Used	**Scaffold ID**	**Predicted Solubility (mg/L)**
GM	101	910
GM	102	1460
GM	103	220
GM	112	490
GM	126	1720
GM	106	190
GM	107	62
SM	B –series	7.39
SM	C –series	7.87
SM	D –series	6.67
SM	E –series	200
SM	F –series	24.94
SM	G –series	7.35
SM	H –series	1.04
SM	I –series	150
SM	J –series	1.27
SM	K –series	0.83
SM	L –series	2.07
SM	M –series	1.22
SM	N –series	1.36

Table 5-2: Comparison of Scaffolds Solubilities from SM and GM

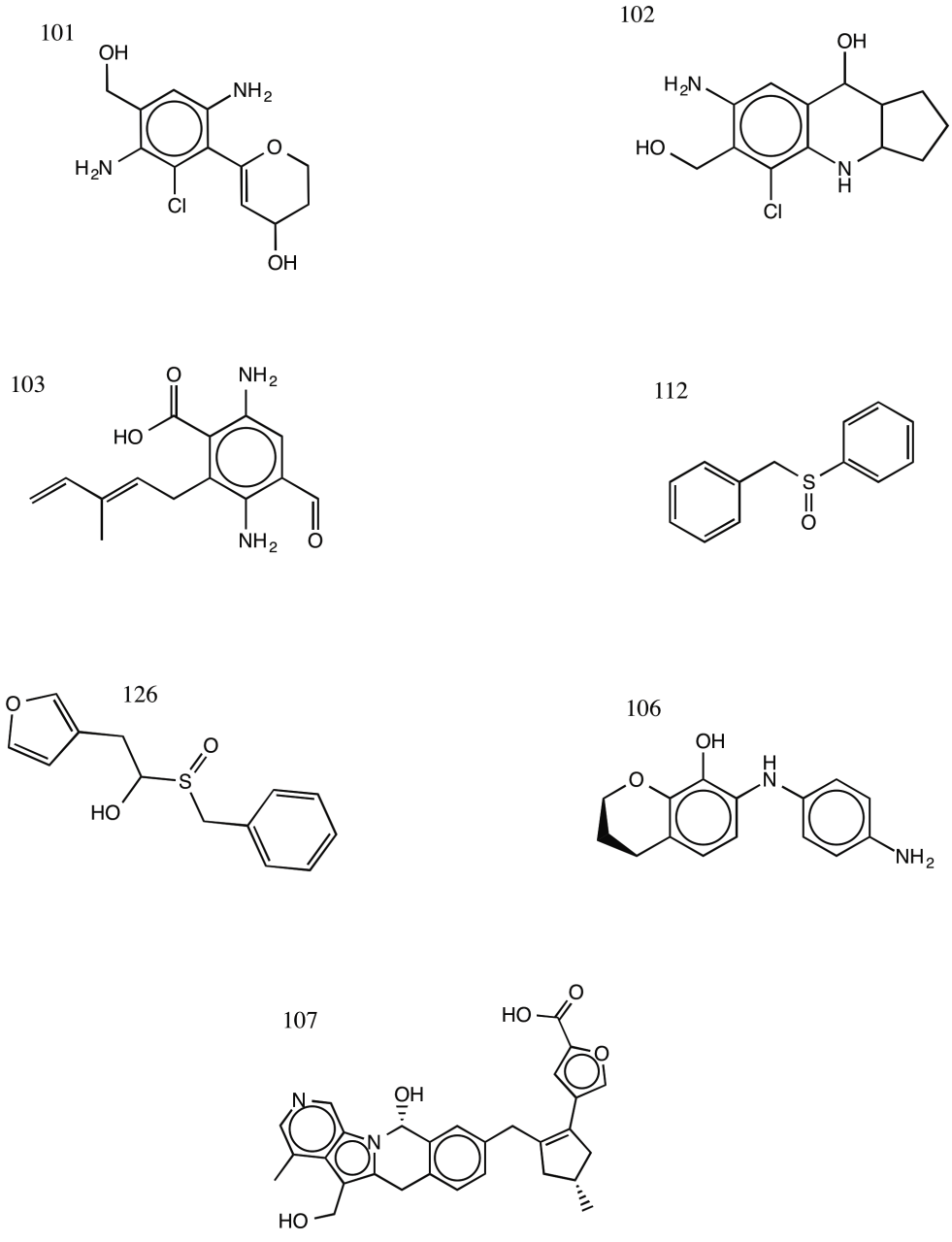

Figure 5-2 Scaffolds generated from the GM

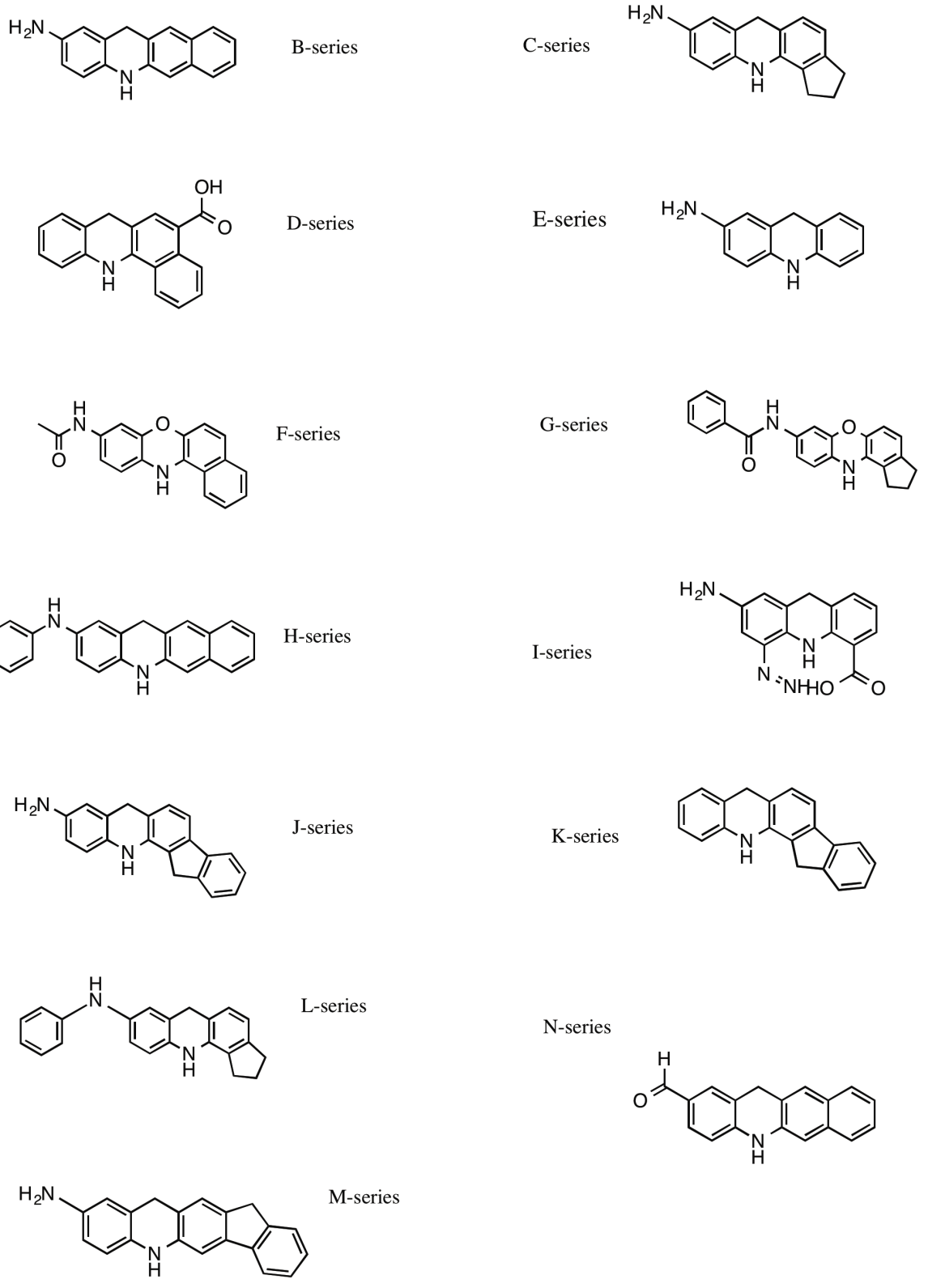

Figure 5-3 Scaffolds generated form the SM

5.3.3 SCAFFOLD 126; 1-(BENZYLSULFINYL)-2-(FURAN-3-YL)ETHANOL

Scaffold 126 contains both a furan ring and a phenyl ring, which are connected by an ethane sulfinyl linker. The ethane portion of the compound is located toward the furan ring and the sulfinyl moiety is benzylic to the phenyl ring. Our QSAR model predicts that scaffold 126 has an inhibition activity of 1131 nM. The solubility for 126 is predicted to be 1720 mg/L respectively. Fourteen analogs were generated having the 126 scaffold. We designed simple analogs of these compounds, A13, A14, A15, and A16.

We were unable to find a synthetic scheme for our 126 scaffold; however, we did find a synthesis for the 126 scaffold precursor ((ABUS) alpha/beta unsaturated sulfoxides) in the patent US 7,744,889 B2 (Scheme 5-1). Briefly, this synthesis is performed by first executing a Williamson ether synthesis to generate a thiolether, followed by a sulfoxidation reaction to form sulfinyl acetic acid on a benzylic chloride analogs. Lastly, a Knoevenagel condensation reaction with aldehyde analogs will generate the alpha/beta unsaturated sulfoxide (126 precursor compound).

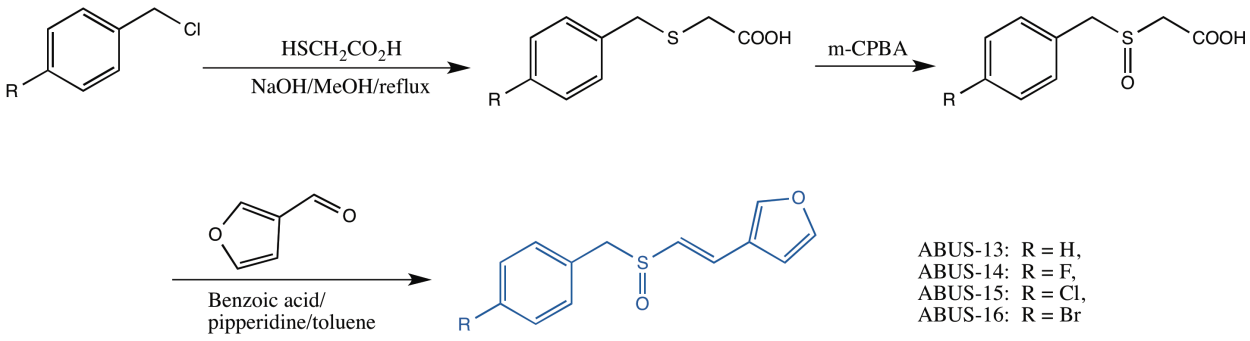

Scheme 5-1. Synthetic scheme for alpha/beta unsaturated sulfoxide (126 precursor) scaffold

Our goal was to use our models to identify scaffolds or point us to scaffolds that had drugable features. While the 126 scaffold was not easily accessible, the ABUS were. Thus, we predicted the activities and solubilities of these scaffold precursors to test our models. It can be seen that the scaffold precursor does not have as significant potency or solubility as the 126 analog; however, there is still marked improvement by 2 orders of magnitude in the solubility of these compounds relative to the sulfonamides (7 mg/L) and in some of the overall CES2 potency considering the broad range of average CES2 inhibitory potency (34 nM to 15665 nM).

126 Scaffold Analog	**nM**	**Solubility (mg/L)**
A13	1550	1720
A14	2280	1700
A15	1130	630
A16	1340	830
Corresponding Scaffold Precoursor		
ABUS-13	8730	940
ABUS-14	5310	150
ABUS-15	6350	160
ABUS-16	10900	320

Table 5-3: Predicted solubility and K_i of 126 analogs and ABUS analogs

5.3.4 SCAFFOLD 112 (BENZYLSULFINYL)BENZENE

Scaffold 112 is (benzylsulfinyl)benzene. LigBuilder designed 114 analogs of scaffold 112. Our previous attempt at producing compounds with enhanced water solubility generated several compounds that were synthetically unfeasible. Thus, this attempt was performed in an effort to overcome this issue. Scaffold 112 was found to be commercially available. Analogs of the 112 scaffold have substituted phenyl and or benzyl rings. The synthetic Scheme shown in scheme 5-2 can be used to develop 112 analogs. The thiolether will be created in step one, using a Williamson ether type synthesis, followed by a sulfoxidation reaction, using MCPBA, to yield the final analog structure. Benzenethiol, benzyl bromide and several analogs of these compounds can be purchased from Sigma Aldrich.

We could find no reported activity of this specific scaffold in carboxylesterases for inhibition, or details of them as substrates. For CES, similar compounds have been reported to be substrates for a modified thermolysin, a bacterial zinc dependent protease, which performs hydrolysis reaction of peptide bonds with hydrophobic amino acids [134]. A sulfonamide scaffold (Figure 5-2) similar in structure to 112 was found to be an inhibitor for the matrix metalloproteinases, another member of the protease family [135]. Finally, this scaffold is similar to the benzil analogs (Figure 5-2), which are used as mammalian carboxylesterase inhibitors [84, 86].

The 112 scaffold had a predicted inhibition of 40 μM, and a solubility of 490 mg/L. Dr. Potter's lab his found this scaffold experimentally to have an activity of < 4% at 100 μM. The 112 scaffold analogs developed by LigBuilder possessed much stronger inhibition values, in the subnanomolar range.

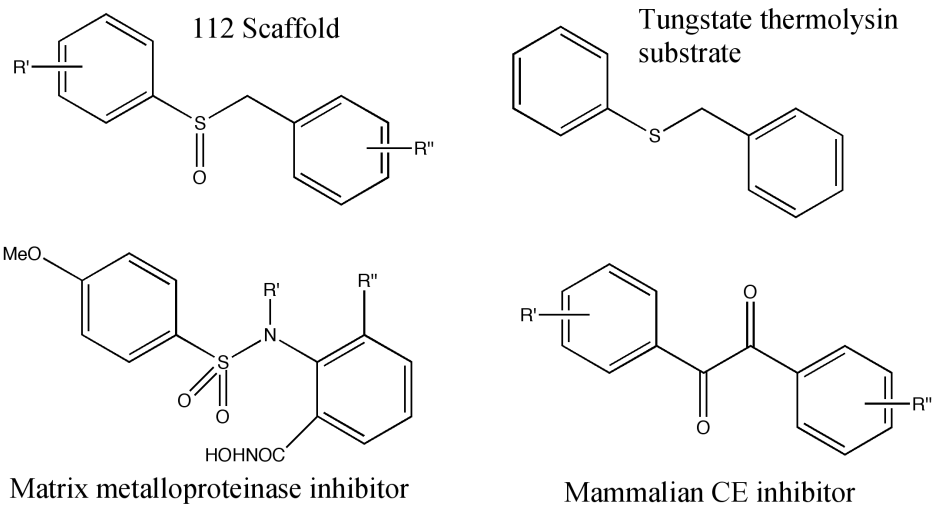

Figure 5-4. Scaffolds similar to 112 that have biological activity against proteins in the alpha/beta hydrolase family

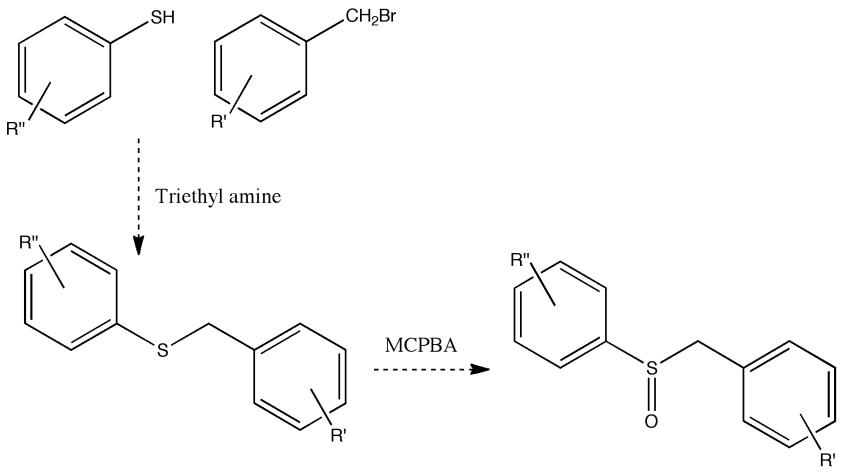

Scheme 5-2. Synthetic scheme for scaffold 112

5.3.5 DOCKING OF SULFONAMIDE CES2 INHIBITORS INTO PNBCE, PNBCE-CES1-LOOP7-MUTANT AND PNBCE-CES2-LOOP7-MUTANTS RECEPTORS

To test our hypothesis that loop 7 contributes to CE inhibitor selectivity, we developed pnbCE mutant homology models, where the loop 7 of pnbCE was substituted with either the loop 7 of CES1 or CES2. The homology models were developed using the MODELLER program. Forty-two sulfonamides were docked into the homology models to determine whether the model could accurately predict their selectivity. In our internal test set, thirty-seven sulfonamides were experimentally found to be selective CES2 inhibitors. Five sulfonamides in the dataset were experimentally shown to have no selectivity between CES1 and CES2. The average difference between receptors was 2.46 kJ/mol in favor of the CES2 mutant receptor (Table 5-4).

Molecule	CES1 Average Dock Score	CES2 Average Dock Score	Difference	Preference
Sulfonamides	-46.55	-49.01	2.46	CES2

Table 5-4: Average docking score of sulfonamide inhibitors

5.4 DISCUSSION

5.4.1 EFFECT OF INCLUDING SEVERAL INHIBITOR SCAFFOLDS INTO QSAR MODEL DEVELOPMENT

We originally hypothesized that including multiple CE inhibitor classes in the development of the QSAR model used for *in silico* design would significantly aid in generating scaffolds with more drugable features, namely enhanced solubility. The SM produced more compounds than the GM. However, after filtering through the compounds produced, the GM

generated more soluble scaffolds. In fact all the scaffolds generated from the GM had improved solubility. Six of the seven scaffolds showed solubility improvement of two to three orders of magnitude compared to that of the sulfonamide scaffold (7 mg/L). In contrast, 10 of the 13 scaffolds outputted from the SM failed to have any solubility enhancement. Six scaffolds actually showed decreased solubility compared to the sulfonamide scaffold. The GM was the only model that generated scaffolds having gram level solubility. This result shows that a multi-class QSAR model as a template for *in silico* generation can produce highly water-soluble scaffold leads.

A combination of factors allows our method to produce novel and soluble inhibitors. We use the program Quasar to develop our QSAR models. Quasar has multiple dimensions most notably the 6th dimension, which factors in solubility. The GM, which was developed using four CE inhibitors classes, was able to capitalize on the best features of each class of inhibitors. The sulfonamides, fluorobenzoins, and benzils have high potency toward CES2, enabling the model to produce compounds having comparable potency against CES2. The isatins and fluorobenzoins, which in general are less specific for CES2, have high solubilities of 1000 mg/L and 9000 mg/L respectively. Thus, including them in the model allowed us to draw from the solubility of these less specific CE inhibitors. The SM generated scaffolds with solubility equivalent to that of the sulfonamides. Since the sulfonamides were the only class included in developing this QSAR model the SM was unable to take advantage of the solubility properties of the other CE inhibitors. Therefore, when generating compounds using the SM, we generated compounds that had features similar to the sulfonamides.

Our 112 scaffold was synthetically accessible and commercially available, illustrating this dual method approach's ability to design compounds that are accessible. We did find that

obtaining the original 126 scaffold was more difficult, as it could not be purchased; however, this scaffold did lead us to the alpha/beta unsaturated sulfoxide scaffold that had reasonable properties (decent potency, solubility, and selectivity) which can be optimized. Therefore we believe that this process was a success overall.

The sulfonamide compounds were shown to favor the pnbCE-CES2-loop7 receptor, supporting the hypothesis that loop 7 plays a role in inhibitor selection. By expanding this model further, to include other regions of importance, we may be able to use this as a predictive model to determine selectivity.

5.5 CONCLUSION

Including several classes of inhibitors is shown to significantly aid in developing scaffolds with enhanced water solubility. While the model is capable of producing promising compounds that have the potency and solubility we desire, the inclusion of the less specific inhibitors could potentially mean that the scaffolds we generate are not specific for the isozyme we desire. However we believe that the inhibitors will have CES2 inhibitory potency. Thus an external model capable of predicting the selectivity of our compounds generated from this dual method would be ideal.

We have shown in this work that loop 7 is another important factor in determining inhibitor selectivity. Our first generation model for selectivity determination of CE inhibitors can be used to help predict the selectivity of untested CE inhibitors compounds. This model however could be improved by further expanding it to entail the other important regions necessary for inhibitor selectivity.

5.6 EXPERIMENTAL

5.6.1 MULTI-DIMENSIONAL QSAR MODELING OF THE SULFONAMIDE MODEL AND THE GRAND MODEL

The SM and the GM QSAR models were developed as previously described in Chapters 3 and 4.

5.6.2 *IN SILICO* DESIGN OF NEW CARBOXYLESTERASE INHIBITORS USING LIGBUILDER

We used our QSAR model as a hypothetical pocket site for *in silico* generation of novel hiCE inhibitors using the GROW module in LigBuilder 1.2v[37]. The atomistic properties of the model were assigned pseudoatomic properties within LigBuilder based on the corresponding property. With this model as a hypothetical pocket site, potential inhibitors for hiCE were constructed from the seed structures 1,2-dione, p-aminoaniline, and benzene. For benzene, growth was allowed from all carbons in the ring. For p-aminoaniline, two seeds were used. The first allowed growth off only the amino group nitrogens, while the second allowed growth off both the amino groups and all unsubstituted ring carbons. The 1,2-dione seed was allowed to grow off both terminal hydrogens. Seeds 1 through 3 were chosen because of their similarity to the core of the sulfonamide analogs. Seed 4 was chosen because the dicarbonyl moiety was found to be important in inhibition of hiCE. The GROW module of the LigBuilder program takes a seed structure, with designated growth points, and attaches new structural fragments onto those growth points. The growth is dictated by identifying fragments that will have the strongest interaction (binding affinity) possible to the receptor at the attachment site. In LigBuilder the binding affinity is calculated by SCORE an empirical scoring function. An example GROW

GROW command file is included in the Appendix. As indicated before, Lipinski's rules were accounted for in this process. Typically, two hundred new compounds are produced per seed, and then ranked. Scaffolds were selected by defining the largest core structure within a family of analogs.

5.6.3 PREDICTION OF INHIBITION SCORES USING GRAND MODEL, AND SOLUBILITIES USING ALOGPS

The previous QSAR model developed was used to predict the activities of the generated compounds. The charges and solvation energies of the generated compounds were calculated using AMSOL 7.1 as previously described**.** Minimizations and alignment of generated compounds was unnecessary since compounds were generated from pre-aligned seed structures, thus not performed. To predict the aqueous solubility the 3D structures in the MOL2 files were converted into SMILES strings to be read into the online server at VCCLAB. The aqueous solubility of all compounds was predicted using the online server ALOGPS program (http://www.vcclab.org) [44, 45].

5.6.4 CE INHIBITION ASSAY OF INHIBITOR CANDIDATES

CE inhibition assays were performed as previously done in [28].

5.6.5 ALIGNMENT OF ALPHA BETA HYDROLASES BY PROTEIN SEQUENCE

Using the DALI pairwise comparison program [136], hCE1 and hiCE were aligned to pnbCE to deteremine corresponding residues for loop 7.

5.6.6 HOMOLOGY MODELING OF PNBCE-CES1-LOOP7 AND PNBCE-CES2-LOOP7 MUTANTS

Homology models of the pnbCE-CES1-loop7 mutant and the pnbCE-CES2-loop7 mutant were generated using MODELLER. Protein fasta sequence were modified then imported into Chimera, after which a BLAST search was performed. The pnbCE wild type structure was chosen as the template structure (pdb: 1QE3). MODELLER was the used to develop 5 homology models. The model with the lowest ZDOPE score was chosen as the docking receptor.

5.6.7 DOCKING ANALYSIS OF SULFONAMIDE INHIBITORS

Computational evaluation can delineate important interactions between the inhibitors and receptors, where mechanisms of inhibition and sites of interactions are unknown. Docking is a technique that has been performed for many biologically-important receptors [137], [54]. It is used here to predict the interactions between pnbCE-wild type, pnbCE-hiCE-loop7-mutants, pnbCE-hCE1-loop7-mutant, hCE1-wild-type and the ten most selective sulfonamide inhibitors, suggesting the inhibitor's binding mode(s).

Using the Marvin Sketch program (Chem Axon), compounds were converted from 2D to 3D structures, after which an initial structural energy minimization was performed using the energy gradient optimization method. Chimera (UCSF [138]) was then used to perform a full structural minimization (using steepest decent followed by conjugate gradient), to calculate total charges on the molecules, and to add all remaining hydrogens not explicitly defined in the 2D structure. DOCK 6.3 was then used for all docking analyses. The success rate, which the percentage of generated conformations that have a heavy atom RMSD equal to or less than 2 Å of the crystal structure pose, for DOCK (70%) is comparable to FlexX (61%), Glide (82%), and GOLD (77%)

[139, 140]. Default parameters were used throughout the flexible docking analysis, with the exception of number of orientations, which was varied through the course of several docking simulations (500 orientations evaluated). The pnbCE-wild type, pnbCE-CES1-loop7-mutants, pnbCE-CES2-loop7-mutant, hCE1-wild-type receptors were used. The active site was identified by aligning each receptor to pnbCE receptor used or MD simulation that included the pNV molecule in the active site. The protein chain from the MD simulation was then deleted leaving the pNV molecule in the active site of the docking receptor. We generated all molecular graphics images using the UCSF Chimera package.

PUBLICATION NOTICE

This work was submitted to Journal of Medicinal Chemistry in 2013

CHAPTER 6 INSIGHTS AND IDEAS GARNERED FROM MARINE METABOLITES FOR DEVELOPMENT OF ACETYLCHOLINESTERSE AND AMYLOID-β AGGREGATION INHIBITORS

6.1 ABSTRACT

Due to the diversity of biological activities that can be found in aquatic ecosystems, marine metabolites have been an active area of drug discovery for the last 30 years. Marine metabolites have been found to inhibit a number of enzymes important in the treatment of human disease. Here, we focus on marine metabolites that inhibit the enzyme acetylcholinesterase, which is the cellular target for treatment of early-stage Alzheimer's disease. Currently, development of anticholinesterase drugs with improved potency, and drugs that act as dual acetylcholinesterase and amyloid-β aggregation inhibitors, are being sought to treat Alzheimer's disease. Seven classes of marine metabolites are reported to possess anti-cholinesterase activity. We compared these metabolites to clinically-used acetylcholinesterase inhibitors having known mechanisms of inhibition. We performed a docking simulation and compared them to published experimental data for each metabolite to determine the most likely mechanism of inhibition for each class of marine inhibitor. Our results indicate that several metabolites use mechanisms of inhibition not currently employed in the clinically-used drugs rivastigmine, galanthamine, donepezil, or tacrine. These new mechanisms may be useful in rational drug design of tighter binding

anticholinesterase drugs, or even development of inhibitors with both acetylcholinesterase and amyloid-β aggregation inhibition properties.

6.2 INTRODUCTION

6.2.1 INTRODUCTION TO ACETYLCHOLINESTERASE STRUCTURE AND FUNCTION

Acetylcholinesterase (AChE) is a member of the α/β hydrolase fold family of enzymes [94]. This enzyme degrades the excitatory neurotransmitter acetylcholine (ACh) in the synaptic junction at an extraordinarily fast catalytic rate, with a 2nd order rate constant almost as fast as a diffusion-controlled reaction [141, 142]. ACh is degraded to choline and acetate through a hydrolysis mechanism, resulting in decreased signal transmission in nerve synapses.

In 1991, using X-ray crystallography, Sussman's lab elucidated a 2.8 Å resolution structure of AChE, from the *Torpedo californica* electric ray [143]. Two sites participate in the hydrolysis reaction of ACh: an anionic site and an esteratic site. The anionic site draws ACh into the active site, followed by hydrolysis in the esteratic site. The catalytic triad (Ser-200, Glu-327 and, His-440) resides at the bottom of a 20 Å gorge. This long, narrow gorge contains 14 conserved aromatic residues (e.g., Tyr-70, Trp-84, Tyr-121, Trp-279, Phe-288, Phe-290, Phe-330, and Tyr-334) leading to the active site [144]. Residues Phe-288 and Phe-290 and the catalytic triad create the esteratic site. Residues Trp-84 and Phe-330 are located in the anionic site [144]. Approximately 14 Å away from the anionic site is another negatively charged site called the peripheral anionic binding site (PAS), composed of residues Tyr-70, Asp-72, Tyr-121, Trp-279, and Tyr-334. Binding of substrates and inhibitors to the PAS causes a conformational change to

AChE, reducing ACh's ability to enter the active site [144, 145]. A schematic of AChE is shown in Figure 6-1.

Acetylcholinesterase is the drug target for treating the neural degenerative disorder Alzheimer's disease (AD). AD in elderly individuals is characterized by memory loss, difficulty in storing new information, and behavioral and cognitive difficulties [146, 147]. The progressive nature of AD can require a high level of care since patients lose the ability to perform simple daily functions.

There are two hypotheses to explain the pathology of AD. One suggests that the decrease in ACh production within the synaptic junction contributes to the onset of AD (cholinergic hypothesis) [148-150]. The other suggests that the development of toxic amyloid-β peptide aggregates in the brain contributes to the progression of AD a (Amyloid hypothesis) [148, 151]. The cholinergic hypothesis suggests that inhibition of AChE can result in improved cognition by increasing ACh activity. The amyloid hypothesis suggests that drugs that inhibit amyloid plaque formation will slow the progression of AD. Inestrosa demonstrated that AChE promotes the formation of amyloid-β peptide aggregates, and that compounds that bind to the PAS of AChE can act as amyloid-β aggregation inhibitors [152]. Therefore, some AChE inhibitors (AChE-I) can effectively prevent both ACh hydrolysis and plaque aggregation in AD. These dual-function inhibitors (DFI) have the potential to be more effective than single-function inhibitors.

Current clinical AD therapies use the anticholinesterase drugs rivastigmine, tacrine, galanthamine, and donepezil [150], [153]. (Figure 6-2) Binding modes of these drugs are depicted in Figure 6-1. The inhibition of AChE increases the amount, and prolongs the duration, of ACh present in the synaptic junction. More ACh is then allowed to enter the nicotinic receptors due to increased ACh levels. The current chemotherapeutic options have low

specificity toward AChE and are poorly tolerated in some patients [149]. Patients receiving donepezil show only moderate improvement of symptoms of AD [148, 153]. Thus development of higher affinity inhibitors may also help to alleviate the mental impairment associated with AD. Recently, inhibitors that inhibit both AChE and prevent amyloid-β aggregation have been suggested as a new therapeutic route [154, 155], although there are none currently in use.

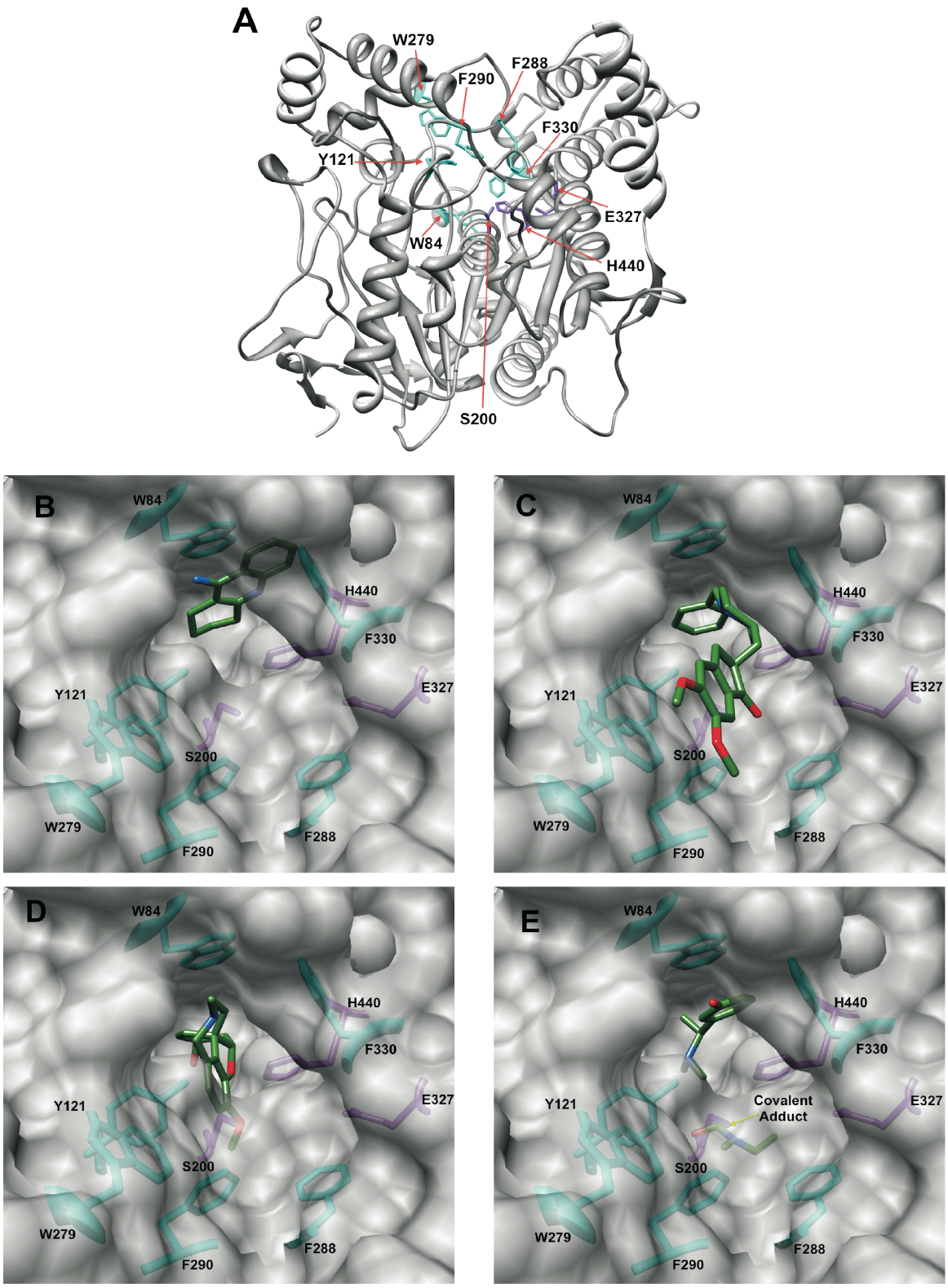
A
W279
F288
F290
F330
Y121
E327
W84
H440
S200
B
W84
H440
F330
Y121
E327
S200
W279
F290
F288
C
W84
H440
F330
Y121
E327
S200
W279
F290
F288
D
W84
H440
F330
Y121
E327
S200
W279
F290
F288
E
W84
H440
F330
Y121
Covalent
Adduct
E327
S200
W279
F290
F288

Figure 6-1 Binding modes for tacrine, donepezil, galanthamine and rivastigmine AChE inhibitors.

Modes of binding to acetylcholinesterase of current anticholinesterase drugs. A. Acetylcholinesterase structure, B. Tacrine, C. Donepezil, D, Galanthamine, E. Rivastigmine. Residues highlighted are known to interact with inhibitors. Residues with purple ribbon are catalytic triad (Ser-200, Glu-327, and His-440). Cyan residues with labels represent residues having interactions to inhibitor. We generated all molecular graphics images using the UCSF Chimera package (a resource for biocomputing, visualization, and informatics at the University of California, San Francisco; supported by NIH P41 RR001081).

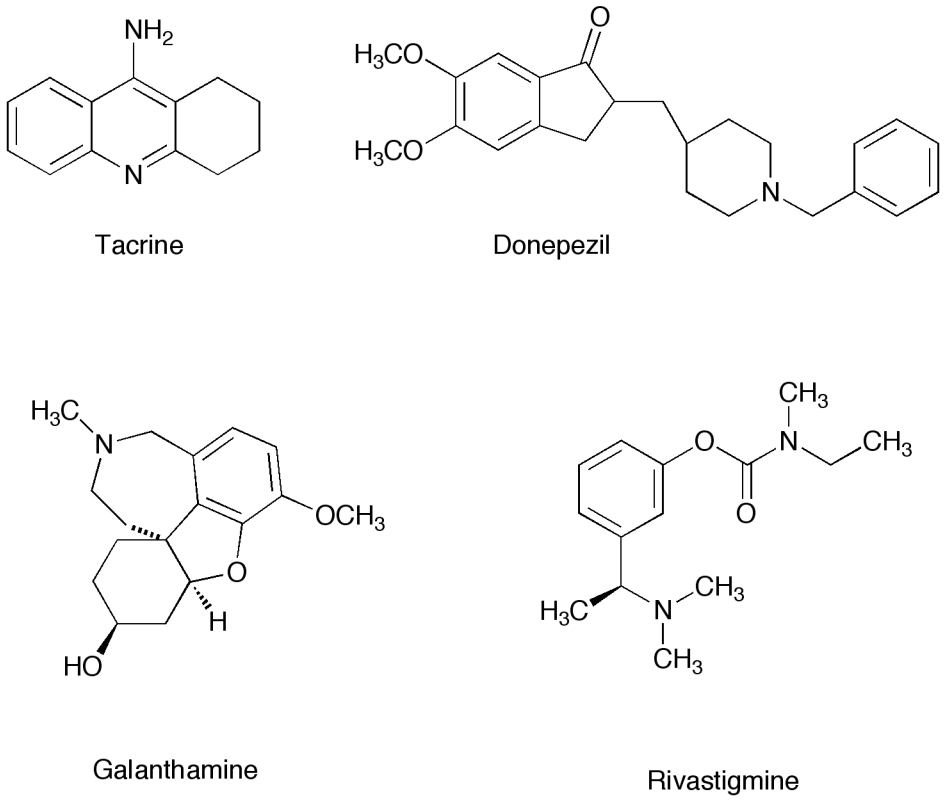

Figure 6-2: Current clinically-used acetylcholinesterase inhibitors

6.2.2 MARINE METABOLITES AS ACETYLCHOLINESTERASE INHIBITORS

Presently, there are no marine natural products in clinical use as AChE-I. Given the past success of drugs derived from marine organisms [156], exploring marine metabolites (MM) for novel lead anticholinesterase compounds may identify new compounds with novel interactions with AChE that garner selectivity and gain potency in treating AD. The purpose of this chapter, then, is the comparison of known marine-derived compounds having anticholinesterase activity to compounds whose mechanism of action are well understood to identify both similarities as well as novel properties of the marine compounds.

Marine metabolites vary greatly in structure, mass, and chemical composition [157]. Only 7 different classes of MM are reported to have anticholinesterase activity: a sesquiterpene acetate [158, 159], (**2**) a pyrrole derivative [160, 161], (**4**) a tetrazacyclopentazulene [162], (**1**) a bromotyrosine derivative [163, 164], (6, **7**) plastoquinones [165], (**3, 5**) farnesylacetones [165, 166], and poly-alkylpyridinium polymers (Poly-APS) [167-169]. Overall, these metabolites have been found to have moderate levels of anticholinesterase activity and generate inhibition through several different mechanisms. A review by Hostettmann was published in 2006 on all acetylcholinesterase inhibitors known up to that point, including those of marine origin [170]. Our paper includes new inhibitors discovered from marine species since 2006. Hostettmann's review detailed the structural information but not the enzyme-inhibitor interactions. Our focus is illustrating the inhibitor interactions within the AChE receptor and comparing them to compounds with known inhibition mechanisms. We have incorporated both experimental studies from the literature and our molecular ensemble docking studies of MM into the AChE receptor to better understand the molecular interactions of each inhibitor class. Four acetylcholinesterase structures (pdb codes 1ACL, 1DX6, 1EVE and 1ACJ) were used for all docking analysis. The

marine products aplysamine and Poly-APS were excluded from the docking analysis since aplysamine is an allosteric site inhibitor [163], and the Poly-APS are large molecular weight polymers; these compounds are not discussed in this paper. All other compounds were docked in their neutral state.

6.3 RESULTS AND DISCUSSION

6.3.1 THE OPISTOBRANCH MOLLUSK AND ITS METABOLITE, ONCHIDAL: A SESQUITERPENE ACETATE

In 1978, the compound onchidal (Figure 6-3), a sesquiterpene acetate containing an α/β-unsaturated aldehyde and an acetate ester, was isolated from the mucous secretion of the *O. binneyi* mollusk species by Ireland and Faulkner [158]. Onchidal was shown to interact with the acetylcholine recognition site, specifically the esteratic site, and found to have a K_d of 300 μM.

Docking of Onchidal into AChE

Onchidal was shown to interact with the esteratic site in our simulation, which is consistent with Abramson's work [159]. Three poses were generated for onchidal Figure 6-4. In all three poses the cyclohexane ring is positioned in the bottleneck. In two of the three poses the acetate ester is in the oxyanion hole. The lowest energy pose (scores listed in Table 6-1) for onchidal (Figure 6-5a) was generated using the 1DX6 receptor and places the acetate ester in the oxyanion hole, the aldehyde in the acyl pocket and onchidal's cyclohexane ring in the bottleneck created by Phe-330 and Tyr-121. The major interactions were potential hydrogen bonding (H-bonding) interactions with Gly-118 and Gly-119 of the oxyanion hole, hydrophobic contacts with the bottleneck, and a H-bond with His-440 of the catalytic triad (Figure 6-5a). It should be noted that potential H-bonds meet the distance requirements for H-bonds, but were not selected by the

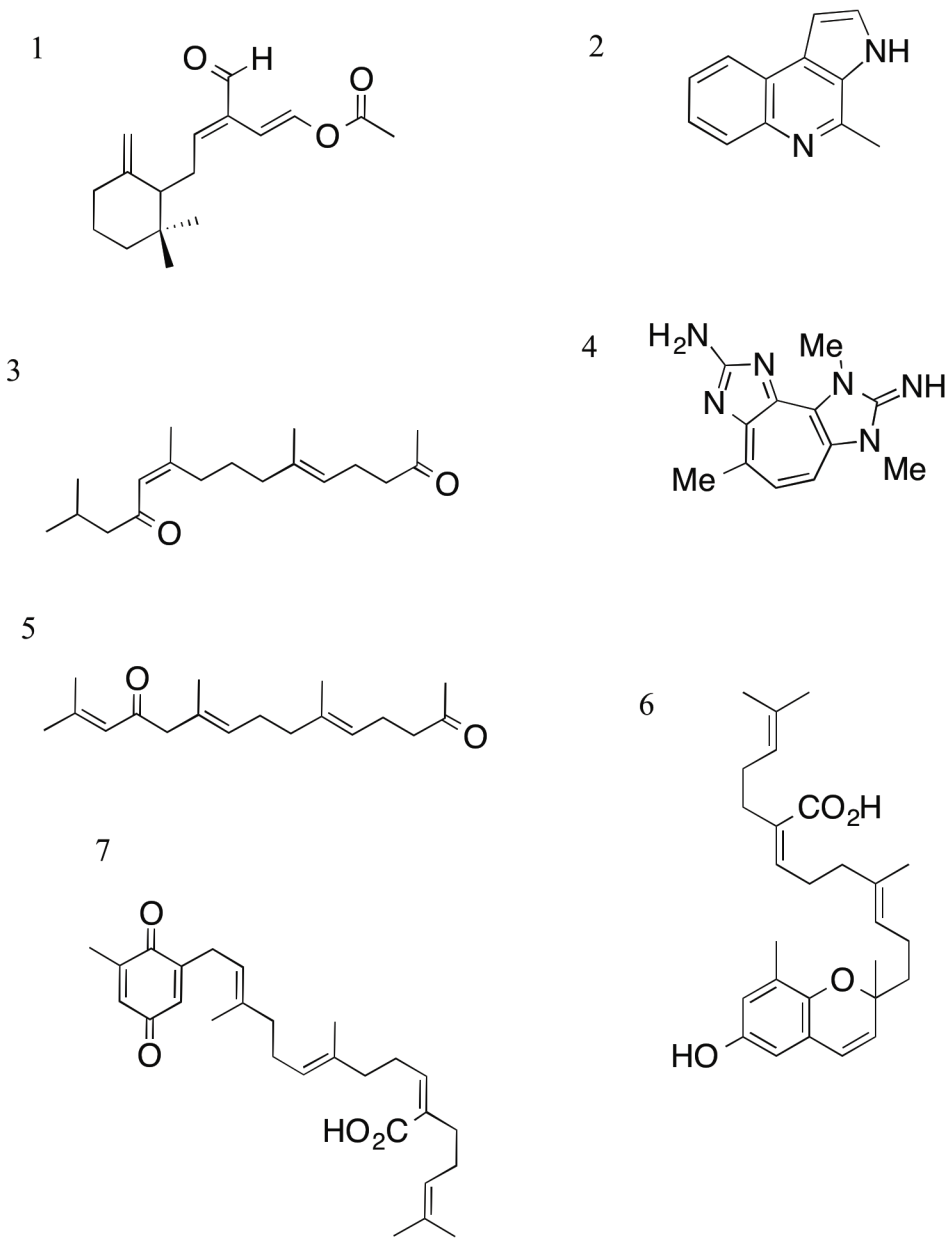

Figure 6-3: Marine metabolites with anticholinesterase activity: 1. Onchidal,[20,21] 2. Marinoquinoline,[22,23] 3. Dihydromonooxofarnesylacetone,[27,28] 4. Pseudozoanthoxanthin-like compound,[24] 5. Monooxofarnesylacetone,[27,28] 6. Sargachromenol.[27] 7. Sargaquinoic acid,[27]

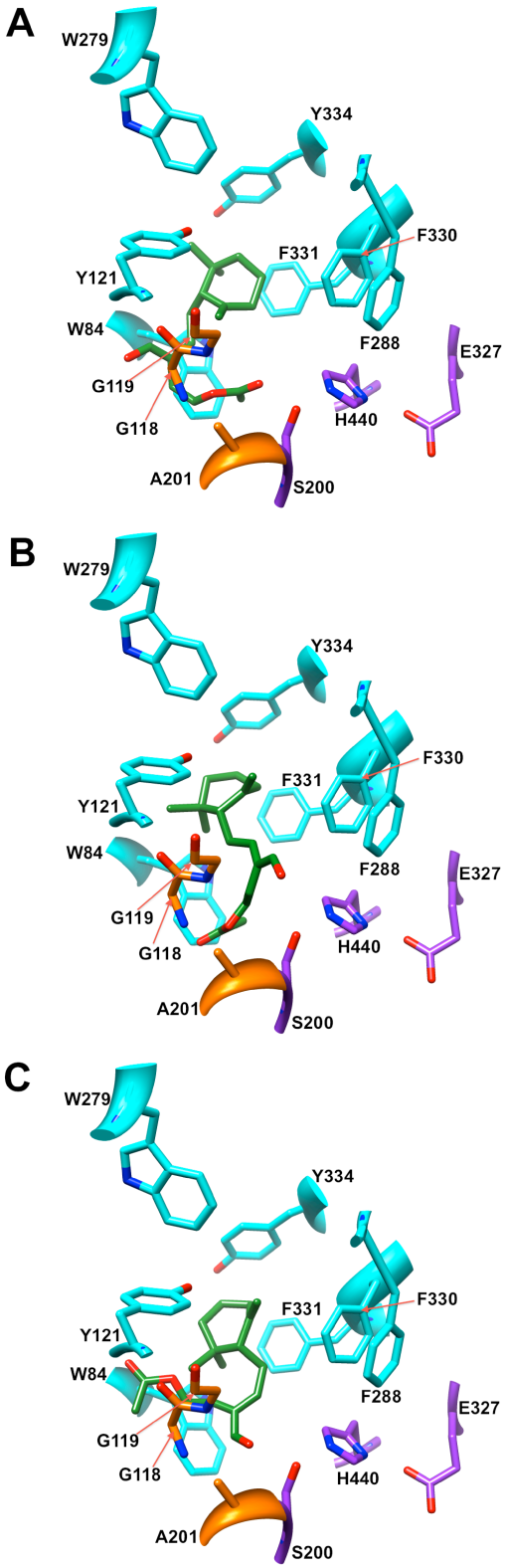
A
W279
Y334
F330
F331
Y121
W84
F288
E327
G119
H440
G118
A201
S200
B
W279
Y334
F330
F331
Y121
W84
F288
E327
G119
H440
G118
A201
S200
C
W279
Y334
F330
F331
Y121
W84
F288
E327
G119
H440
G118
A201
S200

Figure 6-4: Three docking pose generated for onchidal in various AChE receptors.

A. Onchidal poses docked in 1ACL receptor. B. Onchidal pose docked in 1DX6 receptor C. Onchidal pose docked in 1EVE receptor.

	Receptor				
	1ACL	**1ACJ**	**1DX6**	**1DX6 w/H20**	**1EVE**
Ligand	all scores in kJ/mol				
Donepezil	-59.79	-10.86	-53.65	-61.18	-56.74
Tacrine	-35.28	-33.83	-33.91	-34.09	-34.36
Galanthamine	-35.28	-35.77	-36.47	-38.76	-36.38
Acetylcholine	-31.78	-34.06	-31.99	-31.25	-31.61
Onchidal	-47.51	-44.28	-48.55	-47.37	-46.14
Marinoquinoline	-30.77	-34.27	-31.09	-30.50	-31.05
Tetracyclopentazulene	-42.34[1]	-44.03[1]	-41.77[2]	-42.03[1]	-42.51[2]
Sargaquinoic acid	-67.92	ND	-63.14	-69.81	-67.15
Sargachromenol	-62.98	-61.45	-62.82	-67.67	-65.16
Monooxofarnesylactone	-59.00	-55.34	-57.81	-50.22	-57.36
Dihydromonooxofarnesylactone	-56.00	-55.38	-55.94	-52.83	-55.51

Docking galanthamine into its own receptor with and without this conserved water molecule both resulted in the crystallographic pose being selected.
All inhibitors generated similar scores and poses in each receptor with the exception of donepezil in the 1ACJ receptor and onchidal. The best pose for onchidal was chosen.
[1,2] - Tetrazacyclopentazulene has two main poses (pose 1 scores are denoted by ([1]), pose 2 scores are denoted by ([2]).
ND - Sargaquinoic acid would not dock into the 1ACJ receptor due to the Phe-330 ring position occluding the active site gorge (see supplementary Figure 4)

Table 6-1. Docking scores of current anticholinesterase drugs and marine metabolites into acetylcholinesterase receptors

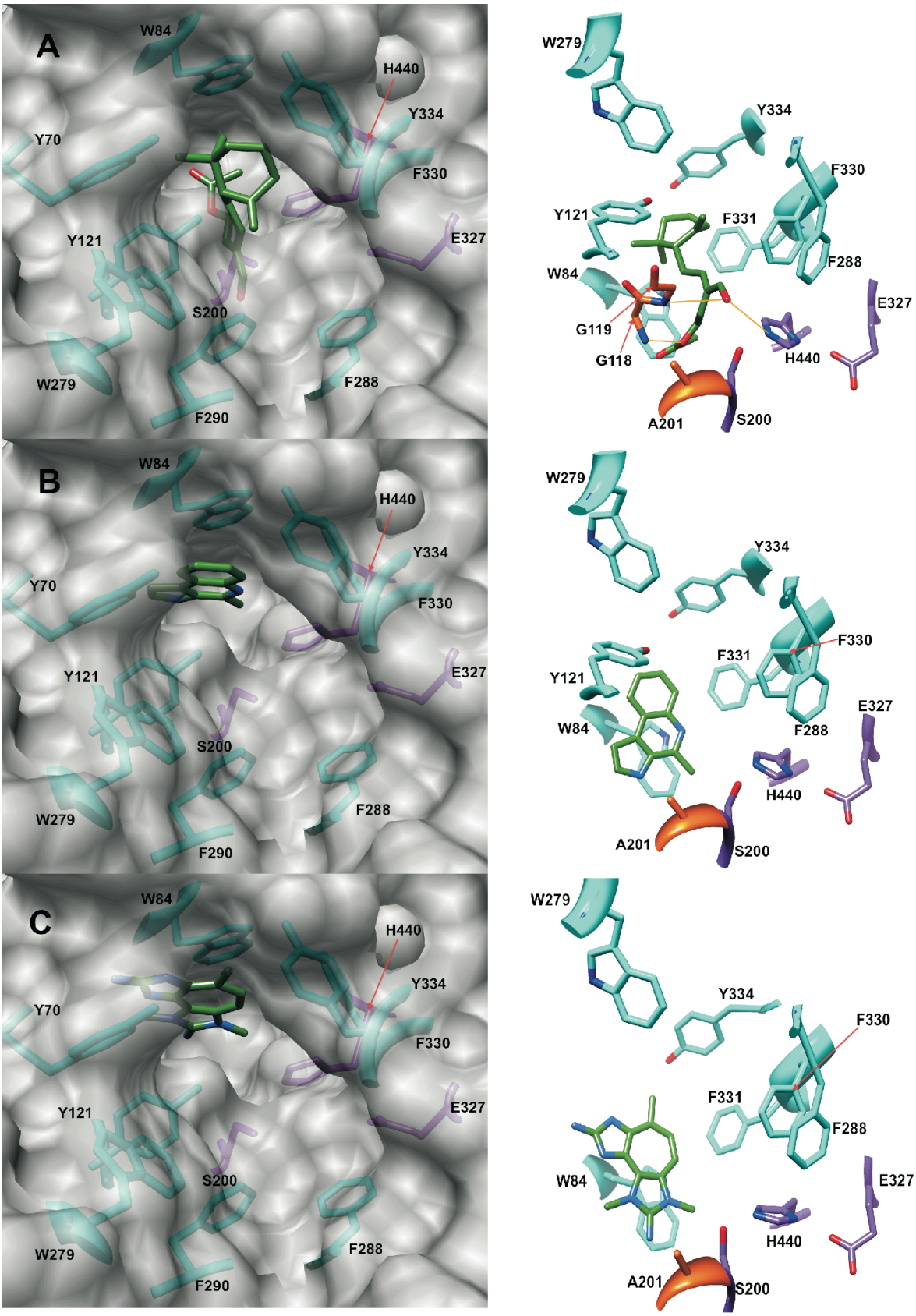
A
W84
H440
Y334
Y70
F330
Y121
E327
S200
W279
F288
F290
B
W84
H440
Y334
Y70
F330
Y121
E327
S200
W279
F288
F290
C
W84
H440
Y334
Y70
F330
Y121
E327
S200
W279
F288
F290
W279
Y334
F330
Y121
F331
F288
W84
E327
G119
G118
H440
A201
S200
W279
Y334
F330
F331
Y121
F288
E327
W84
H440
A201
S200
W279
Y334
F330
F331
F288
W84
E327
H440
A201
S200

Figure 6-5. Binding modes and molecular interactions of onchidal, marinoquinoline and PZT compound metabolites to AChE

Docking poses of A. Onchidal, B. Marinoquinoline, and C. PZT compound in the acetylcholinesterase receptor. Left panel orientation: looking into the active site. Right panel orientation: 90º upward rotation from left panel. Purple, orange, and cyan residues are catalytic triad, oxyanion hole, and aromatic gorge residues respectively. Figures were generated using molecular graphics images using the UCSF Chimera package (a resource for biocomputing, visualization, and informatics at the University of California, San Francisco; supported by NIH P41 RR001081).

automated search criteria due to angle constraints. Due to the flexibility of the enzyme, the proposed H-bonds are plausible.

During catalysis by AChE, H-bonding to the backbone residues Gly-118, Gly-119, and Ala-201 stabilizes the tetrahedral intermediate formed in the substrate. This suggests compounds capable of H-bonding with the oxyanion hole could inhibit AChE in a novel manner. Some aldehyde protease inhibitors have been shown to interact with the oxyanion hole and provide strong inhibition [171, 172]. The H-bonding interaction with oxyanion hole residues in AChE is unique to marine metabolites. Interactions with the oxyanion hole and His-440 are not present when donepezil, galanthamine, tacrine and rivastigmine are bound to AChE. The hydroxyl group of galanthamine does interact with a water molecule that is located in the oxyanion hole, but not the residues of the oxyanion hole itself [173]. When onchidal is docked in the 1DX6 receptor with this conserved water molecule present, it resulted in onchidal performing a clockwise rotation, to prevent steric clashes with the water molecule Figure 6-6. The ester group shifts backwards 2.96 Å away from the catalytic serine; the aldehyde group moves 6.34 Å downward. This may be the initial binding mode onchidal undergoes, after which onchidal may rotate, displacing the water in oxyanion hole; then the catalytic reaction can occur.

Because onchidal is an irreversible inhibitor, a covalent bond should be formed between it and the AChE receptor. Several reaction mechanisms for onchidal inhibition were suggested by Abramson: (i) Schiff base formation with a lysine; (ii) attack on the β-unsaturated carbon in conjugation with the aldehydes by a Cys, Lys, His, or Tyr; and (iii) the formation of 1,4-dialdehyde, which reacts with a Lys to form a pyrrole covalent adduct. Abramson did not have the benefit of the crystal structure of AChE solved by Sussman in 1991, limiting their mechanistic analysis. All lysines in AChE are located on the outside and not buried inside.

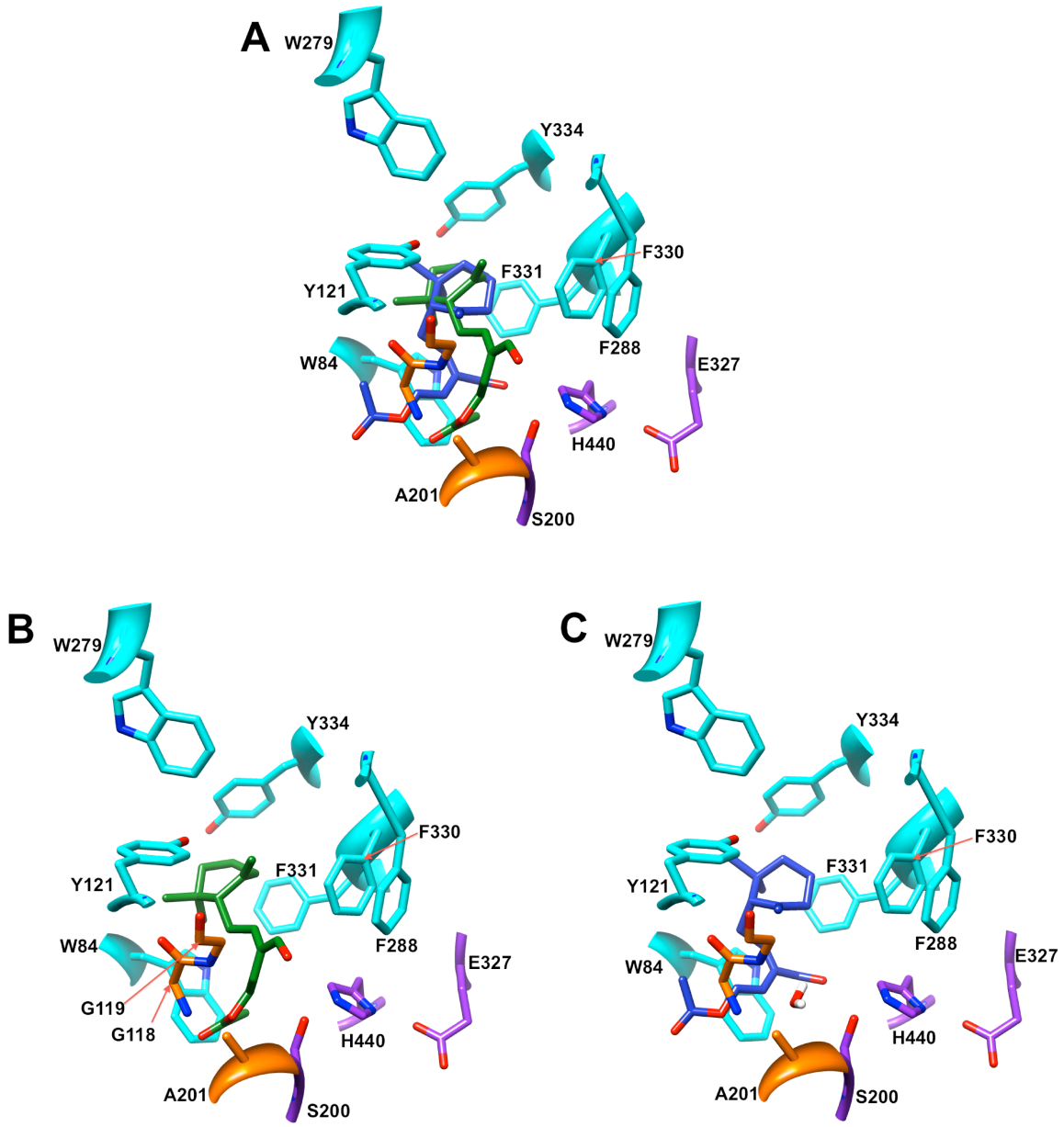

Figure 6-6. Docking pose of onchidal with water molecule present in 1DX6 receptor

A. Overlay of onchidal poses docked with (blue) and without (green) oxyanion hole water molecule. B. Onchidal pose without oxyanion water C. Onchidal with oxyanion water.

There are 7 Cys in AChE, six of which are paired and involved in intrachain di-sulfide bonds, and the last is not near the active site or in the gorge. Only one His, the active site His-440, is located in the gorge. Several tyrosines are located in the gorge; Tyr 442, 334, 130, 121, and 70. Based on the crystal structure and Abramsons' findings, the most probable mechanism is attack on the β-unsaturated carbon in conjugation with the aldehyde by a Tyr; however, attack on this particular moiety or by a Tyr was not supported by our docking analysis. It is also plausible that a direct acylation reaction between Ser-200 and the vinyl ester of onchidal could occur, after which a Lys or Arg residue could react with the aldehyde product. There are however no Lys or Arg residues that are present in the active site.

Here, we consider other possible chemical mechanisms of irreversible inhibition based on our docking analysis. Ser-200 is closest to the α-unsaturated carbon in conjugation with the acetate (3.538 Å). The carbonyl carbon on the aldehyde is 3.736 Å away, and the β-unsaturated carbon in conjugation with the aldehyde is 4.989 Å away from the Ser-200. Nucleophilic attack on the α-unsaturated carbon in conjugation with the acetate could result in the formation of a covalent adduct and acetate production (Scheme 6-1A). This mechanism would be achieved by (i) nucleophilic attack on the α-unsaturated carbon in conjugation with the acetate, followed by (ii) reformation of the double bond releasing acetate (pathway A). We also considered the pathways B and C shown in Scheme 1B and 1C respectively. In pathway B, Ser-200 would attack the β-unsaturated carbon in conjugation with the aldehyde, pushing the electrons onto the aldehyde oxygen. The electronegative oxygen would then attack the α-unsaturated carbon in conjugation with the acetate, forming a five-member ring. Finally, reformation of the double bond would release acetate and then form an aromatic furan ring structure. In pathway C, Ser-200 attacks the aldehyde carbon, pushing the electrons onto the aldehyde oxygen.

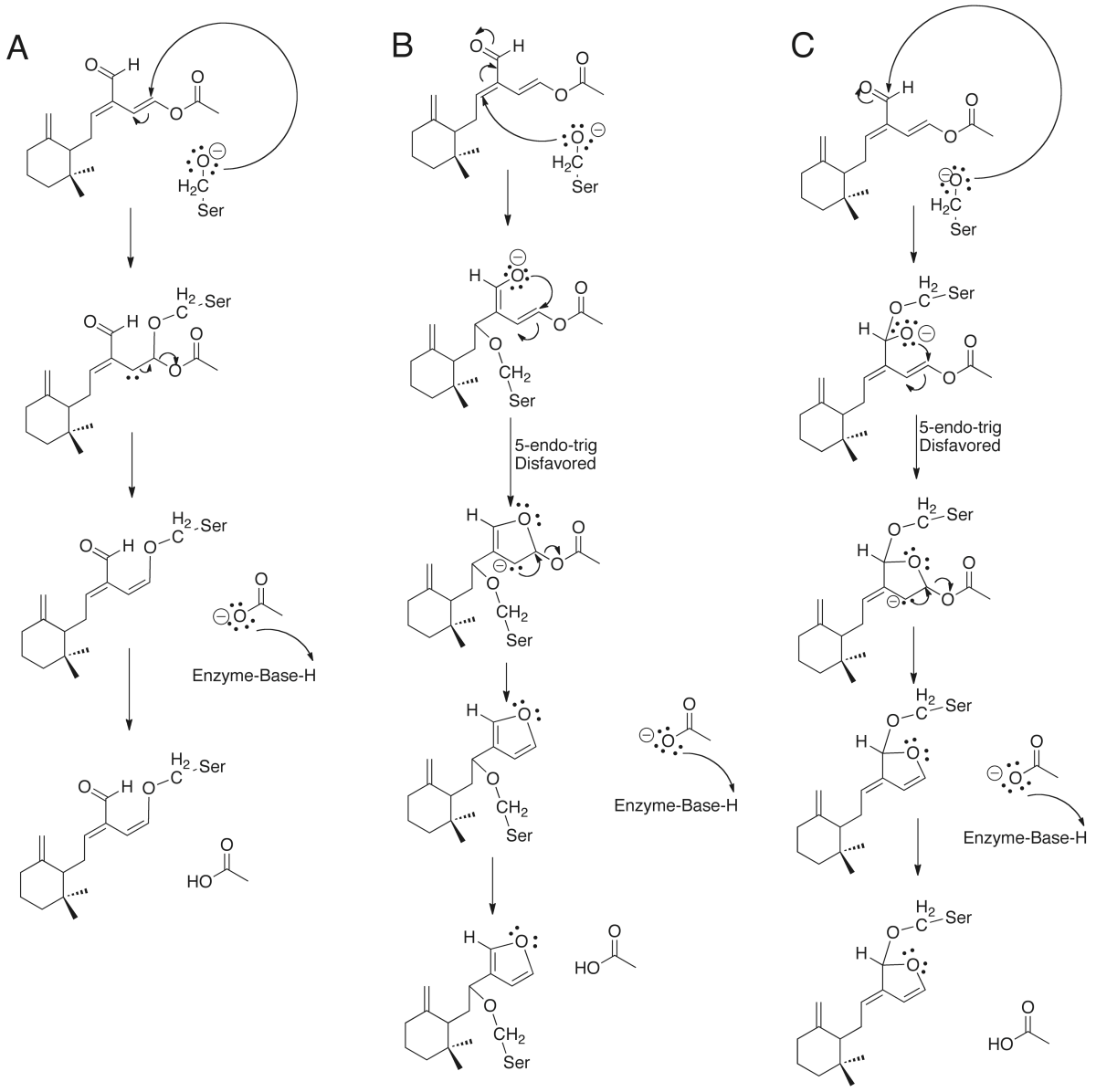

Scheme 6-1. Potential pathways for irreversible inhibition by onchidal. Pathway A is the suggested pathway for irreversible inhibition of AChE.

Like pathway B, the electronegative oxygen would then attack the α-unsaturated carbon in conjugation with the acetate, forming a five-member ring. Reformation of the olefin would release acetate and generate a 2,3-dihydrofuran ring (2-oxolene ring). Pathways B and C employ a disfavored 5-endo-trig pathway, suggesting that they are less probable than pathway A. It should be noted that a disfavored pathway is only disfavored, not impossible [174]. Both the distance and feasibility of pathway A suggest it is most likely the pathway that generates irreversible inhibition of AChE.

Onchidal's irreversible inhibition of AChE makes it unsuitable for direct use as an anticholinesterase inhibitor for human diseases, but it could have potential for use in insecticides or pesticides. However, onchidal's interaction with the oxyanion hole is a new mechanistic area that AChE-I's rivastigmine, tacrine, galanthamine, and donepezil do not use. Onchidal's structure could therefore be used for rational drug design in developing novel inhibitors for use in clinical treatment.

6.3.2 THE GLIDING BACTERIA *RAPIDITHRIX THAILANDICA* AND ITS PYRROLE METABOLITES

Rapidithrix thailandica is a gliding bacterium that was discovered in seaweed extracted from the Andaman Sea off the coast of Thailand by Srisukchayakul [175, 176]. Kanjana-opas and co-workers isolated pyrrole derivatives marinoquinoline (Figure 6-3), 3-(2-aminophenyl)-pyrrole, and 2,2-dimethyl pyrrolo-1,2-dihydroquinoline from *R. thailandica* in 2006 [160]. Marinoquinoline, which has an extended aromatic system, inhibited AChE with an IC_{50} value of 4.9 μM. The other isolated metabolites did not possess anticholinesterase activity. The inactive

pyrrole derivatives isolated lacked an extensive aromatic ring system. This structural difference suggested that inhibition produced by marinoquinoline was due to π-π stacking interactions.

Docking of Marinoquinoline to AChE

No prior work has elucidated which are the specific residue or residues in the aromatic gorge marinoquinoline is potentially stacking against. We hypothesized that marinoquinoline interacts with AChE by participating in π-π stacking with Trp-84, similar to tacrine's mode of binding [144]. We observed marinoquinoline docked against the Trp-84 (Figure 6-5b) in all structures of AChE and having a binding score of -31.09 kJ/mol (1EVE receptor), supporting this hypothesis of π-π stacking to an aromatic residue. In the 1ACJ structure that was crystallized with tacrine as a ligand, Phe-330 is oriented approximately 90º upward compared to its position in the 1ACL, 1DX6 and 1EVE structures (Figure 6-7). Upon binding of tacrine, Phe-330 forms a π-stacking interaction with the inhibitor. It is likely that marinoquinoline would cause Phe-330 to move into a similar position to that observed for tacrine. The rotation of Phe-330 would decrease the 5 Å bottleneck in the gorge, making it more difficult for acetylcholine to reach the active site. Docking marinoquinoline into the 1ACJ structure generated an improved score of -34.27 kJ/mol. Our data suggest that binding of marinoquinoline to AChE results in the compound inhibiting the enzyme in an manner analogous to tacrine (Figure 6-8a).

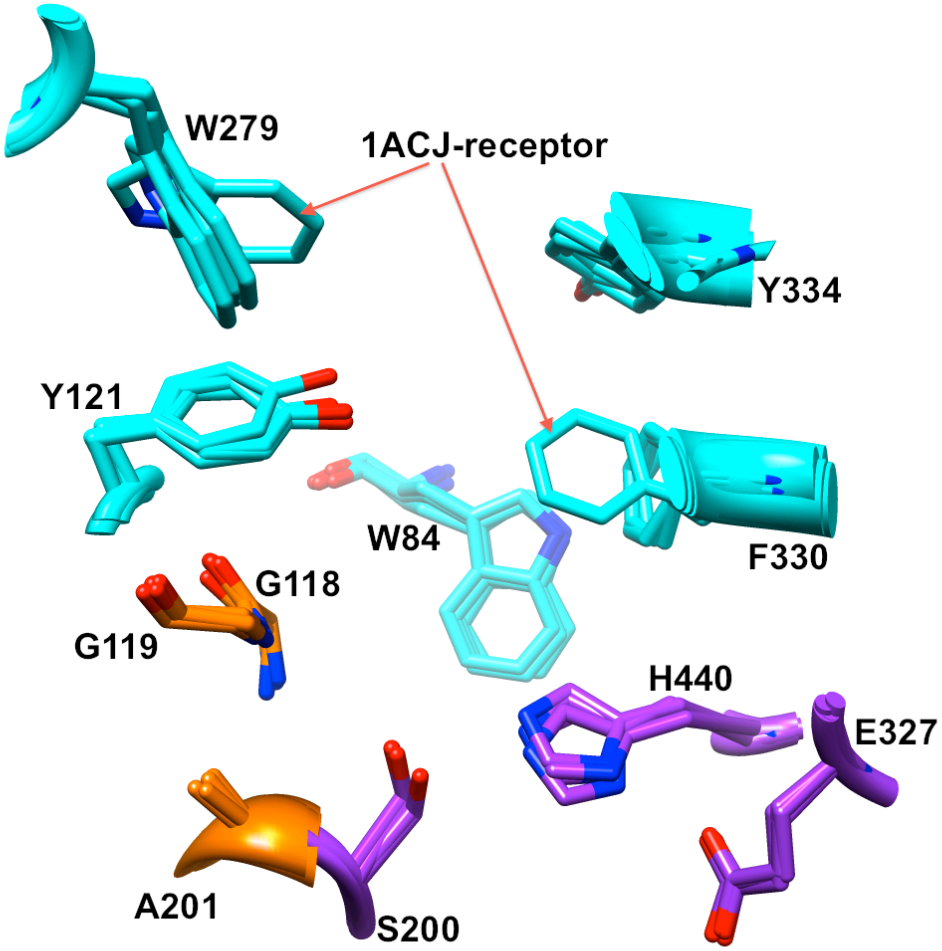

Figure 6-7 Alignment of 1ACJ, 1ACL, 1DX6 and 1EVE receptors

Alignment of tacrine receptor (1ACJ) places the F330 and W279 in a different conformational location than the galanthamine (1DX6) or donepezil (1EVE) or 1ACL receptors. Residues labeled in purple, orange, and cyan represent the catalytic triad, oxyanion hole, and aromatic residues of the gorge.

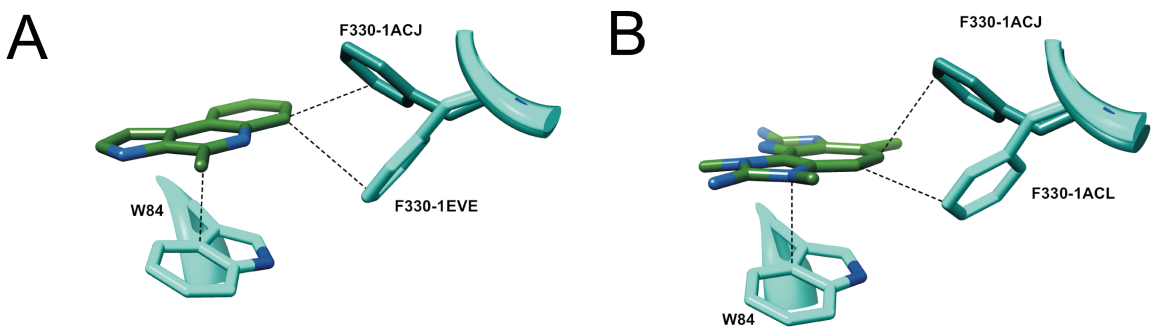

Figure 6-8: Molecular interactions of marinoquinoline and PZT-compound with AChE

Expanded views of molecular interactions for A. Marinoquinoline, B. PZT compound, in the acetylcholinesterase receptor.

6.3.3 THE *PARAZOANTHUS AXINELLAE* (O. SCHMIDT), ZOANTHID CORALS, AND TETRAZACYCLOPENTAZULENE NATURAL PRODUCTS.

The pigmentation of Zoanthid corals is vast, and produced by tetrazacyclopentazulene compounds (TCP; Figure 6-3). One yellow TCP, called a pseudozoanthoxanthin-like compound (PZT compound), was isolated by Turk and co-workers in 1994 [162]. Like onchidal, this compound was shown to be a competitive acetylcholinesterase inhibitor (K_i of 4 μM). Unlike onchidal, which interacts with the esteratic site of acetylcholinesterase, the PZT compound was found to interact with the aromatic residues lining the active site gorge as determined by fluorescence emission spectroscopy. Turk and co-workers found that the signal from the intrinsic tryptophan located in the gorge of acetylcholinesterase was quenched in the presence of the inhibitor. These results suggested that an interaction between a Trp residue and the inhibitor was the mechanism of inhibition.

Binding of a Tetrazacyclopentazulene (PZT) compound to AChE

Using the 1EVE receptor, the pose for the PZT compound scored at -42.51 kJ/mol and showed a T-stacking interaction with Trp-84, and three H-bonding interactions. H-bonding interactions occur between the triad residues Ser-200 and His-440, and the oxyanion hole residue Gly-118 (Figure 6-9). The docking of the PZT compound into the 1ACL receptor resulted in a score of -42.34 kJ/mol, which positioned the PZT compound stacked against Trp-84 (Figure 6-5c). Both poses are in agreement with published experimental data that suggest interaction with a Trp residue. While the authors Turk and coworkers could not determine which Trp residue was interacting with PZT compound, our docking analysis suggest that it interacts with Trp-84 in some way. There are several conserved Trp residues in the gorge, Trp-84, Trp-233, and Trp-279. Trp-279 is located at the entrance, Trp-233 is in the acyl pocket and Trp-84 is in the anionic binding site. Because the PZT compound is a competitive inhibitor, the Trp-279 is unlikely to be a binding partner. Our docking analysis does not support an interaction between Trp-233 and the PZT compound.

A PZT-compound-Trp-84 interaction could share the same binding mode as tacrine [144] and marinoquinoline. Based on the conformational changes that occur when tacrine binds AChE, when PZT compound binds the receptor Phe-330 would rotate to a position to allow for the double π-π stacking interactions (Figure 6-8b). Like marinoquinoline, the binding score improved when docked into the 1ACJ receptor (-44.04 kJ/mol). Thus we believe, upon binding, PZT most likely forms π-π interactions with both Trp-84 and Phe-330, which in turn closes off the bottleneck, disallowing ACh to enter the acyl pocket.

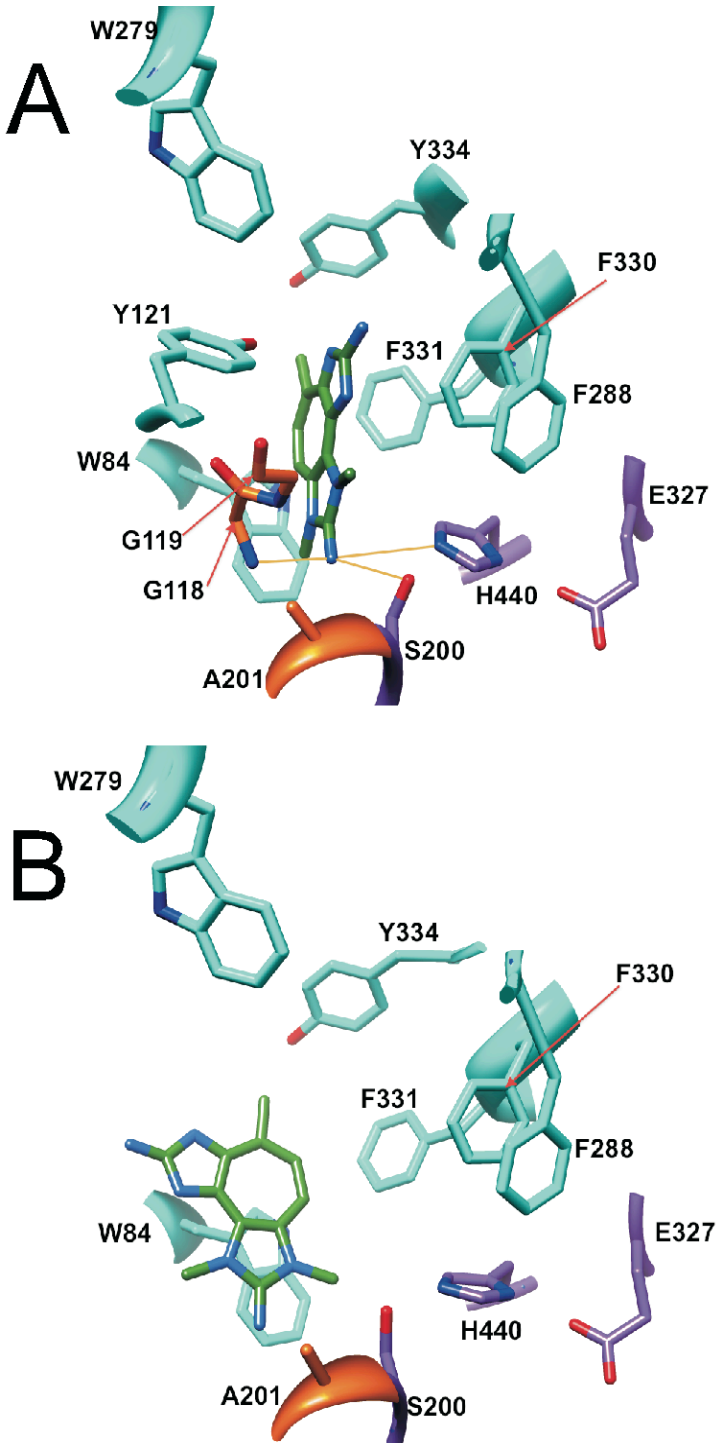

Figure 6-9. Poses generated for PZT-compound. Poses generated from docking PZT-compound in the AChE. A. shows the lowest binding energy pose, B. shows pose consistent with experimental data

Both marinoquinoline and PZT-compound share the same binding mode as tacrine; however the PZT-compound binds tightest to AChE. Tacrine's best docking score was -35.28 kJ/mol, which is 9 kJ weaker then PZT-compound's binding score. A paper by Muñoz-Ruiz [155] used the indole ring of donepezil and the fused ring of tacrine to develop potent dual site inhibitors, with the tacrine moiety bound to the anionic site. Replacement of tacrine by the PZT-compound has the potential to increase the potency of these DFIs even more.

6.3.4 THE BROWN ALGA *SARGASSUM SAGAMIANUM* AND THE PLASTOQUINONES AND FARNESYLACETONES METABOLITES.

Ryu [29] in 2003 and Choi [28] and co-workers in 2007 reported the isolation of a series of terpenoid compounds (Figure 6-3) from the brown alga *Sargussum sagamianum.* Four compounds were isolated from the alga: (**7**) sargaquinoic acid (IC_{50} 23.2 μM), (**6**) sargachromenol (IC_{50} 32.7 μM), (**5**) monooxofarnesylacetone (IC_{50} 65.0 μM) and (**3**) dihydromonooxofarnesylacetone (IC_{50} 48.0 μM). All four compounds have moderate levels of bovine erythrocyte AChE inhibition, with a specificity for butyrylcholinesterase.

Based solely on structural comparisons, we hypothesized these compounds likely inhibit AChE in two ways: stacking interactions with aromatic residues, and interactions with the esteratic site. No experimental work has been done to probe the mechanism of inhibition of the plastoquinones or farnesylacetones thus far.

Docking of the Plastoquinones and Farnesylacetones into AChE

Docking of the two plastoquinones resulted in similar binding modes (Figure 6-10). Three stacking interactions were observed in sargaquinoic acid (**7**): (i) the quinone moiety of sargaquinoic acid positioned next to Trp-84; (ii) the 6-7 olefin stacked with Phe-330; and (iii) the

10-11 olefin stacked against Tyr-334. Sargaquinoic acid's binding score was the best of all metabolites considered, being -67.92 kJ/mol in the 1ACL receptor. Sargachromenol has one less stacking interaction than does sargaquinoic acid. We observed the reduced quinone moiety of sargachromenol stacking against Trp-84 and the 3-4 double bond of sargachromenol stacked against Phe-330 (Figure 6-10). However, sargachromenol's α/β unsaturated carboxylic acid substituent also H-bonds with the backbone of residue Phe-288 located in the esteratic site. Sargachromenol binds slightly weaker to the receptor than sargaquinoic acid, with its best binding score being -65.16 kJ/mol in the 1EVE receptor.

The farnesylacetones, unlike the plastoquinones, do not share a similar binding mode. Dihydromonooxofarnesylacetone (**3**), which participates in two H-bonding interactions, has a binding score of -56.00 kJ/mol in the 1ACL receptor. At the top of the gorge, in the PAS, its α/β unsaturated π bond H-bonds to Tyr-121, at the base of the gorge in the esteratic site (Figure 6-10). This compound is unique for this family in that its major source of interaction with the receptor is through H-bonding compared to stacking interactions. Monooxofarnesylacetone (**5**) also has a H-bond to AChE, albeit to His-440 instead of Gly-119 or Tyr-121. Like sargaquinoic acid, monooxofarnesylacetone π-stacks against Trp-84, Phe-330 and Tyr-334 (Figure 6-10). The binding score for monooxofarnesylacetone is almost 9 kJs weaker than sargaquinoic acid at -59.00 kJ/mol in the 1ACL receptor.

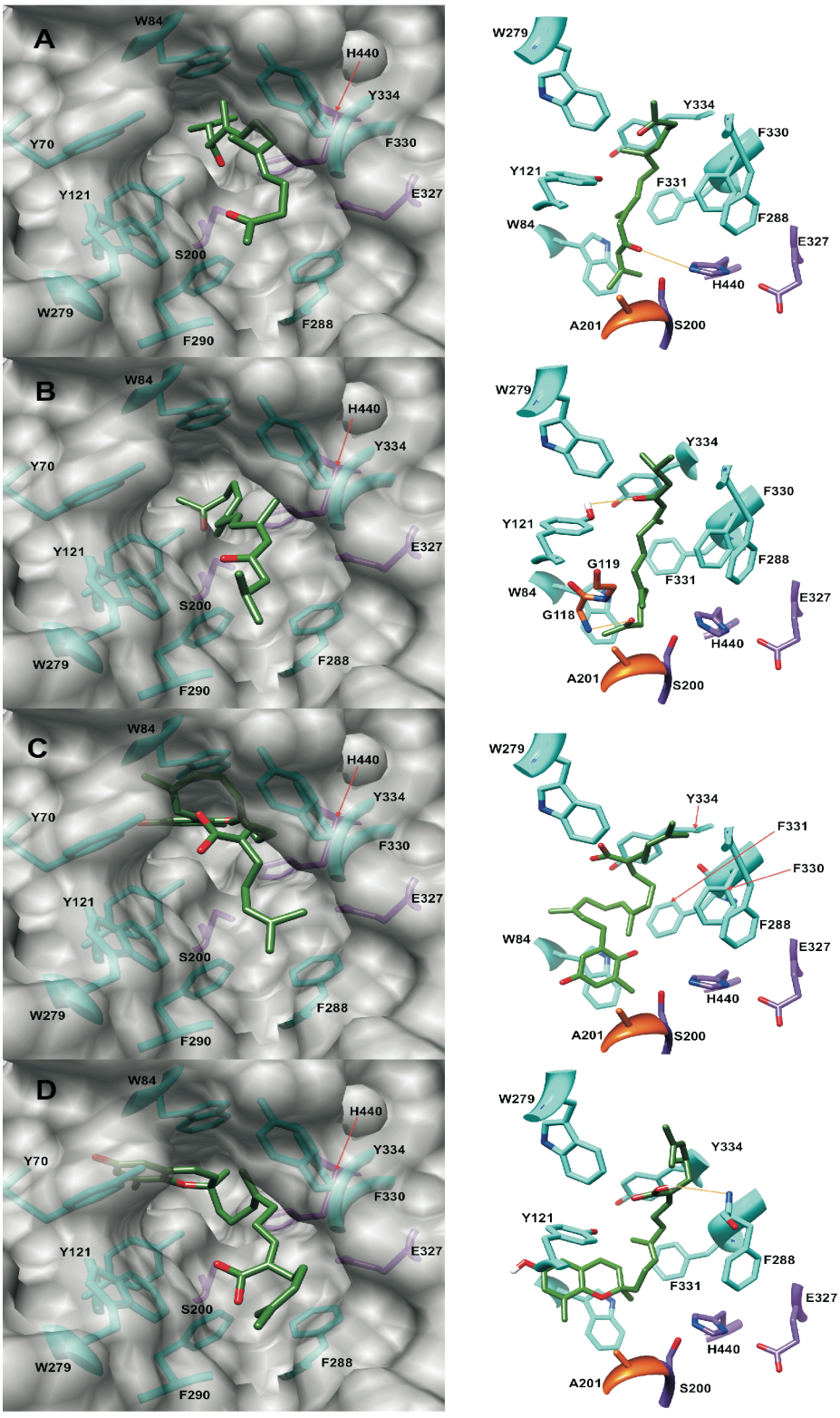
A
W84
H440
Y334
Y70
F330
Y121
E327
S200
W279
F288
F290
B
W84
H440
Y334
Y70
Y121
E327
S200
W279
F288
F290
C
W84
H440
Y334
Y70
F330
Y121
E327
S200
W279
F288
F290
D
W84
H440
Y334
Y70
F330
Y121
E327
S200
W279
F288
F290
W279
Y334
F330
Y121
F331
F288
W84
E327
H440
A201
S200
W279
Y334
F330
Y121
G119
F288
F331
W84
E327
G118
H440
A201
S200
W279
Y334
F331
F330
F288
W84
E327
H440
A201
S200
W279
Y334
Y121
F288
F331
E327
H440
A201
S200

Figure 6-10. Binding modes and molecular interactions of farnesylacetones and plastoquinones metabolites to AChE.

Docking poses of A. monooxofarnesylacetone B. dihydromonooxofarnesylacetone C. sargaquinoic acid and D. sargachromenol in the acetylcholinesterase receptor. Left panel orientation: looking into the active site. Right panel orientation: 90º upward rotation from left panel. Purple, orange, and cyan residues are catalytic triad, oxyanion hole, and aromatic gorge residues respectively.

Both the plastoquinones and farnesylacetones are competitive inhibitors of AChE, which occlude the active site gorge in a manner similar to donepezil. They all protrude somewhat out of the gorge, suggesting that they prevent acetylcholine from entering the AChE binding site. Donepezil stacks against Phe-330 and Trp-84 and interacts with the Trp-279 located in the PAS. The plastoquinones and monooxofarnesylacetone, like donepezil, primarily use stacking interactions to stabilize the receptor ligand complex, stacking against Trp-84, Tyr-334, and Phe-330 within the gorge. The isoprene units of the farnesylacetones and the plastoquinones have the right number of linker carbons and degree of flexibility to allow participation in multiple aromatic interactions simultaneously. In general, the plastoquinones and farnesylacetones bind to the side opposite the PAS at the entrance of the gorge, with the exception of dihydromonooxofarnesylacetone that H-bonds to Tyr-121 of the PAS.

In the development of dual binding site inhibitors that bind to the anionic site and to the peripheral anionic site, a linker is needed which can span the length of the gorge. Linkers that bind strongly to the gorge would greatly increase the potency of these dual site inhibitors. Many linkers used thus far have contained amides [155, 177], aliphatic chains [154, 155], pyrimidine rings [178], piperidine rings [154, 177], and other cyclic aromatic structures [154, 177]. In our docking studies, the plastoquinones bind tighter to AChE than donepezil (best score -59.79 kJ/mol), with farnesylacetones coming in close behind donepezil. The terpene type linker seems to bind well in the gorge, capitalizing on multiple stacking interactions. Thus, it may be a useful new linker to consider in creation of dual site inhibitors. Dihydromonooxofarnesylacetone has two ketone residues, one that binds the oxyanion hole and one that binds to the PAS residue Tyr-121, and therefore suggests a new di-ketone scaffold for amyloid-β aggregation inhibitors.

6.3.5 DESIGN OF NEW DUAL ACHE AND AMYLOID BETA AGGREGATION INHIBITORS

Using the docking scores and poses of marine metabolites investigated, we designed 12 new AChE inhibitor candidates (Figure 6-11). We hypothesized that we could both generate new compounds using the MM as scaffolds that would have better binding scores and that we would be able to predict the pose of these compounds based on the docking data of the MM precursors used. These compounds were then docked into the 1EVE and 1DX6 receptors. Table 2 shows the docking scores of the designed inhibitor candidates. Eleven of the twelve compounds show improved docking scores compared to donepezil. Only one compound, MM-P07 (best dock score -58.26 kJ), showed less favorable binding to the AChE receptor than donepezil. The best compound, MM-P12, had a PZT base, a terpene linker, and the indoline ring of donepezil at the top.

While using the marine metabolites as starting point to develop new AChE inhibitor scaffolds with improved docking scores was successful, it was difficult to accurately predict the interactions they would be calucated to have with the receptor. We found that several new interactions were employed in our new compounds. For example, Tyr-130 was not found to have any major interactions with the marine metabolites themselves; however, we observed 4 compounds having H-bonding interactions with Tyr-130. The best inhibitor candidate, MM-P12 (shown in Figure 6-11; docking score of -73.43 kJs), has an amino group, from the PZT compound scaffold, that hydrogen bonds with Tyr-130. Compounds MM-P04 (quinone moiety from sargaquinoic acid), MM-P05 (quinone moiety from sargachromenol), and MM-P08 also were found to H-bond to with Tyr-130. We will not discus the poses of each new inhibitor in detail but will highlight some important features contributing the increased potency of these

compounds. We also observed that the orientation of compounds could be exactly opposite what we hypothesized. For example, the PZT-compound and marinoquinoline were used in our scaffolds in an effort to drive what we considered the base of the compound to the anionic site through a stacking interaction with Trp-84 that was observed with each of the precursors. However, the addition of the PZT compound to the terpenoid scaffold produced poses where this moiety was at both the base, stacking against Trp-84, as expected, and the periphery of the gorge, participating in stacking reactions with Trp-279 in the PAS, and with Tyr-334. The latter orientation also allows the carbonyl group of the MM-P01 compound, closest to the PZT ring system, to H-bond with Tyr-121. This produces a slightly more favorable dock score for this pose compared to the former pose (-72.93 kJ, versus -71.97 kJ). Both poses, however, show improved binding to the AChE receptor compared to the MM precursors. This inversion of orientation was observed for compounds MM-P08, MM-P07, and MM-P10 (1DX6 receptor only). While some new interactions were shown to occur we were able to develop compounds which posed exactly or fairly close to how we expected, such as the compounds MM-P04, MM-P05, MM-P10), MM-P14, MM-P12, MM-P13, MM-P06, MM-P02, and MM-P01.

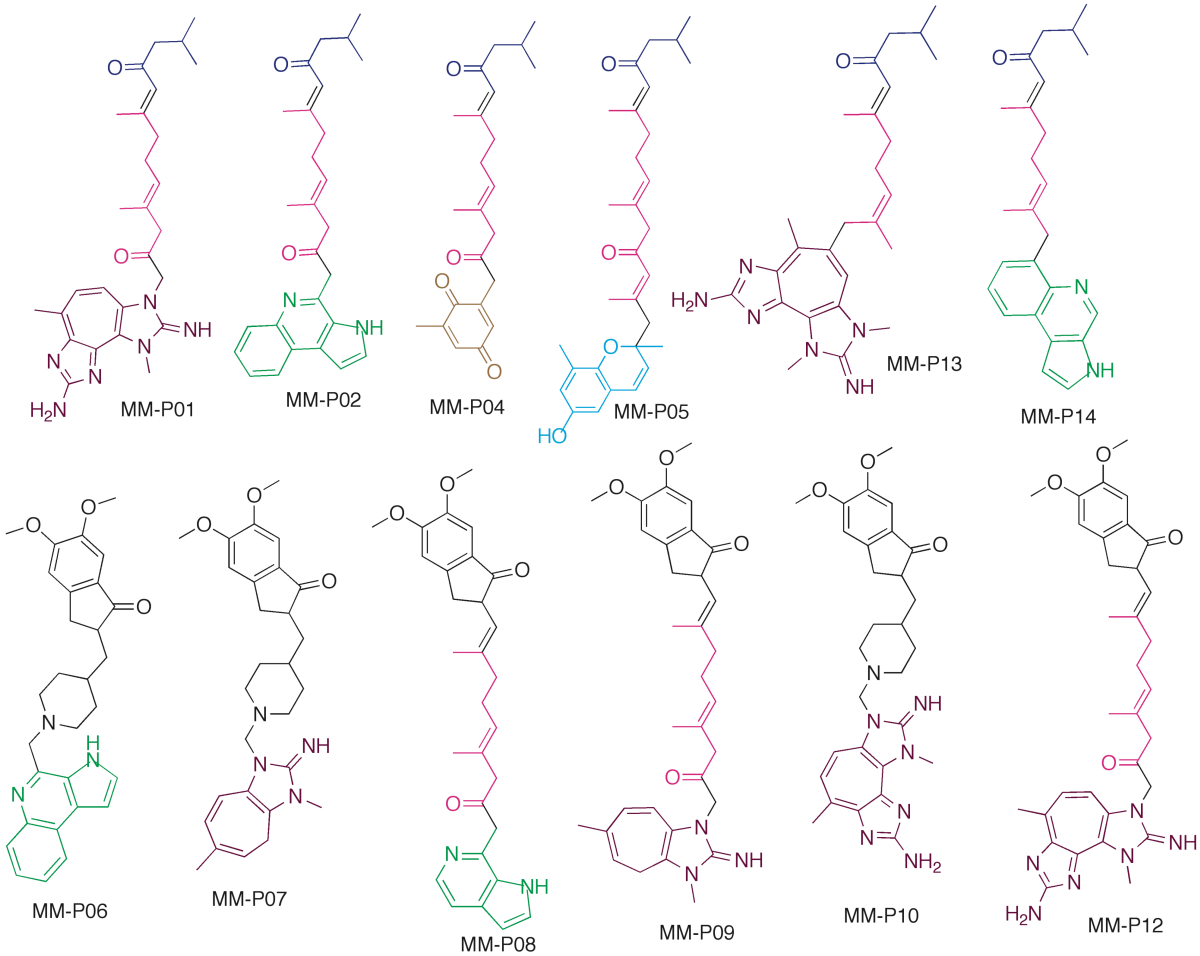

Color code for fragments

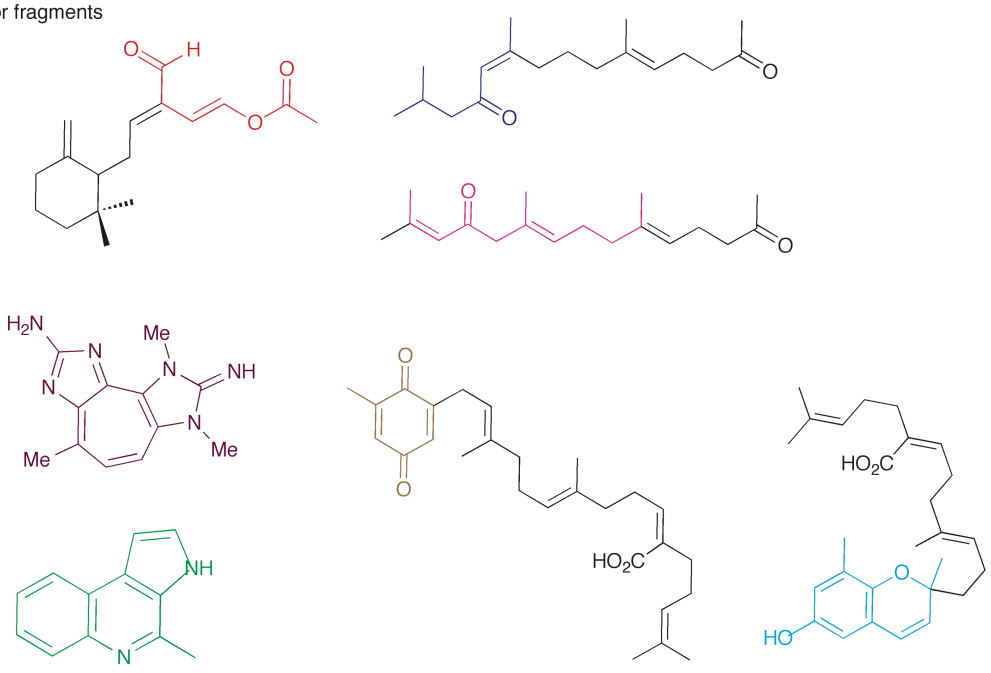

Figure 6-11: Proposed Dual Function Inhibitors developed using MM Scaffolds: The top portion shows the 12 scaffolds, which were successfully docked into the AChE receptor. Each compound was made using portions of MM that had some specific interaction within the AChE receptor. The indoline and piperidino moieties used in some of the compounds are from donepezil. The names for each MM structure can be found in Figure 2.

Dual function inhibitors must interact with the PAS of AChE. Of the 12 compounds we designed, eight have the capability of interaction with the PAS in some fashion (MM-P01, MM-P04, MM-P05, MM-P06, MM-P07, MM-P08, MM-P09, and MM-P10 Table 6-2). Four of these compounds stack with Trp-279 (MM-P06, MM-P07, MM-P09, and MM-P10). MM-P04 and MM-P05 H-bond with Tyr-121. Two compounds interact with both residues (MM-P01, and MM-P08).

Compound	**Best Score (kJ/mol)**	**Receptor**	**Interacts with PAS**	**MM Scaffolds used to create Compound**
MM-P01	-72.93	1EVE	Yes	3, 4, 5
MM-P02	-63.02	1EVE	No	2, 3, 5
MM-P04	-62.62	1EVE	Yes	3, 5, 7
MM-P05	-71.95	1EVE	Yes	3, 5, 6
MM-P06	-62.00	1DX6	Yes	2, and donepezil
MM-P07	-58.26	1DX6	Yes	4 and donepezil
MM-P08	-65.76	1EVE	Yes	2, 5, and donepezil
MM-P09	-72.19	1EVE	Yes	4, 5, and donepezil
MM-P10	-64.77	1DX6	Yes	4 and donepezil
MM-P12	-73.43	1EVE	No	4, 5, and donepezil
MM-P13	-68.90	1DX6	No	3, 4, 5
MM-P14	-60.78	1EVE	No	2, 3, 5

Table 6-2. Docking scores of proposed dual function inhibitors into acetylcholinesterase receptor

6.4 SUMMARY

Exploring marine metabolites (MM) as an option for lead compounds may identify new useful interactions and scaffolds that increase potency and garner selectivity. From these compounds, we can identify new target sites within acetylcholinesterase for development of AChE-I. Future generations of AD drugs could utilize H-bonding to the oxyanion hole residues, stacking interactions with Tyr-334, and H-bonding to Tyr-121 in the PAS to inhibit AChE. Development of novel acetylcholinesterase inhibitors that have characteristics of MM, such as an increased number of protonatable nitrogen atoms that stack against Trp-84, and creation of terpene linkers for dual site inhibitors, may help to develop compounds with greater potencies from optimization of stacking interactions in the gorge. Several of these properties exhibited by the MM can also be included in the design of DFI that prevent both ACh degradation and amyloid-β aggregation. Overall these MM bind tighter to AChE than galanthamine, or tacrine, and several metabolites bind tighter than donepezil. Selectively crossing scaffold features of the MM successfully produced compounds with even better AChE binding than the precursor scaffolds used, yet the overall pose was difficult to predict. Many compounds generated interacted with the PAS site, the critical interaction contributing to inhibition of amyloid-β-aggregation. Determination of isozyme specificity, and effects on amyloid-β aggregation for the sesquiterpene acetate [158, 159], pyrrole derivative, PZT-compound, plastoquinones, and farnesylacetones classes of MM described in this article, would provide an additional guide to development of novel compounds as therapies for Alzheimer's disease.

6.5 MATERIALS AND METHODS

Computational evaluation can delineate important interactions between the inhibitors and receptors, where mechanisms of inhibition and sites of interactions are unknown. Docking is a technique that has been performed for many biologically-important receptors [137], [54]. It is used here to predict the interactions between AChE and an inhibitor, suggesting the inhibitor's binding mode(s).

Using the Marvin Sketch program (Chem Axon), compounds were converted from 2D to 3D structures, after which an initial structural energy minimization was performed using the energy gradient optimization method. Chimera (UCSF [138]) was then used to perform a full structural minimization (using steepest decent followed by conjugate gradient), to calculate total charges on the molecules, and to add all remaining hydrogens not explicitly defined in the 2D structure. DOCK 6.3 was then used for all docking analyses. The success rate, the percentage of generated conformations that have a heavy atom RMSD equal to or less than 2 Å of the crystal structure pose, for DOCK (70%) is comparable to FlexX (61%), Glide (82%), and GOLD (77%) [139, 140]. Default parameters were used throughout the flexible docking analysis, with the exception of number of orientations, which was varied through the course of several docking simulations (1000 to 30,000 orientations evaluated). When the docking simulation did not locate a minimum for a particular compound (incomplete docking) the orientation number was increased for the dataset. Four acetylcholinesterase structures (pdb codes 1ACL, 1DX6, 1EVE and 1ACJ) were used for all docking analysis. The active site was identified using the ligands galanthamine, donepezil and tacrine located in the crystal structures of 1DX6, 1EVE and 1ACJ, respectively. For the 1ACL, to define the active site with a clinically-used inhibitor the decamethonium ion was deleted, donepezil was placed in the active site by aligning the 1EVE receptor to 1ACL then

deleting the 1EVE receptor. A 12 Å receptor box was used for docking inhibitors into the enzyme crystal structures. We generated all molecular graphics images using the UCSF Chimera package.

The marine products aplysamine and Poly-APS were excluded from the docking analysis since aplysamine is an allosteric site inhibitor [163], and the Poly-APS are large molecular weight polymers; these compounds are not discussed in this paper. All other compounds were docked in their neutral state. The inhibitor from the crystal structure of each AChE was also docked into all AChE structures, including its own, to verify that the docking algorithm could correctly identify known crystal structure poses. Galanthamine has a conserved water molecule, to which the hydroxyl group H-bonds. Docking galanthamine into its own receptor with and without this conserved water molecule both resulted in the crystallographic pose being selected. All inhibitors generated similar scores in each receptor with the exception of donepezil in the 1ACJ receptor (Table 6-1). The drastic difference between donepezil in the tacrine receptor makes sense, since the Phe-330 residue is in an orientation that cannot interact with the piperidine moiety, a critical interaction for this inhibitor. Our docking results are consistent with the observed experimental data for onchidal, marinoquinoline, and tetrazacyclozulapentene compound interactions with AChE. Our data also suggest new target regions within the AChE receptor, potential structural scaffolds for novel AChE inhibitors, and reasonable binding modes for the plastoquinones and farnesylacetones. The binding scores from the docking analysis could not accurately be compared to the literature inhibition values determined experimentally since several reported values are given as IC_{50}, a unit that is concentration dependent, and concentrations of enzymes used for performing the assay were not always reported in the literature. The docking scores themselves are internally consistent.

PUBLICATION NOTICE

This work will be submitted to the Journal of Molecular Modeling in 2013.

CHAPTER 7 SUMMARY OF RESEARCH IMPLICATIONS AND FUTURE RESEARCH

This goal of this work was to define contributions that contribute to the potency, solubility, and selectivity of CE inhibitors. This would help us to be able to design novel CES2 specific inhibitors. This work addressed three major questions to help us better design novel CES2 inhibitors. First, how do make potent CES inhibitors? Second, how do we design soluble CES2 inhibitors? Last, how do we develop selective CES2 inhibitors?

In chapter 3 we used an expanded set of sulfonamide inhibitors to develop a new QSAR model. This was performed to further delineate the structural features that made this class of CE inhibitors potent. Our new QSAR model expanded our knowledge on why the sulfonamide inhibitors were potent. It showed that (i. Increasing hydrophobicity of the core sulfonamide scaffold, (ii.) halogen substitution at the distal benzyl rings improved potency (iii.) placement of those halogens in the meta or para position, (iv.) removal of moderately EWG from the para position, and (v.) removal of bulky groups from the core benzene ring would all improve the potency of the sulfonamide scaffold. This information helped us to address the question, "how do we make CES2 inhibitor potent?"

In chapter 4 and 5 a multi-scaffold QSAR model was developed and used as a hypothetical pocket site for in silico design to generate soluble new soluble CE inihibtors. These chapters showed us that we could use a dual method approach of generating a QSAR model

followed by in silico design to generate novel scaffolds that had improved solubility relative to the sulfonamide scaffold. The biggest aid in generating soluble scaffolds however was the use of the four disparate classes of CES2 inhibitor compounds, thus, answering the question of how to design soluble CES2 inhibitors. It was the inclusion of four CE inhibitor classes that allowed us to create compounds with the best features of each class. The novelty of this approach is that it was performed for an enzyme target that has no experimentally derived 3D structure. A process like this could be applied to many targets were no structural information of the target macromolecule is known. This would play a significant role in the drug discovery industry.

In chapter 5, we also developed a docking model that helped us to determine some features that confere specificity on the sulfonamide compounds. Our models showed that interactions with the internal loop 7 were important in determining inhibitor selectivity between CES1 and CES2. With further development this model could be used as a predictive model to filter out nonspecific inhibitors.

Chapter 6 investigated another alpha/beta hydrolase protein acetycholinesterase. We predicted through a docking analysis that the marine metabolite onchidal interacts with the oxyaninon hole of Loop 7 in AChE. We suggested through docking the binding mode of 7 competive acetylcholinesterase inhibitors derived from marine natural products.

Using the three models we have developed, we can develop compounds, which will be potent, soluble, and selective against CES2. A system like this is not limited to just alpha/beta hydrolases, but could be applied to many protein systems. Fuuture studies should synthesize a large pool of the generated compounds and assay them against the CEs and cholinesterases enzymes to deteremine their potency, solubility, and specificity.

BIBLIOGRAPHY

1. Ollis DL, Cheah E, Cygler M, Dijkstra B, Frolow F, Franken SM, Harel M, Remington SJ, Silman I, Schrag J *et al*: **The alpha/beta hydrolase fold**. *Protein Eng* 1992, **5**(3):197-211.

2. Vorobiev SM, Su M, Seetharaman J, Huang YJ, Chen CX, Maglaqui M, Janjua H, Proudfoot M, Yakunin A, Xiao R *et al*: **Crystal structure of human retinoblastoma binding protein 9**. *Proteins* 2009, **74**(2):526-529.

3. Strop P, Bankovich AJ, Hansen KC, Garcia KC, Brunger AT: **Structure of a human A-type potassium channel interacting protein DPPX, a member of the dipeptidyl aminopeptidase family**. *J Mol Biol* 2004, **343**(4):1055-1065.

4. Carr PD, Ollis DL: **Alpha/beta hydrolase fold: an update**. *Protein Pept Lett* 2009, **16**(10):1137-1148.

5. Potter PM, Wadkins RM: **Carboxylesterases--detoxifying enzymes and targets for drug therapy**. *Current Medicinal Chemistry* 2006, **13**(9):1045-1054.

6. Soni KG, Lehner R, Metalnikov P, O'Donnell P, Semache M, Gao W, Ashman K, Pshezhetsky AV, Mitchell GA: **Carboxylesterase 3 (EC 3.1.1.1) is a major adipocyte lipase**. *Journal of Biological Chemistry* 2004, **279**(39):40683-40689.

7. Potter PM, Wadkins RM: **Carboxylesterases--detoxifying enzymes and targets for drug therapy**. *Curr Med Chem* 2006, **13**(9):1045-1054.

8. Carvalho CM, Aires-Barros MR, Cabral JM: **Cutinase: from molecular level to bioprocess development**. *Biotechnol Bioeng* 1999, **66**(1):17-34.

9. Heikinheimo P, Goldman A, Jeffries C, Ollis DL: **Of barn owls and bankers: a lush variety of alpha/beta hydrolases**. *Structure* 1999, **7**(6):R141-146.

10. Nardini M, Dijkstra BW: **Alpha/beta hydrolase fold enzymes: the family keeps growing**. *Curr Opin Struct Biol* 1999, **9**(6):732-737.

11. Satoh T, Hosokawa M: **The mammalian carboxylesterases: from molecules to functions**. *Annual Review of Pharmacology & Toxicology* 1998, **38**:257-288.

12. Khanna R, Morton CL, Danks MK, Potter PM: **Proficient metabolism of irinotecan by a human intestinal carboxylesterase**. *Cancer Research* 2000, **60**(17):4725-4728.

13. Alexson SE, Diczfalusy M, Halldin M, Swedmark S: **Involvement of liver carboxylesterases in the in vitro metabolism of lidocaine**. *Drug Metabolism & Disposition* 2002, **30**(6):643-647.

14. Ross MK, Borazjani A, Edwards CC, Potter PM: **Hydrolytic metabolism of pyrethroids by human and other mammalian carboxylesterases**. *Biochem Pharmacol* 2006, **71**(5):657-669.

15. Jokanovic M, Kosanovic M, Maksimovic M: **Interaction of organophosphorus compounds with carboxylesterases in the rat**. *Arch Toxicol* 1996, **70**(7):444-450.

16. Wallace TJ, Ghosh S, McLean Grogan W: **Molecular cloning and expression of rat lung carboxylesterase and its potential role in the detoxification of organophosphorus compounds**. *American Journal of Respiratory Cell & Molecular Biology* 1999, **20**(6):1201-1208.

17. Humerickhouse R, Lohrbach K, Li L, Bosron WF, Dolan ME: **Characterization of CPT-11 hydrolysis by human liver carboxylesterase isoforms hCE-1 and hCE-2**. *Cancer Research* 2000, **60**(5):1189-1192.

18. Spiller B, Gershenson A, Arnold FH, Stevens RC: **A structural view of evolutionary divergence**. *Proc Natl Acad Sci U S A* 1999, **96**(22):12305-12310.

19. Wierdl M, Morton CL, Nguyen NK, Redinbo MR, Potter PM: **Molecular modeling of CPT-11 metabolism by carboxylesterases (CEs): use of pnb CE as a model**. *Biochemistry* 2004, **43**(7):1874-1882.

20. Yu X, Sigler SC, Hossain D, Wierdl M, Gwaltney SR, Potter PM, Wadkins RM: **Global and local molecular dynamics of a bacterial carboxylesterase provide insight into its catalytic mechanism**. *J Mol Model* 2011, **18**(6):2869-2883.

21. Hatfield MJ, Potter PM: **Carboxylesterase inhibitors**. *Expert Opin Ther Pat* 2011, **21**(8):1159-1171.

22. Wadkins RM, Hyatt JL, Wei X, Yoon KJ, Wierdl M, Edwards CC, Morton CL, Obenauer JC, Damodaran K, Beroza P *et al*: **Identification and characterization of novel benzil (diphenylethane-1,2-dione) analogues as inhibitors of mammalian carboxylesterases**. *J Med Chem* 2005, **48**(8):2906-2915.

23. Hicks LD, Hyatt JL, Stoddard S, Tsurkan L, Edwards CC, Wadkins RM, Potter PM: **Improved, Selective, Human Intestinal Carboxylesterase Inhibitors Designed to Modulate 7-Ethyl-10-[4-(1-piperidino)-1-piperidino]carbonyloxycamptothecin (Irinotecan; CPT-11) Toxicity**. *Journal of Medicinal Chemistry* 2009, **52**(12):3742-3752.

24. Fujita T, Iwasa, J., Hansch, C.: **A New Substituent Constant, π , Derived from Partition Coefficients**. *The Journal of the American Chemical Society* 1964, **86**:5175-5180.

25. Hansch C, Fujita, T.: **ρ - σ - π Analysis - A Method for the Correlation of Biological Activity and Chemical Structure**. *Journal of the American Chemical Society* 1964, **86**:1616-1626.

26. Hansch C: **Quantitative approach to biochemical structure-activity relationships**. *Accounts of chemical research* 1969, **2**:232-239.

27. Wadkins RM, Hyatt JL, Yoon KJ, Morton CL, Lee RE, Damodaran K, Beroza P, Danks MK, Potter PM: **Discovery of novel selective inhibitors of human intestinal carboxylesterase for the amelioration of irinotecan-induced diarrhea: synthesis, quantitative structure-activity relationship analysis, and biological activity**. *Molecular Pharmacology* 2004, **65**(6):1336-1343.

28. Hicks LD, Hyatt JL, Stoddard S, Tsurkan L, Edwards CC, Wadkins RM, Potter PM: **Improved, selective, human intestinal carboxylesterase inhibitors designed to modulate 7-ethyl-10-[4-(1-piperidino)-1-piperidino]carbonyloxycamptothecin (Irinotecan; CPT-11) toxicity**. *Journal of Medicinal Chemistry* 2009, **52**(12):3742-3752.

29. Meek AR, Simms GA, Weaver DF: **Searching for an endogenous anti-Alzheimer molecule: identifying small molecules in the brain that slow Alzheimer disease progression by inhibition of beta-amyloid aggregation**. *J Psychiatry Neurosci* 2012, **38**(1):120166.

30. Gueto C, Torres J, Vivas-Reyes R: **CoMFA, LeapFrog and blind docking studies on sulfonanilide derivatives acting as selective aromatase expression regulators**. *Eur J Med Chem* 2009, **44**(9):3445-3451.

31. Gueto C, Ruiz JL, Torres JE, Mendez J, Vivas-Reyes R: **Three-dimensional quantitative structure-activity relationship studies on novel series of benzotriazine based compounds acting as Src inhibitors using CoMFA and CoMSIA**. *Bioorg Med Chem* 2008, **16**(5):2439-2447.

32. Speck-Planche A, Kleandrova VV, Cordeiro MN: **New insights toward the discovery of antibacterial agents: multi-tasking QSBER model for the simultaneous prediction of anti-tuberculosis activity and toxicological profiles of drugs**. *Eur J Pharm Sci* 2012, **48**(4-5):812-818.

33. Freyhult EK, Andersson K, Gustafsson MG: **Structural modeling extends QSAR analysis of antibody-lysozyme interactions to 3D-QSAR**. *Biophys J* 2003, **84**(4):2264-2272.

34. Pasquale G, Romanelli GP, Autino JC, Garcia J, Ortiz EV, Duchowicz PR: **Quantitative structure-activity relationships of mosquito larvicidal chalcone derivatives**. *J Agric Food Chem*, **60**(2):692-697.

35. Hawkins GDG, D.; Lynch, G.; Chambers, C.; Rossi, I.; Storer, J.; Li, J.; Zhu, T.; Thompson, J.; Winget, P.; Lynch, B.; Rinaldi, D.; Liotad, D.; Cramer, C. J.; Truhlar, D. G.: **Amsol version 7.1**. In. Minneapolis: University of Minnesota; 2004.

36. Winget P, Thompson JD, Cramer CJ, Truhlar DG: **Parametrization of a universal solvation model for molecules containing silicon**. *Journal of Physical Chemistry A* 2002, **106**(20):5160-5168.

37. Wang RX, Gao Y, Lai LH: **LigBuilder: A multi-purpose program for structure-based drug design**. *Journal of Molecular Modeling* 2000, **6**(7-8):498-516.

38. Pearlman DA, Murcko MA: **CONCERTS: dynamic connection of fragments as an approach to de novo ligand design**. *Journal of Medicinal Chemistry* 1996, **39**(8):1651-1663.

39. Goodford PJ: **A computational procedure for determining energetically favorable binding sites on biologically important macromolecules**. *Journal of Medicinal Chemistry* 1985, **28**(7):849-857.

40. Payne AW, Glen RC: **Molecular recognition using a binary genetic search algorithm**. *Journal of Molecular Graphics* 1993, **11**(2):74-91.

41. Gillet VJ, Newell W, Mata P, Myatt G, Sike S, Zsoldos Z, Johnson AP: **SPROUT: recent developments in the de novo design of molecules**. *Journal of Chemical Information & Computer Sciences* 1994, **34**(1):207-217.

42. Law JMS, Fung DYK, Zsoldos Z, Simon A, Szabo Z, Csizmadia IG, Johnson AP: **Validation of the SPROUT de novo design program**. *J Mol Struc-Theochem* 2003, **666**:651-657.

43. Vinkers HM, de Jonge MR, Daeyaert FF, Heeres J, Koymans LM, van Lenthe JH, Lewi PJ, Timmerman H, Van Aken K, Janssen PA: **SYNOPSIS: SYNthesize and OPtimize System in Silico**. *Journal of Medicinal Chemistry* 2003, **46**(13):2765-2773.

44. Tetko IV, Gasteiger J, Todeschini R, Mauri A, Livingstone D, Ertl P, Palyulin VA, Radchenko EV, Zefirov NS, Makarenko AS *et al*: **Virtual computational chemistry laboratory--design and description**. *J Comput Aided Mol Des* 2005, **19**(6):453-463.

45. **VCCLAB Virtual Computational Chemistry Lab, http://www.vcclab.org**

46. Qu H, Ricklin D, Bai H, Chen H, Reis ES, Maciejewski M, Tzekou A, Deangelis RA, Resuello RR, Lupu F *et al*: **New analogs of the clinical complement inhibitor compstatin with subnanomolar affinity and enhanced pharmacokinetic properties**. *Immunobiology* 2012.

47. Tanabe G, Nakamura S, Tsutsui N, Balakishan G, Xie W, Tsuchiya S, Akaki J, Morikawa T, Ninomiya K, Nakanishi I *et al*: **In silico design, synthesis and evaluation of 3'-O-benzylated analogs of salacinol, a potent alpha-glucosidase inhibitor isolated from an Ayurvedic traditional medicine "Salacia"**. *Chem Commun (Camb)* 2012, **48**(69):8646-8648.

48. Simonelli L, Beltramello M, Yudina Z, Macagno A, Calzolai L, Varani L: **Rapid structural characterization of human antibody-antigen complexes through experimentally validated computational docking**. *J Mol Biol* 2010, **396**(5):1491-1507.

49. Weidlich IE, Dexheimer T, Marchand C, Antony S, Pommier Y, Nicklaus MC: **Inhibitors of human tyrosyl-DNA phospodiesterase (hTdp1) developed by virtual screening using ligand-based pharmacophores**. *Bioorg Med Chem* 2010, **18**(1):182-189.

50. Goodsell DS, Olson AJ: **Automated docking of substrates to proteins by simulated annealing**. *Proteins* 1990, **8**(3):195-202.

51. Welch W, Ruppert J, Jain AN: **Hammerhead: fast, fully automated docking of flexible ligands to protein binding sites**. *Chem Biol* 1996, **3**(6):449-462.

52. Rarey M, Kramer B, Lengauer T, Klebe G: **A fast flexible docking method using an incremental construction algorithm**. *J Mol Biol* 1996, **261**(3):470-489.

53. Oshiro CM, Kuntz ID, Dixon JS: **Flexible ligand docking using a genetic algorithm**. *J Comput Aided Mol Des* 1995, **9**(2):113-130.

54. Ewing TJ, Makino S, Skillman AG, Kuntz ID: **DOCK 4.0: search strategies for automated molecular docking of flexible molecule databases**. *J Comput Aided Mol Des* 2001, **15**(5):411-428.

55. McGann MR, Almond HR, Nicholls A, Grant JA, Brown FK: **Gaussian docking functions**. *Biopolymers* 2003, **68**(1):76-90.

56. Morris GM, Huey R, Lindstrom W, Sanner MF, Belew RK, Goodsell DS, Olson AJ: **AutoDock4 and AutoDockTools4: Automated docking with selective receptor flexibility**. *J Comput Chem* 2009, **30**(16):2785-2791.

57. Friesner RA, Banks JL, Murphy RB, Halgren TA, Klicic JJ, Mainz DT, Repasky MP, Knoll EH, Shelley M, Perry JK *et al*: **Glide: a new approach for rapid, accurate docking and scoring. 1. Method and assessment of docking accuracy**. *J Med Chem* 2004, **47**(7):1739-1749.

58. Jones G, Willett P, Glen RC, Leach AR, Taylor R: **Development and validation of a genetic algorithm for flexible docking**. *J Mol Biol* 1997, **267**(3):727-748.

59. Jain AN: **Surflex: fully automatic flexible molecular docking using a molecular similarity-based search engine**. *J Med Chem* 2003, **46**(4):499-511.

60. Leach AR, Dolata DP, Prout K: **Automated conformational analysis and structure generation: algorithms for molecular perception**. *J Chem Inf Comput Sci* 1990, **30**(3):316-324.

61. Cashman JR, Perotti BY, Berkman CE, Lin J: **Pharmacokinetics and molecular detoxication**. *Environ Health Perspect* 1996, **104 Suppl 1**:23-40.

62. Kunimoto T, Nitta K, Tanaka T, Uehara N, Baba H, Takeuchi M, Yokokura T, Sawada S, Miyasaka T, Mutai M: **Antitumor activity of 7-ethyl-10-[4-(1-piperidino)-1-piperidino]carbonyloxy-camptothec in, a novel water-soluble derivative of camptothecin, against murine tumors**. *Cancer Res* 1987, **47**(22):5944-5947.

63. Bencharit S, Morton CL, Xue Y, Potter PM, Redinbo MR: **Structural basis of heroin and cocaine metabolism by a promiscuous human drug-processing enzyme**. *Nat Struct Biol* 2003, **10**(5):349-356.

64. Brzezinski MR, Spink BJ, Dean RA, Berkman CE, Cashman JR, Bosron WF: **Human liver carboxylesterase hCE-1: binding specificity for cocaine, heroin, and their metabolites and analogs**. *Drug Metab Dispos* 1997, **25**(9):1089-1096.

65. Kamendulis LM, Brzezinski MR, Pindel EV, Bosron WF, Dean RA: **Metabolism of cocaine and heroin is catalyzed by the same human liver carboxylesterases**. *J Pharmacol Exp Ther* 1996, **279**(2):713-717.

66. Pindel EV, Kedishvili NY, Abraham TL, Brzezinski MR, Zhang J, Dean RA, Bosron WF: **Purification and cloning of a broad substrate specificity human liver carboxylesterase that catalyzes the hydrolysis of cocaine and heroin**. *J Biol Chem* 1997, **272**(23):14769-14775.

67. Potter PM, Pawlik CA, Morton CL, Naeve CW, Danks MK: **Isolation and partial characterization of a cDNA encoding a rabbit liver carboxylesterase that activates the prodrug irinotecan (CPT-11)**. *Cancer Res* 1998, **58**(12):2646-2651.

68. Quinney SK, Sanghani SP, Davis WI, Hurley TD, Sun Z, Murry DJ, Bosron WF: **Hydrolysis of capecitabine to 5'-deoxy-5-fluorocytidine by human carboxylesterases and inhibition by loperamide**. *J Pharmacol Exp Ther* 2005, **313**(3):1011-1016.

69. Shi D, Yang J, Yang D, LeCluyse EL, Black C, You L, Akhlaghi F, Yan B: **Anti-influenza prodrug oseltamivir is activated by carboxylesterase human carboxylesterase 1, and the activation is inhibited by antiplatelet agent clopidogrel**. *J Pharmacol Exp Ther* 2006, **319**(3):1477-1484.

70. Tabata T, Katoh M, Tokudome S, Nakajima M, Yokoi T: **Identification of the cytosolic carboxylesterase catalyzing the 5'-deoxy-5-fluorocytidine formation from capecitabine in human liver**. *Drug Metab Dispos* 2004, **32**(10):1103-1110.

71. Tsuji T, Kaneda N, Kado K, Yokokura T, Yoshimoto T, Tsuru D: **CPT-11 converting enzyme from rat serum: purification and some properties**. *J Pharmacobiodyn* 1991, **14**(6):341-349.

72. Wierdl M, Tsurkan L, Hyatt JL, Edwards CC, Hatfield MJ, Morton CL, Houghton PJ, Danks MK, Redinbo MR, Potter PM: **An improved human carboxylesterase for enzyme/prodrug therapy with CPT-11**. *Cancer Gene Ther* 2008, **15**(3):183-192.

73. Zhang J, Burnell JC, Dumaual N, Bosron WF: **Binding and hydrolysis of meperidine by human liver carboxylesterase hCE-1**. *J Pharmacol Exp Ther* 1999, **290**(1):314-318.

74. Stampfli HF, Quon CY: **Polymorphic metabolism of flestolol and other ester containing compounds by a carboxylesterase in New Zealand white rabbit blood and cornea**. *Res Commun Mol Pathol Pharmacol* 1995, **88**(1):87-97.

75. Morton CL, Iacono L, Hyatt JL, Taylor KR, Cheshire PJ, Houghton PJ, Danks MK, Stewart CF, Potter PM: **Activation and antitumor activity of CPT-11 in plasma esterase-deficient mice**. *Cancer Chemother Pharmacol* 2005, **56**(6):629-636.

76. Beroza P, Damodaran K, Lum RT: **Target-related affinity profiling: Telik's lead discovery technology**. *Curr Top Med Chem* 2005, **5**(4):371-381.

77. Bencharit S, Morton CL, Hyatt JL, Kuhn P, Danks MK, Potter PM, Redinbo MR: **Crystal structure of human carboxylesterase 1 complexed with the Alzheimer's drug tacrine: From binding promiscuity to selective inhibition**. *Chemistry & Biology* 2003, **10**(4):341-349.

78. Webb JL: **Enzyme and Metabolic Inhibitors, Volume 1. General Principles of Inhibition**: Academic Press Inc.: New York, 1963; 1963.

79. Lundstedt T, Seifert, E., Abramo, L., Thelin, B., Nystrom, A., Petterson, J., Bergman R.: **Experimental design and optimization**. *Chemometrics and Intellignet Laboratory Systems* 1998, **42**:3-40.

80. Wadkins RM, Morton CL, Weeks JK, Oliver L, Wierdl M, Danks MK, Potter PM: **Structural constraints affect the metabolism of 7-ethyl-10-[4-(1-piperidino)-1-piperidino]carbonyloxycamptothecin (CPT-11) by carboxylesterases**. *Molecular Pharmacology* 2001, **60**(2):355-362.

81. Merritt EA, Bacon DJ: **Raster3D: photorealistic molecular graphics**. *Methods Enzymol* 1997, **277**:505-524.

82. Hicks LD, Hyatt JL, Moak T, Edwards CC, Tsurkan L, Wierdl M, Ferreira AM, Wadkins RM, Potter PM: **Analysis of the inhibition of mammalian carboxylesterases by novel fluorobenzoins and fluorobenzils**. *Bioorganic & Medicinal Chemistry* 2007, **15**(11):3801-3817.

83. Hyatt JL, Moak T, Hatfield MJ, Tsurkan L, Edwards CC, Wierdl M, Danks MK, Wadkins RM, Potter PM: **Selective inhibition of carboxylesterases by isatins, indole-2,3-diones**. *Journal of Medicinal Chemistry* 2007, **50**(8):1876-1885.

84. Hyatt JL, Stacy V, Wadkins RM, Yoon KJ, Wierdl M, Edwards CC, Zeller M, Hunter AD, Danks MK, Crundwell G *et al*: **Inhibition of carboxylesterases by benzil (diphenylethane-1,2-dione) and heterocyclic analogues is dependent upon the aromaticity of the ring and the flexibility of the dione moiety**. *J Med Chem* 2005, **48**(17):5543-5550.

85. Wadkins RM, Hyatt JL, Edwards CC, Tsurkan L, Redinbo MR, Wheelock CE, Jones PD, Hammock BD, Potter PM: **Analysis of mammalian carboxylesterase inhibition by trifluoromethylketone-containing compounds**. *Molecular Pharmacology* 2007, **71**(3):713-723.

86. Wadkins RM, Hyatt JL, Wei X, Yoon KJ, Wierdl M, Edwards CC, Morton CL, Obenauer JC, Damodaran K, Beroza P *et al*: **Identification and characterization of novel benzil (diphenylethane-1,2-dione) analogues as inhibitors of mammalian carboxylesterases**. *Journal of Medicinal Chemistry* 2005, **48**(8):2906-2915.

87. Brandstetter H, Turk D, Hoeffken HW, Grosse D, Sturzebecher J, Martin PD, Edwards BF, Bode W: **Refined 2.3 A X-ray crystal structure of bovine thrombin complexes formed with the benzamidine and arginine-based thrombin inhibitors NAPAP, 4-TAPAP and MQPA. A starting point for improving antithrombotics**. *J Mol Biol* 1992, **226**(4):1085-1099.

88. Okamoto S, Kinjo K, Hijikata A, Kikumoto R, Tamao Y, Ohkubo K, Tonomura S: **Thrombin inhibitors. 1. Ester derivatives of N alpha-(arylsulfonyl)-L-arginine**. *J Med Chem* 1980, **23**(8):827-830.

89. Sturzebecher J, Markwardt F, Voigt B, Wagner G, Walsmann P: **Cyclic amides of N alpha-arylsulfonylaminoacylated 4-amidinophenylalanine--tight binding inhibitors of thrombin**. *Thromb Res* 1983, **29**(6):635-642.

90. Stewart JJ: **MOPAC: a semiempirical molecular orbital program**. *J Comput Aided Mol Des* 1990, **4**(1):1-105.

91. Vedani A, Dobler M: **5D-QSAR: the key for simulating induced fit?** *Journal of Medicinal Chemistry* 2002, **45**(11):2139-2149.

92. Vedani A, Dobler M, Lill MA: **Combining protein modeling and 6D-QSAR. Simulating the binding of structurally diverse ligands to the estrogen receptor**. *J Med Chem* 2005, **48**(11):3700-3703.

93. Nardini M, Dijkstra BW: **Alpha/beta hydrolase fold enzymes: the family keeps growing**. *Current Opinion in Structural Biology* 1999, **9**(6):732-737.

94. Ollis DL, Cheah E, Cygler M, Dijkstra B, Frolow F, Franken SM, Harel M, Remington SJ, Silman I, Schrag J: **The alpha/beta hydrolase fold**. *Protein Engineering* 1992, **5**(3):197-211.

95. Satoh T, Hosokawa M: **Structure, function and regulation of carboxylesterases**. *Chem Biol Interact* 2006, **162**(3):195-211.

96. Kweekel D, Guchelaar HJ, Gelderblom H: **Clinical and pharmacogenetic factors associated with irinotecan toxicity**. *Cancer Treat Rev* 2008, **34**(7):656-669.

97. Hatfield JM, Wierdl M, Wadkins RM, Potter PM: **Modifications of human carboxylesterase for improved prodrug activation**. *Expert Opin Drug Metab Toxicol* 2008, **4**(9):1153-1165.

98. Lenz DE, Yeung D, Smith JR, Sweeney RE, Lumley LA, Cerasoli DM: **Stoichiometric and catalytic scavengers as protection against nerve agent toxicity: a mini review**. *Toxicology* 2007, **233**(1-3):31-39.

99. Hemmert AC, Tamara C. Otto, Monika Weirdl, Carol C. Edwards, Christopher D. Fleming, Mary MacDonald, John R. Cashman, Philip M. Potter, Cerasoli DM, Redinbo M: **Human Carboxylesterase 1 Stereoselectively Binds the Nerve Agent Cyclosarin and Spontaneously Hydrolyzes the Nerve Agent Sarin**. *molecular pharmacology* 2010.

100. McGleenon BM, Dynan KB, Passmore AP: **Acetylcholinesterase inhibitors in Alzheimer's disease**. *British Journal of Clinical Pharmacology* 1999, **48**(4):471-480.

101. Hyatt JL, Tsurkan L, Morton CL, Yoon KJ, Harel M, Brumshtein B, Silman I, Sussman JL, Wadkins RM, Potter PM: **Inhibition of acetylcholinesterase by the anticancer prodrug CPT-11**. *Chem Biol Interact* 2005, **157-158**:247-252.

102. Yoon KJ, Hyatt JL, Morton CL, Lee RE, Potter PM, Danks MK: **Characterization of inhibitors of specific carboxylesterases: development of carboxylesterase inhibitors for translational application**. *Molecular Cancer Therapeutics* 2004, **3**(8):903-909.

103. Morton CL, Wadkins RM, Danks MK, Potter PM: **The anticancer prodrug CPT-11 is a potent inhibitor of acetylcholinesterase but is rapidly catalyzed to SN-38 by butyrylcholinesterase**. *Cancer Res* 1999, **59**(7):1458-1463.

104. Hsu N, Cai D, Damodaran K, Gomez RF, Keck JG, Laborde E, Lum RT, Macke TJ, Martin G, Schow SR *et al*: **Novel cyclooxygenase-1 inhibitors discovered using affinity fingerprints**. *Journal of Medicinal Chemistry* 2004, **47**(20):4875-4880.

105. Fleming CD, Bencharit S, Edwards CC, Hyatt JL, Tsurkan L, Bai F, Fraga C, Morton CL, Howard-Williams EL, Potter PM *et al*: **Structural insights into drug processing by human carboxylesterase 1: tamoxifen, mevastatin, and inhibition by benzil**. *Journal of Molecular Biology* 2005, **352**(1):165-177.

106. Hyatt JL, Wadkins RM, Tsurkan L, Hicks LD, Hatfield MJ, Edwards CC, Ross CR, 2nd, Cantalupo SA, Crundwell G, Danks MK *et al*: **Planarity and constraint of the carbonyl groups in 1,2-diones are determinants for selective inhibition of human carboxylesterase 1**. *Journal of Medicinal Chemistry* 2007, **50**(23):5727-5734.

107. Lushington GH, Guo JX, Hurley MM: **Acetylcholinesterase: molecular modeling with the whole toolkit**. *Curr Top Med Chem* 2006, **6**(1):57-73.

108. Bencharit S, Morton CL, Howard-Williams EL, Danks MK, Potter PM, Redinbo MR: **Structural insights into CPT-11 activation by mammalian carboxylesterases**. *Nature Structural Biology* 2002, **9**(5):337-342.

109. Tara S, Helms V, Straatsma TP, McCammon JA: **Molecular dynamics of mouse acetylcholinesterase complexed with huperzine A**. *Biopolymers* 1999, **50**(4):347-359.

110. Suhre K, Sanejouand YH: **ElNemo: a normal mode web server for protein movement analysis and the generation of templates for molecular replacement**. *Nucleic Acids Res* 2004, **32**(Web Server issue):W610-614.

111. Kua J, Zhang Y, McCammon JA: **Studying enzyme binding specificity in acetylcholinesterase using a combined molecular dynamics and multiple docking approach**. *J Am Chem Soc* 2002, **124**(28):8260-8267.

112. Harada T, Nakagawa Y, Wadkins RM, Potter PM, Wheelock CE: **Comparison of benzil and trifluoromethyl ketone (TFK)-mediated carboxylesterase inhibition using classical and 3D-quantitative structure-activity relationship analysis**. *Bioorganic & Medicinal Chemistry* 2009, **17**(1):149-164.

113. Vangrevelinghe E, Rudisser S: **Computational approaches for fragment optimization**. *Curr Comput-Aid Drug* 2007, **3**(1):69-83.

114. Gueto C, Torres J, Vivas-Reyes R: **CoMFA, LeapFrog and blind docking studies on sulfonanilide derivatives acting as selective aromatase expression regulators**. *European Journal of Medicinal Chemistry* 2009, **44**(9):3445-3451.

115. Kapou A, Benetis NP, Durdagi S, Nikolaropoulos S, Mavromoustakos T: **3D QSAR/CoMFA and CoMSIA studies on antileukemic steroidal esters coupled with conformationally flexible nitrogen mustards**. *Journal of Chemical Information & Modeling* 2008, **48**(11):2254-2264.

116. Kumar A, Siddiqi MI: **CoMFA based de novo design of pyrrolidine carboxamides as inhibitors of enoyl acyl carrier protein reductase from Mycobacterium tuberculosis**. *Journal of Molecular Modeling* 2008, **14**(10):923-935.

117. Makhija MT, Kasliwal RT, Kulkarni VM, Neamati N: **De novo design and synthesis of HIV-1 integrase inhibitors**. *Bioorganic & Medicinal Chemistry* 2004, **12**(9):2317-2333.

118. Nair PC, Sobhia ME: **CoMFA based de novo design of pyridazine analogs as PTP1B inhibitors**. *Journal of Molecular Graphics & Modelling* 2007, **26**(1):117-123.

119. Spreafico M, Ernst B, Lill MA, Smiesko M, Vedani A: **Mixed-model QSAR at the glucocorticoid receptor: predicting the binding mode and affinity of psychotropic drugs**. *ChemMedChem* 2009, **4**(1):100-109.

120. Kraulis PJ: **Similarity of protein G and ubiquitin**. *Science* 1991, **254**(5031):581-582.

121. Lipinski CA: **Drug-like properties and the causes of poor solubility and poor permeability**. *J Pharmacol Toxicol Methods* 2000, **44**(1):235-249.

122. Tondel K, Drablos F: **Design of selective inhibitors of tyrosine kinase 2**. *Lett Drug Des Discov* 2005, **2**(7):507-515.

123. Morton CL, Potter PM: **Comparison of Escherichia coli, Saccharomyces cerevisiae, Pichia pastoris, Spodoptera frugiperda, and COS7 cells for recombinant gene expression. Application to a rabbit liver carboxylesterase**. *Mol Biotechnol* 2000, **16**(3):193-202.

124. Topai A, Breccia P, Minissi F, Padova A, Marini S, Cerbara I: **In silico scaffold evaluation and solid phase approach to identify new gelatinase inhibitors**. *Bioorg Med Chem* 2012, **20**(7):2323-2337.

125. Limbachiya MI: **Solubility Enhancement Techniques for Porrly Soluble Drugs: A Review**. *International Journal of Pharmaceutical Research and Development* 2012, **4**(4):071-086.

126. Jatwani S, Rana AC, Singh G, Aggarwal G: **An Overview on Solubility Enhancement Techniques for Poorly Soluble Drugs and Solid Dispersion as an Eminent Strategic Approach**. *International journal of pharmaceutical Sciences and Research* 2012, **3**(4):942-956.

127. Visentin S, Ermondi G, Medana C, Pedemonte N, Galietta L, Caron G: **Ligand-based design, in silico ADME-Tox filtering, synthesis and biological evaluation to discover new soluble 1,4-DHP-based CFTR activators**. *Eur J Med Chem* 2012, **55**:188-194.

128. Ohashi T, Oguro Y, Tanaka T, Shiokawa Z, Tanaka Y, Shibata S, Sato Y, Yamakawa H, Hattori H, Yamamoto Y *et al*: **Discovery of the investigational drug TAK-441, a pyrrolo[3,2-c]pyridine derivative, as a highly potent and orally active hedgehog signaling inhibitor: modification of the core skeleton for improved solubility**. *Bioorg Med Chem* 2012, **20**(18):5507-5517.

129. Guantai EM, Ncokazi K, Egan TJ, Gut J, Rosenthal PJ, Bhampidipati R, Kopinathan A, Smith PJ, Chibale K: **Enone- and chalcone-chloroquinoline hybrid analogues: in silico guided design, synthesis, antiplasmodial activity, in vitro metabolism, and mechanistic studies**. *J Med Chem* 2011, **54**(10):3637-3649.

130. Emmitte KA, Adjabeng GM, Andrews CW, Alberti JG, Bambal R, Chamberlain SD, Davis-Ward RG, Dickson HD, Hassler DF, Hornberger KR *et al*: **Design of potent thiophene inhibitors of polo-like kinase 1 with improved solubility and reduced protein binding**. *Bioorg Med Chem Lett* 2009, **19**(6):1694-1697.

131. Young BM, Hyatt JL, Bouck DC, Chen T, Hanumesh P, Price J, Boyd VA, Potter PM, Webb TR: **Structure-activity relationships of substituted 1-pyridyl-2-phenyl-1,2-ethanediones: potent, selective carboxylesterase inhibitors**. *J Med Chem* 2010, **53**(24):8709-8715.

132. Yoshizawa Y, Ogawara KI, Fushimi A, Abe S, Ishikawa K, Araki T, Molema G, Kimura T, Higaki K: **Deeper Penetration into Tumor Tissues and Enhanced in Vivo Antitumor Activity of Liposomal Paclitaxel by Pretreatment with Angiogenesis Inhibitor SU5416**. *Mol Pharm* 2012.

133. Stoddard SV, Yu XZ, Potter PM, Wadkins RM: **In silico design and evaluation of carboxylesterase inhibitors**. *Journal of Pesticide Science* 2010, **35**(3):240-249.

134. Bakker M, van Rantwijk F, Sheldon RA: **Metal substitution in thermolysin: Catalytic properties of tungstate thermolysin in sulfoxidation with H2O2**. *Canadian Journal of Chemistry-Revue Canadienne De Chimie* 2002, **80**(6):622-625.

135. Levin JI: **The design and synthesis of aryl hydroxamic acid inhibitors of MMPs and TACE**. *Curr Top Med Chem* 2004, **4**(12):1289-1310.

136. Hasegawa H, Holm L: **Advances and pitfalls of protein structural alignment**. *Current Opinion in Structural Biology* 2009, **19**(3):341-348.

137. Leach AR, Shoichet BK, Peishoff CE: **Prediction of protein-ligand interactions. Docking and scoring: successes and gaps**. *J Med Chem* 2006, **49**(20):5851-5855.

138. Pettersen EF, Goddard TD, Huang CC, Couch GS, Greenblatt DM, Meng EC, Ferrin TE: **UCSF Chimera--a visualization system for exploratory research and analysis**. *J Comput Chem* 2004, **25**(13):1605-1612.

139. Lang PT, Brozell SR, Mukherjee S, Pettersen EF, Meng EC, Thomas V, Rizzo RC, Case DA, James TL, Kuntz ID: **DOCK 6: combining techniques to model RNA-small molecule complexes**. *RNA* 2009, **15**(6):1219-1230.

140. Moustakas DT, Lang PT, Pegg S, Pettersen E, Kuntz ID, Brooijmans N, Rizzo RC: **Development and validation of a modular, extensible docking program: DOCK 5**. *J Comput Aided Mol Des* 2006, **20**(10-11):601-619.

141. Silverman R, B.: **The Organic Chemistry of Enzyme Catalyzed Reactions**, Revised Edition edn. San Diego, California: Academic Press; 2002.

142. Quinn DM: **Acetylcholinesterase - Enzyme Structure, Reaction Dynamics, and Virtual Transition-States**. *Chemical Reviews* 1987, **87**(5):955-979.

143. Sussman JL, Harel M, Frolow F, Oefner C, Goldman A, Toker L, Silman I: **Atomic structure of acetylcholinesterase from Torpedo californica: a prototypic acetylcholine-binding protein**. *Science* 1991, **253**(5022):872-879.

144. Harel M, Schalk I, Ehret-Sabatier L, Bouet F, Goeldner M, Hirth C, Axelsen PH, Silman I, Sussman JL: **Quaternary ligand binding to aromatic residues in the active-site gorge of acetylcholinesterase**. *Proc Natl Acad Sci U S A* 1993, **90**(19):9031-9035.

145. Shafferman A, Velan B, Ordentlich A, Kronman C, Grosfeld H, Leitner M, Flashner Y, Cohen S, Barak D, Ariel N: **Substrate inhibition of acetylcholinesterase: residues affecting signal transduction from the surface to the catalytic center**. *EMBO J* 1992, **11**(10):3561-3568.

146. Lahiri DK, Farlow MR, Sambamurti K, Greig NH, Giacobini E, Schneider LS: **A critical analysis of new molecular targets and strategies for drug developments in Alzheimer's disease**. *Curr Drug Targets* 2003, **4**(2):97-112.

147. Kandel E, R., Schwartx, James, H., Jessell, Thomas, M. In: *Principles of Neural Science.* Third edn. East Norfolk: Appelton; 1991: 975-983.

148. Fisher A: **Cholinergic modulation of amyloid precursor protein processing with emphasis on M1 muscarinic receptor: perspectives and challenges in treatment of Alzheimer's disease**. *J Neurochem*, **120 Suppl 1**:22-33.

149. Colombres M, Sagal JP, Inestrosa NC: **An overview of the current and novel drugs for Alzheimer's disease with particular reference to anti-cholinesterase compounds**. *Curr Pharm Des* 2004, **10**(25):3121-3130.

150. Farlow MR: **Pharmacokinetic profiles of current therapies for Alzheimer's disease: implications for switching to galantamine**. *Clin Ther* 2001, **23 Suppl A**:A13-24.

151. Selkoe DJ: **Alzheimer's disease: genes, proteins, and therapy**. *Physiol Rev* 2001, **81**(2):741-766.

152. Inestrosa NC, Alvarez A, Perez CA, Moreno RD, Vicente M, Linker C, Casanueva OI, Soto C, Garrido J: **Acetylcholinesterase accelerates assembly of amyloid-beta-peptides into Alzheimer's fibrils: possible role of the peripheral site of the enzyme**. *Neuron* 1996, **16**(4):881-891.

153. Greenberg SM, Tennis MK, Brown LB, Gomez-Isla T, Hayden DL, Schoenfeld DA, Walsh KL, Corwin C, Daffner KR, Friedman P *et al*: **Donepezil therapy in clinical practice: a randomized crossover study**. *Arch Neurol* 2000, **57**(1):94-99.

154. Castro A, Martinez A: **Peripheral and dual binding site acetylcholinesterase inhibitors: implications in treatment of Alzheimer's disease**. *Mini Rev Med Chem* 2001, **1**(3):267-272.

155. Munoz-Ruiz P, Rubio L, Garcia-Palomero E, Dorronsoro I, del Monte-Millan M, Valenzuela R, Usan P, de Austria C, Bartolini M, Andrisano V *et al*: **Design, synthesis, and biological evaluation of dual binding site acetylcholinesterase inhibitors: new disease-modifying agents for Alzheimer's disease**. *J Med Chem* 2005, **48**(23):7223-7233.

156. Newman DJ, Cragg GM: **Natural products as sources of new drugs over the last 25 years**. *J Nat Prod* 2007, **70**(3):461-477.

157. Mayer AM, Rodriguez AD, Berlinck RG, Hamann MT: **Marine pharmacology in 2003-4: marine compounds with anthelmintic antibacterial, anticoagulant, antifungal, anti-inflammatory, antimalarial, antiplatelet, antiprotozoal, antituberculosis, and antiviral activities; affecting the cardiovascular, immune and nervous systems, and other miscellaneous mechanisms of action**. *Comp Biochem Physiol C Toxicol Pharmacol* 2007, **145**(4):553-581.

158. Ireland CF, D. J.: **The Defensive Secretion of the Opisthobranch Mollusc *Onchidella binneyi*** *Bioorganic Chemistry* 1978, **7**:125-131.

159. Abramson SN, Radic Z, Manker D, Faulkner DJ, Taylor P: **Onchidal: a naturally occurring irreversible inhibitor of acetylcholinesterase with a novel mechanism of action**. *Mol Pharmacol* 1989, **36**(3):349-354.

160. Kanjana-Opas A, Panphon S, Fun HK, Chantrapromma S: **4-methyl-3H-pyrrolo[2,3-c]quinoline**. *Acta Crystallographica Section E-Structure Reports Online* 2006, **62**:O2728-O2730.

161. Sangnoi Y, Sakulkeo O, Yuenyongsawad S, Kanjana-opas A, Ingkaninan K, Plubrukarn A, Suwanborirux K: **Acetylcholinesterase-inhibiting activity of pyrrole derivatives from a novel marine gliding bacterium, Rapidithrix thailandica**. *Mar Drugs* 2008, **6**(4):578-586.

162. Turk T, Macek P, Suput D: **Inhibition of acetylcholinesterase by a pseudozoanthoxanthin-like compound isolated from the zoanthid Parazoanthus axinellae (O. Schmidt)**. *Toxicon* 1995, **33**(2):133-142.

163. Sepcic K, Mancini I, Vidic I, Franssanito R, Pietra F, Macek P, Turk T: **Antibacterial and anticholinesterase activities of aplysamine-4, a bromotyrosine-derived metabolite of a Red Sea marine sponge**. *J Nat Toxins* 2001, **10**(3):181-191.

164. Goud TV, Srinivasulu M, Reddy VL, Reddy AV, Rao TP, Kumar DS, Murty US, Venkateswarlu Y: **Two new bromotyrosine-derived metabolites from the sponge Psammaplysilla purpurea**. *Chem Pharm Bull (Tokyo)* 2003, **51**(8):990-993.

165. Choi BW, Ryu G, Park SH, Kim ES, Shin J, Roh SS, Shin HC, Lee BH: **Anticholinesterase activity of plastoquinones from Sargassum sagamianum: lead compounds for Alzheimer's disease therapy**. *Phytother Res* 2007, **21**(5):423-426.

166. Ryu G, Park SH, Kim ES, Choi BW, Ryu SY, Lee BH: **Cholinesterase inhibitory activity of two farnesylacetone derivatives from the brown alga Sargassum sagamianum**. *Archives of Pharmacal Research* 2003, **26**(10):796-799.

167. Turk T, Frangez R, Sepcic K: **Mechanisms of Toxicity of 3-Alkylpyridinium Polymers from Marine Sponge Reniera sarai**. *Mar Drugs* 2007, **5**(4):157-167.

168. Sepcic K, Marcel V, Klaebe A, Turk T, Suput D, Fournier D: **Inhibition of acetylcholinesterase by an alkylpyridinium polymer from the marine sponge, Reniera sarai**. *Biochimica Et Biophysica Acta-Protein Structure and Molecular Enzymology* 1998, **1387**(1-2):217-225.

169. Sepcic K: **Bioactive alkylpyridinium compounds from marine sponges**. *Journal of Toxicology-Toxin Reviews* 2000, **19**(2):139-160.

170. Hostettmann K, Borloz A, Urbain A, Marston A: **Natural product inhibitors of acetylcholinesterase**. *Current Organic Chemistry* 2006, **10**(8):825-847.

171. Robin G, Chappell K, Stoermer MJ, Hu SH, Young PR, Fairlie DP, Martin JL: **Structure of West Nile virus NS3 protease: ligand stabilization of the catalytic conformation**. *J Mol Biol* 2009, **385**(5):1568-1577.

172. Zhu L, George S, Schmidt MF, Al-Gharabli SI, Rademann J, Hilgenfeld R: **Peptide aldehyde inhibitors challenge the substrate specificity of the SARS-coronavirus main protease**. *Antiviral Res*, **92**(2):204-212.

173. Greenblatt HM, Kryger G, Lewis T, Silman I, Sussman JL: **Structure of acetylcholinesterase complexed with (-)-galanthamine at 2.3 angstrom resolution**. *Febs Letters* 1999, **463**(3):321-326.

174. Smith MM, J.: **MARCH's Advanced Organic Chemistry Reactions, Mechanisms, and Structure** 5edn: John Wiley & Sons; 2001.

175. Srisukchayakul P, Suwanachart C, Sangnoi Y, Kanjana-Opas A, Hosoya S, Yokota A, Arunpairojana V: **Rapidithrix thailandica gen. nov., sp. nov., a marine gliding**

bacterium isolated from samples collected from the Andaman sea, along the southern coastline of Thailand. *Int J Syst Evol Microbiol* 2007, **57**(Pt 10):2275-2279.

176. Hosoya S, Arunpairojana V, Suwannachart C, Kanjana-Opas A, Yokota A: **Aureispira marina gen. nov., sp. nov., a gliding, arachidonic acid-containing bacterium isolated from the southern coastline of Thailand**. *Int J Syst Evol Microbiol* 2006, **56**(Pt 12):2931-2935.

177. Gupta S, Fallarero A, Jarvinen P, Karlsson D, Johnson MS, Vuorela PM, Mohan CG: **Discovery of dual binding site acetylcholinesterase inhibitors identified by pharmacophore modeling and sequential virtual screening techniques**. *Bioorg Med Chem Lett* 2011, **21**(4):1105-1112.

178. Mohamed T, Zhao X, Habib LK, Yang J, Rao PP: **Design, synthesis and structure-activity relationship (SAR) studies of 2,4-disubstituted pyrimidine derivatives: dual activity as cholinesterase and Abeta-aggregation inhibitors**. *Bioorg Med Chem* 2011, **19**(7):2269-2281.

LIST OF APPENDICES

APPENDIX A1: QSAR SCRIPTS

A.1.1 MASTERSCRIPT FOR PREDICTION

```
# This program prepares files to be read into the Quasar Program
# Shana Stoddard
#!/bin/sh

#input file will be the mol2 files from ligbuilder
#the output files will be the corresponding pdb files

echo "mol2 files are being converted to pdb files"
cd /Users/shana/Desktop/Tanshionones/ligbuilder/OD_GM_seed-v3mTan.results.mdb
sudo cp /Users/My_Research/QSAR/Prediction-scripts-1/babel-mol2-pdb
/Users/shana/Desktop/Tanshionones/ligbuilder/OD_GM_seed-v3mTan.results.mdb
chmod ugo+x babel-mol2-pdb
./babel-mol2-pdb

echo "mol2 files are being converted to canonical files"

cp /Users/My_Research/QSAR/Prediction-scripts-1/babel-mol2-pdb
/Users/shana/Desktop/Tanshionones/ligbuilder/OD_GM_seed-v3mTan.results.mdb
chmod ugo+x babel-mol2-smi
./babel-mol2-smi

#
echo "mol2 files are being converted to mopint files"
cp /Users/My_Research/QSAR/Prediction-scripts-1/babel-mol2-mopint
/Users/shana/Desktop/Tanshionones/ligbuilder/OD_GM_seed-v3mTan.results.mdb
chmod ugo+x babel-mol2-mopint
./babel-mol2-mopint

#echo "Keywords are being written in mopint files"

cp /Users/My_Research/QSAR/Prediction-scripts-1/Keywords-start
/Users/shana/Desktop/Tanshionones/ligbuilder/OD_GM_seed-v3mTan.results.mdb
cp /Users/My_Research/QSAR/Prediction-scripts-1/Keywords-write.py
/Users/shana/Desktop/Tanshionones/ligbuilder/OD_GM_seed-v3mTan.results.mdb
chmod ugo+x Keywords-start
chmod ugo+x Keywords-write.py
./Keywords-start

echo "AMSOL run file is being written"

cp /Users/My_Research/QSAR/Prediction-scripts-1/AMSOL-Print-part1-start
/Users/shana/Desktop/Tanshionones/ligbuilder/OD_GM_seed-v3mTan.results.mdb
cp /Users/My_Research/QSAR/Prediction-scripts-1/Print.part1.AMSOL.py
/Users/shana/Desktop/Tanshionones/ligbuilder/OD_GM_seed-v3mTan.results.mdb
```

```
cp /Users/My_Research/QSAR/Prediction-scripts-1/AMSOL-insertion-start
/Users/shana/Desktop/Tanshionones/ligbuilder/OD_GM_seed-v3mTan.results.mdb
cp /Users/My_Research/QSAR/Prediction-scripts-1/Amsol-outname.py
/Users/shana/Desktop/Tanshionones/ligbuilder/OD_GM_seed-v3mTan.results.mdb
cp /Users/My_Research/QSAR/Prediction-scripts-1/AMSOL-Print-part2-start
/Users/shana/Desktop/Tanshionones/ligbuilder/OD_GM_seed-v3mTan.results.mdb
cp /Users/My_Research/QSAR/Prediction-scripts-1/Print.part2.AMSOL.py
/Users/shana/Desktop/Tanshionones/ligbuilder/OD_GM_seed-v3mTan.results.mdb
cp /Users/My_Research/QSAR/Prediction-scripts-1/multiplestest.run_all.pl
/Users/shana/Desktop/Tanshionones/ligbuilder/OD_GM_seed-v3mTan.results.mdb

chmod ugo+x AMSOL-Print-part1-start
chmod ugo+x Print.part1.AMSOL.py
chmod ugo+x AMSOL-insertion-start
chmod ugo+x Amsol-outname.py
chmod ugo+x AMSOL-Print-part2-start
chmod ugo+x Print.part2.AMSOL.py

./AMSOL-Print-part1-start
./AMSOL-insertion-start
./AMSOL-Print-part2-start

echo "AMSOL is being run"
chmod ugo+x AMSOL-list.pl
cp /Applications/amsol7.1/amsol7.1.exe
/Users/shana/Desktop/Tanshionones/ligbuilder/OD_GM_seed-v3mTan.results.mdb
perl AMSOL-list.pl

echo "Charges are being extracted from AMSOL output files"

cp /Users/My_Research/QSAR/Prediction-scripts-1/charges
/Users/shana/Desktop/Tanshionones/ligbuilder/OD_GM_seed-v3mTan.results.mdb
cp /Users/My_Research/QSAR/Prediction-scripts-1/charge_finder-SVS-FL.py
/Users/shana/Desktop/Tanshionones/ligbuilder/OD_GM_seed-v3mTan.results.mdb
chmod ugo+x charges
chmod ugo+x charge_finder-SVS-FL.py
./charges

echo "Solvation charges are being extracted from AMSOL output files"

cp /Users/My_Research/QSAR/Prediction-scripts-1/Solv_extraction
/Users/shana/Desktop/Tanshionones/ligbuilder/OD_GM_seed-v3mTan.results.mdb
cp /Users/My_Research/QSAR/Prediction-scripts-1/Solvation-finish.py
/Users/shana/Desktop/Tanshionones/ligbuilder/OD_GM_seed-v3mTan.results.mdb
cp /Users/My_Research/QSAR/Prediction-scripts-1/Solvator
/Users/shana/Desktop/Tanshionones/ligbuilder/OD_GM_seed-v3mTan.results.mdb
```

```
chmod ugo+x Solv_extraction
chmod ugo+x solvator
chmod ugo+x Solvation-finish.py
./Solv_extraction
./solvator
python Solvation-finish.py

#echo "QSAR input pdb files are being written"

cp /Users/My_Research/QSAR/Prediction-scripts-1/pdb.Namechange
/Users/shana/Desktop/Tanshiononones/ligbuilder/OD_GM_seed-v3mTan.results.mdb
cp /Users/My_Research/QSAR/Prediction-scripts-1/svs-pdb-filename-exchange.py
/Users/shana/Desktop/Tanshiononones/ligbuilder/OD_GM_seed-v3mTan.results.mdb
chmod ugo+x pdb.Namechange
chmod ugo+x svs-pdb-filename-exchange.py
./pdb.Namechange

echo "Copying clean up program to folder. Use only if everything is correct!!!"
echo "Clean up program must be run from directory"
cp /Users/My_Research/QSAR/Prediction-scripts-1/clean-up
/Users/shana/Desktop/Tanshiononones/ligbuilder/OD_GM_seed-v3mTan.results.mdb
chmod ugo+x clean-up

echo "at"
date
echo "Program is finished"
```

A.1.2 BABEL-MOL2-PDB SCRIPT

```
babel -imol2 *.mol2 -opdb *.pdb
```

A.1.3 BABEL-MOL2-SMI SCRIPT

```
babel -imol2 *.mol2 -osmi *.smi
```

A.1.4 BABEL-MOL2-MOPINT

```
#!/bin/sh

for file in `ls -1 *.mol2`

do
        babel -imol2 $file -omopin $file.mopin
done
```

A.1.5 KEYWORDS-START SCRIPT

```
#!/bin/sh

for file in `ls -1 *.mol2.mopin`
do
        python Keywords-write.py $file
done
```

A.1.6 KEYWORDS-WRITE.PY SCRIPT

```
import string
import os
import sys

# This will only work for file names ending with .#.mo.out or the like, where
#the file number is in the 1st from last position in the filename.

inFile = sys.argv[1]
inParts = string.split(inFile, ".")
print inParts
print ("%s is running." %inFile)
outName = inParts[0]
outName = outName+".mo.dat"


input = open('%s' %inFile,'r')

#input = open(Benz.svs.mo.out, 'r')
outFile = open('%s' %outName,'a')
#outFile = open(test.keywords.mo.dat, 'a')
outFile.write("SM5.42R SOLVNT=WATER 1SCF TRUES PM3 HFCALC=1SCF \n")
outFile.write("(aqueous) \n")
        #outFile = open(Benz.chg, 'a')


infile = open('%s' %inFile,'r')
infile.readline()
infile.readline()
for i in range (1, 100):
        line = infile.readline()
        outFile.write(line)
```

A.1.7 AMSOL-PRINT-PART1-START

```
#!/bin/sh

for file in `ls -1 multiplestest.run_all.pl`
do
        python Print.part1.AMSOL.py $file
done
```

A.1.8 PRINT.PART1.AMSOL.PY

```
outfile = open("AMSOL-list.pl", 'w')
infile = open("multiplestest.run_all.pl", 'r')

def main():

        for i in range (1, 21):
                line = infile.readline()
                print line
                outfile.write(line)

main ()
```

A.1.9 AMSOL-INSERTION-START

```
#!/bin/sh

for file in `ls -1 *.mo.dat`
do
        python Amsol-outname.py $file
done
```

A.1.10 AMSOL-OUTNAME.PY

```
import string
import os
import sys

outfile = open("AMSOL-list.pl", 'a')

inFile = sys.argv[1]
inParts = string.split(inFile, ".")
print ("name is being written to AMSOL file")
#print ("%s is running." %inFile)
```

```
outName = inParts[0]
outName = outName+".mo.dat "
print outName
outfile.write(outName)
```

A.1.11 AMSOL-PRINT-PART2-START

```
#!/bin/sh

for file in `ls -1 multiplestest.run_all.pl`
do
        python Print.part2.AMSOL.py $file
done
```

A.1.12 PRINT.PART2.AMSOL.PY

```
outfile = open("AMSOL-list.pl", 'a')
infile = open("multiplestest.run_all.pl", 'r')

def main():

        infile.readline()
        infile.readline()
        infile.readline()
        infile.readline()
        infile.readline()
        infile.readline()
        infile.readline()
        infile.readline()
        infile.readline()
        infile.readline()
        infile.readline()
        infile.readline()
        infile.readline()
        infile.readline()
        infile.readline()
        infile.readline()
        infile.readline()
        infile.readline()
        infile.readline()
        infile.readline()
        infile.readline()
        infile.readline()
        for i in range (1, 65):
                line = infile.readline()
                print line
```

```
                outfile.write(line)

main ()
```

A.1.13 MULTIPLESTEST.RUN_ALL.PL

```
#!/usr/bin/perl
#
#

$amsol_exe='./amsol7.1.exe';
$cp_command = 'cp -f';


#uncomment the next 2 lines if running in Windows
#$amsol_exe='..\amsol7.1.exe';
#$cp_command = 'copy /Y';



################################################################################
########
# delete any files from this list if you do not want to run any particular test runs #
################################################################################
########


$test_input_files="
multiples.test.mo.dat
";
$test_input_files2 = "     ";

$test_input_files3 = "     ";

@files  = ($test_input_files  =~ /\S{1,}/g);
@files2 = ($test_input_files2 =~ /\S{1,}/g);
@files3 = ($test_input_files3 =~ /\S{1,}/g);


foreach $file (@files){
  chop $file;chop $file;
  chop $file;chop $file;
  print "running $file  ...";
  $error_flag = system ("$amsol_exe \< $file.dat \> $file.out");
  if ($error_flag) {print "error running $file \n"}
```

```
  else{print "finished \n"}
}

foreach $file (@files2){
  chop $file;chop $file;
  chop $file;chop $file;
  print "running $file  ...";
  system ("$cp_command $file.xsm fort.19");
  $error_flag = system ("$amsol_exe \< $file.dat \> $file.out");
  if ($error_flag) {print "error running $file \n"}
  else{print "finished \n"}
}

foreach $file (@files3){
  chop $file;chop $file;
  chop $file;chop $file;
  print "running $file  ...";
  system ("$cp_command $file.xkw fort.20");
  $error_flag = system ("$amsol_exe \< $file.dat \> $file.out");
  if ($error_flag) {print "error running $file \n"}
  else{print "finished \n"}
}
```

A.1.14 AMSOL-LIST.PL

```
#!/usr/bin/perl
#
#

$amsol_exe='./amsol7.1.exe';
$cp_command = 'cp -f';


#uncomment the next 2 lines if running in Windows
#$amsol_exe='..\amsol7.1.exe';
#$cp_command = 'copy /Y';



################################################################################
########
# delete any files from this list if you do not want to run any particular test runs #
################################################################################
########
```

```
$test_input_files="
";
$test_input_files2 = "     ";

$test_input_files3 = "     ";

@files  = ($test_input_files  =~ /\S{1,}/g);
@files2 = ($test_input_files2 =~ /\S{1,}/g);
@files3 = ($test_input_files3 =~ /\S{1,}/g);


foreach $file (@files){
  chop $file;chop $file;
  chop $file;chop $file;
  print "running $file  ...";
  $error_flag = system ("$amsol_exe \< $file.dat \> $file.out");
  if ($error_flag) {print "error running $file \n"}
  else{print "finished \n"}
}

foreach $file (@files2){
  chop $file;chop $file;
  chop $file;chop $file;
  print "running $file  ...";
  system ("$cp_command $file.xsm fort.19");
  $error_flag = system ("$amsol_exe \< $file.dat \> $file.out");
  if ($error_flag) {print "error running $file \n"}
  else{print "finished \n"}
}

foreach $file (@files3){
  chop $file;chop $file;
  chop $file;chop $file;
  print "running $file  ...";
  system ("$cp_command $file.xkw fort.20");
  $error_flag = system ("$amsol_exe \< $file.dat \> $file.out");
  if ($error_flag) {print "error running $file \n"}
  else{print "finished \n"}
}
```

A.1.15 CHARGES

```
#!/bin/sh
```

```
for file in `ls -1 *.mo.out`
do
        python charge_finder-SVS-FL.py $file
done
```

A.1.16 CHARGE FINDER

```
DEVELOPED BY SHAWN YU
import string
import os
import sys

# This will only work for file names ending with .#.mo.out or the like, where
#the file number is in the 1st from last position in the filename.

inFile = sys.argv[1]
inParts = string.split(inFile,"_")
print inParts
outParts = inParts[1]
newparts = string.split(outParts, ".")
print newparts
lastparts = newparts[0]
print lastparts
print ("%s is running." %inFile)
outName = lastparts+".chg"
print outName

input = open('%s' %inFile,'r')
#input = open(Benz.svs.mo.out, 'r')
outFile = open('%s' %outName,'w')
#outFile = open(Benz.chg, 'a')
#outFile.write("#Charges extracted from file: %s\n" %inFile)

while 1:
        inputline = input.readline()
        if inputline == '                              calculated with CM2 \n' :
                inputline = input.readline()
                inputline = input.readline()
                inputline = input.readline()
                while len(inputline) > 1:
                        splitline = string.split(inputline)
                        outFile.write("%s00\n" %splitline[2])  # %s is defined by %(name)
                        inputline = input.readline()
                break
outFile.close()
```

```
input.close()


# The command while 1: is a loop the condition is inputline = input.readline().  Which creates
# a string if it is the correct line it will continue trough the loop and this part of the
# program skips two lines then begins to read the next line.
```

A.1.17 SOLV_EXTRACTION

```
#!/bin/sh
#Solv_extration
#this is the solvation extration program
#Shana stoddard 5/30.08

#!/bin/sh

for file in `ls -1 *.mo.out`
do
        grep "DeltaG-S" $file > Solv.int,$file
        #grep "DeltaG-S" Solv.int,* > Intermediate-Solvation.txt
        #rm -r Test_Solv.NS.int
done
```

A.1.18 SOLVATOR

```
#!/bin/sh

for file in `ls -1 S*.mo.out`
do
        python Solvation-finish.py $file
done
```

A.1.19 SOLVATION-FINISH.PY

```
# printfile.py
# Prints a file to the screen
import sys
import os
import string

inFile = sys.argv[1]
inParts = string.split(inFile,"_")
#print inParts
outParts = inParts[1]
```

```
newparts = string.split(outParts, ".")
#print newparts
lastparts = newparts[0]
print lastparts
print ("%s is running." %inFile)
#outName = lastparts+".solv.txt"
#print outName

input = open('%s' %inFile,'r')
#input = open('Intermediate-Solvation.txt','r')
#input = open(Benz.svs.mo.out, 'r')
outfile = open("Solvation-File2.txt", 'a')   #%outName
#outFile = open(Benz.chg, 'a')
#outFile.write("#Charges extracted from file: %s\n" %inFile)

for i in range (50):
        line = input.readline()
        print line
        Score = line[67:75]
        print Score
        outfile.write(lastparts+" "+ Score+'\n')
        outfile.close()
```

A.1.21 PDB.NAMECHANGE

```
#!/bin/sh

for file in `ls -1 *.pdb`
do
        python svs-pdb-filename-exchange.py $file
done
```

A.1.22 SVS-PDB-FILENAME-EXCHANGE.PY

```
#READ.line.py separate lines
#This program reads separate lines

import string
import os
import sys

# This will only work for file names ending with .#.mo.out or the like, where
#the file number is in the 1st from last position in the filename.
```

```
#inFile = "result_001.pdb"
inFile = sys.argv[1]
inParts = string.split(inFile,"_")
print inParts
outParts = inParts[1]
newparts = string.split(outParts, ".")
print newparts
lastparts = newparts[0]
print lastparts
print ("%s is running." %inFile)
outName = lastparts+".pdb"
print outName

input = open('%s' %inFile,'r')
#input = open(Prepare-inputfile.pdb,'r')
outFile = open("Prepare-input-file.pdb",'a')

#input = open('%s' %inFile,'r')
#outFile = open('%s' %outName,'w')

def main():

        for i in range (1, 200):
                        line = input.readline()
                        if len(line) < 75:
                                line = input.readline()
                        line = line.replace("LIG", lastparts)
                        line = line.replace("UNK", lastparts)
                        line = line.replace("AUTHOR    GENERATED BY OPEN BABEL
2.3.1", "\n")
                        line = line.replace("HETATM", "ATOM  ")
                        line = line.replace("1.00  0.00          C  ", "                    ")
                        line = line.replace("1.00  0.00          N  ", "                    ")
                        line = line.replace("1.00  0.00          O  ", "                    ")
                        line = line.replace("1.00  0.00         Cl  ", "                    ")
                        line = line.replace("1.00  0.00         Br  ", "                    ")
                        line = line.replace("1.00  0.00          I  ", "                   ")
                        line = line.replace("1.00  0.00          F  ", "                    ")
                        line = line.replace("1.00  0.00          S  ", "                    ")
                        line = line.replace("END", "\n")
                        line = line.replace("1.00  0.00          H  ", "                    ")
                        #line = input.readline()
                        #print line
                        outFile.write(line)

main ()
```

APPENDIX A2: LIGBUILDER RUN FILES

A.2.1 EXAMPLE POCKET INPUT FILE

```
#
   #input file
   #
   RECEPTOR_FILE
         /Users/Shana/Desktop/Tanshionones/Ligbuilder/Grandmodelversion3.14particles.pdb
   LIGAND_FILE
         /Users/Shana/Desktop/Tanshionones/Ligbuilder/Grand-Model-ligand.mol2
   PARAMETER_DIRECTORY
         /Applications/LigBuilder/LigBuilderv1.2/parameter/
   #
   #Output files
   #
   POCKET_ATOM_FILE
         /Users/Shana/Desktop/Tanshionones/Ligbuilder/Poc_atom_file_GM-tanshionones.txt
   POCKET_GRID_FILE
         /Users/Shana/Desktop/Tanshionones/Ligbuilder/Poc_atom_file_GM-tanshionones.txt
   #
   #Key interaction sites and pharmacophore
   #
   KEY_SITE_FILE
         /Users/Shana/Desktop/Tanshionones/Ligbuilder/Key_site-File_GM-tanshionones.pdb
   PHARMACOPHORE_TXT_FILE
         /Users/Shana/Desktop/Tanshionones/Ligbuilder/Phar_txt_file_GM-tanshionones.txt
   PHARMACOPHORE_PDB_FILE
         /Users/Shana/Desktop/Tanshionones/Ligbuilder/Phar_pdb_file_GM-tanshionones.pdb
   MINIMAL_FEATURE_DISTANCE          3.50
   MAXIMAL_FEATURE_NUMBER                  8
   #
   # vwl particle size
```

A.2.2 EXAMPLE GROW INPUT FILE

```
         #
         # input files
         #
         SEED_LIGAND_FILE
         /Users/Shana/Desktop/Tanshionones/Ligbuilder/Seeds-v2-1DT.mol2
         POCKET_ATOM_FILE
         /Users/Shana/Desktop/Tanshionones/Ligbuilder/Poc_atom_file_GM3.14-
tanshionones.txt
```

```
POCKET_GRID_FILE
/Users/Shana/Desktop/Tanshionones/Ligbuilder/Poc_grid_file_GM3.14-tanshionones.txt
#
# force field directory
#
PARAMETER_DIRECTORY
/Applications/LigBuilder/LigBuilderv1.2/parameter/
#
# fragment libraries
#
BUILDING_BLOCK_LIBRARY
/Applications/LigBuilder/LigBuilderv1.2/fragment.mdb/
FORBIDDEN_STRUCTURE_LIBRARY
/Applications/LigBuilder/LigBuilderv1.2/forbidden.mdb/
TOXIC_STRUCTURE_LIBRARY
/Applications/LigBuilder/LigBuilderv1.2/toxicity.mdb/
#
# structural construction parameters
#
GROWING_PROBABILITY                 1.00
LINKING_PROBABILITY                 0.50
MUTATION_PROBABILITY                0.50
#
# chemical viability rules
#
APPLY_CHEMICAL_RULES                YES
APPLY_FORBIDDEN_STRUCTURE_CHECK     YES
APPLY_TOXIC_STRUCTURE_CHECK         YES
MAXIMAL_MOLECULAR_WEIGHT            350
MINIMAL_MOLECULAR_WEIGHT            250
MAXIMAL_LOGP                        5.00
MINIMAL_LOGP                        2.00
MAXIMAL_HB_DONOR_ATOM               5
MINIMAL_HB_DONOR_ATOM               2
MAXIMAL_HB_ACCEPTOR_ATOM            10
MINIMAL_HB_ACCEPTOR_ATOM            2
MAXIMAL_PKD                             10.00
MINIMAL_PKD                             5.00
#
# genetic algorithm parameters
#
NUMBER_OF_GENERATION                20
NUMBER_OF_POPULATION                3000
NUMBER_OF_PARENTS                   200
ELITISM_RATIO                       0.10
SIMILARITY_CUTOFF                   0.90
```

```
#
# output files
#
POPULATION_RECORD_FILE
/Users/Shana/Desktop/Tanshionones/Ligbuilder/PRF_GM-seed-v2Tan-run1.lig
LIGAND_COLLECTION_FILE
/Users/Shana/Desktop/Tanshionones/Ligbuilder/LCF_GM-seed-v2Tan-run1.lig
#
```

A.2.3 EXAMPLE PROCES INPUT FILE

```
#
# input files
#
LIGAND_COLLECTION_FILE
/Users/Shana/Desktop/Tanshionones/Ligbuilder/LCF_GM-seed-v6Tan-run1.lig
#
# chemical rules
#
MAXIMAL_MOLECULAR_WEIGHT        500
MINIMAL_MOLECULAR_WEIGHT        300
MAXIMAL_LOGP                    5.00
MINIMAL_LOGP                    0.00
MAXIMAL_PKD                             10.00
MINIMAL_PKD                             0.00
#
# similarity threshhold
#
SIMILARITY_CUTOFF               0.90
#
# output files
#
NUMBER_OF_OUTPUT_MOLECULES      200
OUTPUT_DIRECTORY
/Users/Shana/Desktop/Tanshionones/Ligbuilder/OD_GM_seed-v6Tan.results.mdb
#
```

APPENDIX A3: PROTEIN AND DNA SEQUENCES

A.3.1 DNA SEQUENCE FOR PNBCE-WILD-TYPE ENZYME

ATGACTCATC AAATAGTAAC GACTCAATAC GGCAAAGTAA AAGGCACAAC

GGAAAACGGC GTACATAAGT GGAAAGGCAT CCCCTATGCC AAGCCGCCTG

TCGGACAATG GCGTTTTAAA GCACCTGAGC CGCCTGAAGT GTGGGAAGAT

GTGCTTGATG CCACAGCGTA CGGCTCTATT TGCCCGCAGC CGTCTGATTT

GCTGTCACTT TCGTATACTG AGCTGCCCCG CCAGTCCGAG GATTGCTTGT

ATGTCAATGT ATTTGCGCCT GACACCCCAA GTAAAAATCT TCCTGTCATG

GTGTGGATTC ACGGAGGCGC TTTTTATCTA GGAGCGGGCA GTGAGCCATT

GTATGACGGA TCAAAACTTG CGGCACAGGG AGAAGTCATT GTCGTTACAT

TGAACTATCG GCTGGGGCCG TTTGGCTTTT TGCACTTGTC TTCATTTAAT

GAGGCGTATT CTGATAACCT TGGGCTTTTA GACCAAGCCG CCGCGCTGAA

ATGGGTGCGA GAGAATATTT CAGCGTTTGG CGGTGATCCC GATAACGTAA

CAGTATTTGG AGAATCCGCC GGCGGGATGA GCATTGCCGC GCTGCTTGCT

ATGCCTGCGG CAAAAGGCCT GTTCCAGAAA GCAATCATGG AAAGCGGCGC

TTCTCGAACG ATGACGAAAG AACAAGCGGC GAGCACCTCG GCAGCCTTTT

TACAGGTCCT TGGGATTAAC GAGGGCCAAC TGGATAAATT GCATACGGTT

TCTGCGGAAG ATTTGCTAAA AGCGGCTGAT CAGCTTCGGA TTGCAGAAAA

AGAAAATATC TTTCAGCTGT TCTTCCAGCC CGCCCTTGAT CCGAAAACGC

TGCCTGAAGA ACCAGAAAAA GCGATCGCAG AAGGGGCTGC TTCCGGTATT

CCGCTATTAA TTGGAACAAC CCGTGATGAA GGATATTTAT TTTTCACCCC

GGATTCAGAC GTTCATTCTC AGGAAACGCT TGATGCAGCG CTCGAGTATT

TACTAGGGAA GCCGCTGGCA GAGAAAGTTG CCGATTTGTA TCCGCGTTCT

CTGGAAAGCC AAATTCATAT GATGACTGAT TTATTATTTT GGCGCCCTGC

CGTCGCCTAT GCATCCGCAC AGTCTCATTA CGCCCCTGTC TGGATGTACA

GGTTCGATTG GCACCCGAAG AAGCCGCCGT ACAATAAAGC GTTTCACGCA

TTAGAGCTTC CTTTTGTCTT TGGAAATCTG GACGGATTGG AACGAATGGC

AAAAGCGGAG ATTACGGATG AGGTGAAACA GCTTTCTCAC ACGATACAAT

CAGCGTGGAT CACGTTCGCC AAAACAGGAA ACCCAAGCAC CGAAGCTGTG

AATTGGCCTG CGTATCATGA AGAAACGAGA GAGACGCTGA TTTTAGACTC

AGAGATTACG ATCGAAAACG ATCCCGAATC TGAAAAAAGG CAGAAGCTAT

TCCCTTCAAA AGGAGAATAA

A.3.2 DNA SEQUENCE FOR PNBCE-CES1-LOOP7-MUTANT ENZYME

ATGACTCATC AAATAGTAAC GACTCAATAC GGCAAAGTAA AAGGCACAAC

GGAAAACGGC GTACATAAGT GGAAAGGCAT CCCCTATGCC AAGCCGCCTG

TCGGACAATG GCGTTTTAAA GCACCTGAGC CGCCTGAAGT GTGGGAAGAT

GTGCTTGATG CCACAGCGTA CGGCTCTATT TGCCCGCAGC CGTCTGATTT

GCTGTCACTT TCGTATACTG AGCTGCCCCG CCAGTCCGAG GATTGCTTGT

ATGTCAATGT ATTTGCGCCT GACACCCCAA GTAAAAATCT TCCTGTCATG

GTGTGGATTC ACGGAGGCGG CCTAATGGTG GGAGCGCTTA GTGAGCCATT

GTATGACGGA TCAAAACTTG CGGCACAGGG AGAAGTCATT GTCGTTACAT

TGAACTATCG GCTGGGGCCG TTTGGCTTTT TGCACTTGTC TTCATTTAAT

GAGGCGTATT CTGATAACCT TGGGCTTTTA GACCAAGCCG CCGCGCTGAA

ATGGGTGCGA GAGAATATTT CAGCGTTTGG CGGTGATCCC GATAACGTAA

CAGTATTTGG AGAATCCGCC GGCGGGATGA GCATTGCCGC GCTGCTTGCT
ATGCCTGCGG CAAAAGGCCT GTTCCAGAAA GCAATCATGG AAAGCGGCGC
TTCTCGAACG ATGACGAAAG AACAAGCGGC GAGCACCTCG GCAGCCTTTT
TACAGGTCCT TGGGATTAAC GAGGGCCAAC TGGATAAATT GCATACGGTT
TCTGCGGAAG ATTTGCTAAA AGCGGCTGAT CAGCTTCGGA TTGCAGAAAA
AGAAAATATC TTTCAGCTGT TCTTCCAGCC CGCCCTTGAT CCGAAAACGC
TGCCTGAAGA ACCAGAAAAA GCGATCGCAG AAGGGGCTGC TTCCGGTATT
CCGCTATTAA TTGGAACAAC CCGTGATGAA GGATATTTAT TTTTCACCCC
GGATTCAGAC GTTCATTCTC AGGAAACGCT TGATGCAGCG CTCGAGTATT
TACTAGGGAA GCCGCTGGCA GAGAAAGTTG CCGATTTGTA TCCGCGTTCT
CTGGAAAGCC AAATTCATAT GATGACTGAT TTATTATTTT GGCGCCCTGC
CGTCGCCTAT GCATCCGCAC AGTCTCATTA CGCCCCTGTC TGGATGTACA
GGTTCGATTG GCACCCGAAG AAGCCGCCGT ACAATAAAGC GTTTCACGCA
TTAGAGCTTC CTTTTGTCTT TGGAAATCTG GACGGATTGG AACGAATGGC
AAAAGCGGAG ATTACGGATG AGGTGAAACA GCTTTCTCAC ACGATACAAT
CAGCGTGGAT CACGTTCGCC AAAACAGGAA ACCCAAGCAC CGAAGCTGTG
AATTGGCCTG CGTATCATGA AGAAACGAGA GAGACGCTGA TTTTAGACTC
AGAGATTACG ATCGAAAACG ATCCCGAATC TGAAAAAAGG CAGAAGCTAT
TCCCTTCAAA AGGAGAATAA

A.3.3 DNA SEQUENCE FOR PNBCE-CES2-LOOP7-MUTANT ENZYME

ATGACTCATC AAATAGTAAC GACTCAATAC GGCAAAGTAA AAGGCACAAC

GGAAAACGGC GTACATAAGT GGAAAGGCAT CCCCTATGCC AAGCCGCCTG

TCGGACAATG GCGTTTTAAA GCACCTGAGC CGCCTGAAGT GTGGGAAGAT

GTGCTTGATG CCACAGCGTA CGGCTCTATT TGCCCGCAGC CGTCTGATTT

GCTGTCACTT TCGTATACTG AGCTGCCCCG CCAGTCCGAG GATTGCTTGT

ATGTCAATGT ATTTGCGCCT GACACCCCAA GTAAAAATCT TCCTGTCATG

GTGTGGATTC ACGGAGGCGC TCTAGTGTTTG GAATGCTTA GTGAGCCATT

GTATGACGGA TCAAAACTTG CGGCACAGGG AGAAGTCATT GTCGTTACAT

TGAACTATCG GCTGGGGCCG TTTGGCTTTT TGCACTTGTC TTCATTTAAT

GAGGCGTATT CTGATAACCT TGGGCTTTTA GACCAAGCCG CCGCGCTGAA

ATGGGTGCGA GAGAATATTT CAGCGTTTGG CGGTGATCCC GATAACGTAA

CAGTATTTGG AGAATCCGCC GGCGGGATGA GCATTGCCGC GCTGCTTGCT

ATGCCTGCGG CAAAAGGCCT GTTCCAGAAA GCAATCATGG AAAGCGGCGC

TTCTCGAACG ATGACGAAAG AACAAGCGGC GAGCACCTCG GCAGCCTTTT

TACAGGTCCT TGGGATTAAC GAGGGCCAAC TGGATAAATT GCATACGGTT

TCTGCGGAAG ATTTGCTAAA AGCGGCTGAT CAGCTTCGGA TTGCAGAAAA

AGAAAATATC TTTCAGCTGT TCTTCCAGCC CGCCCTTGAT CCGAAAACGC

TGCCTGAAGA ACCAGAAAAA GCGATCGCAG AAGGGGCTGC TTCCGGTATT

CCGCTATTAA TTGGAACAAC CCGTGATGAA GGATATTTAT TTTTCACCCC

GGATTCAGAC GTTCATTCTC AGGAAACGCT TGATGCAGCG CTCGAGTATT

TACTAGGGAA GCCGCTGGCA GAGAAAGTTG CCGATTTGTA TCCGCGTTCT

CTGGAAAGCC AAATTCATAT GATGACTGAT TTATTATTTT GGCGCCCTGC

CGTCGCCTAT GCATCCGCAC AGTCTCATTA CGCCCCTGTC TGGATGTACA

GGTTCGATTG GCACCCGAAG AAGCCGCCGT ACAATAAAGC GTTTCACGCA

TTAGAGCTTC CTTTTGTCTT TGGAAATCTG GACGGATTGG AACGAATGGC AAAAGCGGAG ATTACGGATG AGGTGAAACA GCTTTCTCAC ACGATACAAT CAGCGTGGAT CACGTTCGCC AAAACAGGAA ACCCAAGCAC CGAAGCTGTG AATTGGCCTG CGTATCATGA AGAAACGAGA GAGACGCTGA TTTTAGACTC AGAGATTACG ATCGAAAACG ATCCCGAATC TGAAAAAAGG CAGAAGCTAT TCCCTTCAAA AGGAGAATAA

A.3.4 PROTEIN SEQUENCE FOR PNBCE-WILD-TYPE ENZYME

MTHQIVTTQY GKVKGTTENG VHKWKGIPYA KPPVGQWRFK APEPPEVWED VLDATAYGPI CPQPSDLLSL SYTELPRQSE DCLYVNVFAP DTPSQNLPVM VWIHGGAFY LGAGSEPLY DGSKLAAQGE VIVVTLNYRL GPFGFLHLSS FDEAYSDNLG LLDQAAALKW VRENISAFGG DPDNVTVFGE SAGGMSIAA LLAMPAAKGL FQKAIMESGA SRTMTKEQAA STAAAFLQVL GINESQLDRL HTVAAEDLLK AADQLRIAEK ENIFQLFFQP ALDPKTLPEE PEKSIAEGAA SGIPLLIGTT RDEGYLFFTP DSDVHSQETL DAALEYLLGK PLAEKAADLY PRSLESQIHM MTDLLFWRPA VAYASAQSHY APVWMYRFDW HPEKPPYNKA FHALELPFVF GNLDGLERMA KAEITDEVKQ LSHTIQSAWI TFAKTGNPST EAVNWPAYHE ETRETVILDS EITIENDPES EKRQKLFPSK GEP

A.3.5 PROTEIN SEQUENCE FOR PNBCE-CES1-LOOP7-MUTANT ENZYME

MTHQIVTTQY GKVKGTTENG VHKWKGIPYA KPPVGQWRFK APEPPEVWED
VLDATAYGPI CPQPSDLLSL SYTELPRQSE DCLYVNVFAP DTPSQNLPVM
VWIHGGGLMV GAASEPLYDG SKLAAQGEVI VVTLNYRLGP FGFLHLSSFD
EAYSDNLGLL DQAAALKWVR ENISAFGGDP DNVTVFGESA GGMSIAALLA
MPAAKGLFQK AIMESGASRT MTKEQAASTA AAFLQVLGIN ESQLDRLHTV
AAEDLLKAAD QLRIAEKENI FQLFFQPALD PKTLPEEPEK SIAEGAASGI
PLLIGTTRDE GYLFFTPDSD VHSQETLDAA LEYLLGKPLA EKAADLYPRS
LESQIHMMTD LLFWRPAVAY ASAQSHYAPV WMYRFDWHPE KPPYNKAFHA
LELPFVFGNL DGLERMAKAE ITDEVKQLSH TIQSAWITFA KTGNPSTEAV
NWPAYHEETR ETVILDSEIT IENDPESEKR QKLFPSKGE

A.3.6 PROTEIN SEQUENCE FOR PNBCE-CES2-LOOP7-MUTANT ENZYME

MTHQIVTTQY GKVKGTTENG VHKWKGIPYA KPPVGQWRFK APEPPEVWED
VLDATAYGPI CPQPSDLLSL SYTELPRQSE DCLYVNVFAP DTPSQNLPVM
VWIHGGALVF GMASEPLYDG SKLAAQGEVI VVTLNYRLGP FGFLHLSSFD
EAYSDNLGLL DQAAALKWVR ENISAFGGDP DNVTVFGESA GGMSIAALLA
MPAAKGLFQK AIMESGASRT MTKEQAASTA AAFLQVLGIN ESQLDRLHTV
AAEDLLKAAD QLRIAEKENI FQLFFQPALD PKTLPEEPEK SIAEGAASGI
PLLIGTTRDE GYLFFTPDSD VHSQETLDAA LEYLLGKPLA EKAADLYPRS
LESQIHMMTD LLFWRPAVAY ASAQSHYAPV WMYRFDWHPE KPPYNKAFHA
LELPFVFGNL DGLERMAKAE ITDEVKQLSH TIQSAWITFA KTGNPSTEAV
NWPAYHEETR ETVILDSEIT IENDPESEKR QKLFPSKGE

VITA

Shana V. Stoddard

Research Interests:

My research interests include investigation of enzyme specificity for the development of specific inhibitors and drugs. I am particularly interested in using computational chemistry, organic chemistry, and biochemistry to complete these research endeavors. The impact of my research I would like to see translated into clinical therapies.

Education and Corresponding Research Experience:

University of Mississippi; Oxford, MS: *Doctor of Philosophy*, Chemistry, (**Expected, 2013)**

Doctoral Dissertation Project – Molecular considerations in the design of novel alpha/beta hydrolase inhibitors.

Advisor: Randy Wadkins Ph.D., Biophysical and Computational Chemistry **May 2008-July 2013**

University of Mississippi, Department of Chemistry and Biochemistry

Project Description: This project includes evaluation of the interactions important for substrate and inhibitor recognition in a family of enzymes called alpha/beta hydrolases with emphasis on a carboxylesterase subfamily. The contributions from this work will be applicable to the design of

novel inhibitors and drugs. This project is being accomplished through a combination of protein mutagenesis and kinetic analysis, quantitative structure activity relationship, de novo drug design, and other biochemical, computational, basic molecular and cellular biology, and organic chemistry protocols.

Prairie View A&M University; Prairie View, TX: *Post Baccalaureate studies* in Chemistry (2007-2008)

Research Project – PDK/CDK ligand interactions and mode of binding.

Advisor: Hua-jun Fan Ph.D., Computational Chemistry **Jan 2007-May 2008**

Prairie View A&M University, ***Prairie View, TX***

Project Description: Elucidated important ligand protein interactions present within the cyclin dependent kinases (CDK2 and CDK5) and 3-phosphoinositide-dependent protein kinase 1 (PDK1) through use of docking methodology (DOCK 6.0) coupled with statistical analysis (SPSS software).

Texas A&M University; College Station, TX: *Post Baccalaureate studies* in Chemistry (2005-2006)

Research Project – Synthesis of alpha/beta unsaturated cyclohexadienes.

Advisor: Coran Watanabe Ph.D., Organic and Bioorganic Chemistry **Oct 2005-Jun 2006**

Texas A&M University, ***College Station, TX***

Project Description: Synthesized a series of homo- and heterodimeric cyclohexadiene analogs. This project was conducted using proline mediated catalysis and basic organic chemistry, and synthetic protocols.

Prairie View A&M University; Prairie View, TX: *Bachelor of Science* (August 2005),

Major: Chemistry, Biomedical Science Track

Minor: Biology

Research Project – Expression of sialyl lewis-X carbohydrate antigen within the female caprine

reproductive tract.

Advisor: Gary Newton Ph.D., Reproductive Physiology **Sep 2002-Feb 2004**

Cooperative Agricultural Research Center, Prairie View, TX

Project Description: Investigation of the presence of L-selectin, E-selectin and sialyl lewis-x on caprine reproductive tract and conceptus tissues. This project was carried out using immunohistochemistry techniques and fluorescence microscopy.

Other Research Experience:

Project – Trends in cardiovascular disease **Summer 2000**

Advisor: Irving Joushua Ph.D., Physiology and Biophysics

National Institute of Health at University of Louisville Medical School, Louisville, KY

Project Description: This project included evaluation of the prevalence of trends in cardiovascular disease and stroke.

Peer-Reviewed Publications:

1. Combining Quantitative Structure Activity Relationship (QSAR) Modeling with *In silico* Design to Develop Carboxylesterase Inhibitors, **Shana V. Stoddard**, Philip M. Potter, Randy M. Wadkins *Bioorganic and Medicinal Chemistry Letters* (**In preparation)**

2. Insights and Ideas Garnered from Marine Metabolites for Development of Acetylcholinesterase and Amyloid-β Aggregation Inhibitors, **Shana V. Stoddard**, Mark T. Hamann, Randy M. Wadkins, *Journal of Molecular Modeling* (**In Preparation**)

3. *In Silico* Design and Evaluation of Carboxylesterase Inhibitors, **Shana V. Stoddard**, Xiaozhen Yu, Philip M. Potter, Randy M. Wadkins. *Journal of Pesticide Science* 35 (2010) 240-249 – invited review

4. Improved, Selective, Human Intestinal Carboxylesterase Inhibitors Designed to Modulate CPT-11 Toxicity, Latorya D. Hicks, Janice L. Hyatt, **Shana Stoddard**, Lyudmila Tsurkan, Carol C. Edward, Monika Wierdl, Randy M. Wadkins, Philip M. Potter. *Journal of Medicinal Chemistry* 52 (2009) 3742-3752

Technical Skills:

In addition to biochemical expertise I am proficient with UNIX, Chimera, DOCK 6.0, Quasar 6.0. I have familiarity with SPSS software; VMD software; NMR 300, 400, and 500MHz; IR and UV spectroscopy; HPLC; UNIX shell and python script writing. I am skilled in program development, event organization and implementation.

Presentations:

1. Development of Cutinase Deletion Mutant Plasmids for the Investigation of Structure Function Relationships in α/β Hydrolases L. Jennie Fan, Erica M. Stoddard, **Shana V. Stoddard**, Randy M. Wadkins, University of Mississippi, Oxford, MS

2. Combining Quantitative Structure Activity Relationship (QSAR) Modeling with In silico Design to Develop Carboxylesterase Inhibitors (Poster Presentation) **Shana V. Stoddard**, Mississippi State EPSCoR meeting April 18th, 2013: Hattiesburg, MS. **Placed 3rd**

3. Insights and Ideas Garnered from Marine Metabolites for Development of Acetylcholinesterase and Amyloid-β Aggregation Inhibitors, (Poster Presentation) **Shana V. Stoddard**, Mark T. Hamann, Randy M. Wadkins, National Organization for the Professional Advancement of Black Chemists and Chemical Engineers (NOBCChE) national meeting, September – 25th, 2012: Washington, DC.

4. Combining Quantitative Structure Activity Relationship (QSAR) Modeling with In silico Design to Develop Carboxylesterase Inhibitors (Poster Presentation) **Shana V. Stoddard**, Mississippi State EPSCoR meeting April 10th, 2012: Oxford, MS.

5. Combining Quantitative Structure Activity Relationship (QSAR) Modeling with In silico Design to Develop Carboxylesterase Inhibitors (Poster Presentation) **Shana V. Stoddard**, Philip M. Potter, Randy M. Wadkins, 2nd Annual Poster Symposium and Research Day, April 5th, 2012: Oxford, MS. **Conference Organizer**

6. In silico Generation and Evaluation of Carboxylesterase Inhibitor Scaffolds (Oral Presentation) **Shana V. Stoddard**, Mississippi Academy of Sciences Annual Meeting, February 23rd -24th, 2012: Hattiesburg, MS. **Placed 1st**

7. Combining Quantitative Structure Activity Relationship (QSAR) Modeling with In silico Design to Develop Carboxylesterase Inhibitors (Oral Presentation) **Shana V. Stoddard** Midsouth Computational Biology & Bioinformatics Society, February 17th-18th, 2012: Oxford, MS. **Placed 1st**

8. Structural Alignment and Normal Mode Analysis of Deletion Mutants of Cutinase to Determine Substructure Function in Alpha/Beta Hydrolases (Poster Presentation) Erica M. Stoddard, Austin E. Pernell, **Shana V. Stoddard**, Dawn Wilkins, Randy M. Wadkins. Midsouth Computational Biology & Bioinformatics Society, February 17th-18th, 2012: Oxford, MS

9. In silico Design and Evaluation of Carboxylesterase Inhibitors, (Poster Presentation) **Shana V. Stoddard**, Philip M. Potter, Randy M. Wadkins: 4th Mississippi Biophysical Consortium, June 2nd - 3rd, 2011: Oxford, MS.

10. In silico Design and Evaluation of Carboxylesterase Inhibitors, (Poster Presentation) **Shana V. Stoddard**, Philip M. Potter, Randy M. Wadkins: National Organization for the Professional Advancement of Black Chemists and Chemical Engineers (NOBCChE) national meeting, April 18th -

22nd, 2011: Houston, TX. **Placed 3rd**

11. In silico Design and Evaluation of Carboxylesterase Inhibitors, (Poster Presentation) **Shana V. Stoddard**, Philip M. Potter, Randy M. Wadkins: Mississippi State EPSCoR meeting April 14th, 2011: Starkville, MS. **Placed 2nd**

12. In silico Design and Evaluation of Carboxylesterase Inhibitors, (Poster Presentation) **Shana V. Stoddard**, Philip M. Potter, Randy M. Wadkins: 1st Annual Poster Symposium and Research Day, April 8th, 2011: Oxford, MS. **Placed 1st**

13. In silico Design of Carboxylesterase Inhibitors, (Poster Presentation) **Shana V. Stoddard**, Philip M. Potter, Randy M. Wadkins: The Twenty-fourth Annual Gibbs Conference on Biothermodynamics, September 25th - 28th, 2010: Carbondale, IL.

14. Graduate School at the University of Mississippi: Pursuing an Advanced Degree in the Field of Chemistry: (Oral Presentation) **Shana V. Stoddard**: April 16th, 2010: Prairie View A&M University, Prairie View, TX. **Invited speaker**

15. In Silico Methods for Determination of Selective Inhibitors for Human Intestinal Carboxylesterase (hiCE), (Poster Presentation) **Shana V. Stoddard**, Randy M. Wadkins: Mississippi State EPSCoR meeting, April 15th, 2010: Jackson, MS.

16. A New QSAR Model for the Development of Inhibitors of Human Intestinal Carboxylesterase: (Oral Presentation) **Shana V. Stoddard**, Latorya D. Hicks, Janice L. Hyatt, Philip M. Potter, Randy M. Wadkins: 61st Southeast Regional Meeting of the ACS (SERMACS), Bioorganic Chemistry Session I, October 21st – October 25th: San Juan, Puerto Rico.

17. Improved, Selective, Human Intestinal Carboxylesterase Inhibitor Designed to Modulate CPT-11 Toxicity, (Poster Presentation) Latorya D. Hicks, Janice L. Hyatt, **Shana Stoddard**, Lyudmila Tsurkan,

Carol C. Edward, Monika Wierdl, Randy M. Wadkins, Philip M. Potter: 61st Southeast Regional Meeting of the ACS (SERMACS), Bioorganic Chemistry Session I, October 21st – October 25th: San Juan, Puerto Rico.

18. QSAR Study on Human Intestinal Carboxylesterase Enzyme (hiCE) using Sulfonamide Analog Inhibitors, (Poster Presentation) **Shana Stoddard**, Randy Wadkins: Mississippi State EPSCoR meeting, April 16th, 2009: Starkville, MS.

19. Molecular Modeling the Interaction between the Chemical Ligands and Cyclin-Dependent Kinase, (Poster Presentation) **Shana Stoddard**, Hua-jun Fan: 236th ACS National Meeting, Medicinal Chemistry Division, August 20th, 2008: Philadelphia, PA.

20. A Chemical Interpretation of the Interaction between the Ligand and CDK Binding Site, (Poster Presentation) **Shana Stoddard**, Milton Jackson, Okioa Uket, Hua-jun Fan: 4th Annual Research Symposium Research in the Changing Times, Sponsored by the College of Juvenile Justice and Psychology: April 18th, 2008: Prairie View, TX. **Placed 1st**

21. Carbohydrate Antigen Expression by Caprine Oviductal Tissue, (Poster Presentation) Gary Newton, **Shana Stoddard**, Ramón Garcia, NneNna Igbo, Jamila Leake, Selamawit Woldesenbet: The Society for the Study of Reproduction, 38th Annual Meeting, July 24th – July 27th, 2005: Quebec City, Quebec, Canada.

22. The Expression of the Sialyl Lewis-X Carbohydrate Antigen within the Female Caprine Reproductive Tract, (Poster Presentation) **Shana Stoddard**, Ramón F. Garcia, NneNna Igbo, Jamila Leake, Selamawit Woldesenbet, Gary Newton, Agricultural Regional Directors Symposium, March 29th – April 2nd, 2003: Atlanta, GA.

23. The Expression of the Sialyl Lewis-X Carbohydrate Antigen within the Female Caprine Reproductive Tract, (Poster Presentation) **Shana Stoddard**, Ramón F. Garcia, NneNna Igbo, Jamila Leake, Selamawit

Woldesenbet, Gary Newton, University of Texas Medical Branch at Galveston 17th Annual Undergraduate Research Symposium, February 2003: Galveston, TX. **Placed 2nd**

24. Alpha(1-2)Fucosyltransferase gene expression by caprine endometrial tissues obtained during the estrous cycle and early pregnancy, (Poster Presentation) Selamawit Woldesenbet, Ramón Garcia, S. Lewis, NneNna Igbo, Jamila Leake, **Shana V. Stoddard,** G. Rickettes, N. Ing, Gary Newton, Biology of Reproduction, July 2003: Cincinnati, OH.

25. An Alternative Light Color for Lights that Need to be Seen at Low Intensities of Light: (Oral Presentation) **Shana Stoddard**: Kentucky Junior Association of Science (KJAS), Morehead State University, March 2001: Morehead, KY.

26. The Minimal Amount of Light Detectable by the Human Eye: (Oral Presentation) **Shana Stoddard** Kentucky Junior Science Symposium, March 2001, Louisville, KY. **Won all expense paid trip to National Science Camp; selected as Kentucky State alternate for National Science Fair Competition**

27. How to Organize a Scientific Research Project: (Oral Presentation) **Shana Stoddard** and Sarah Swope, Invited Speaker at Ballard High School, October 2000, Ballard High School, Louisville, KY.

28. Trends in Cardiovascular Disease: (Oral Presentation) **Shana Stoddard** National Institute of Health, August 2000 Washington DC.

Honors, Awards, and Scholarships By Year:

2013

• Outstanding Graduate Student Academics, Research, and Service award.

Highest award given in the Ole Miss Local section of the American Chemical Society. This award is not given annually, and has only been given 6 times in 20 years. I am tenth recipient of the award, and the only 2012/2013 recipient.

• Placed 3rd in Graduate poster competition in the computational chemistry section at the Mississippi State EPSCoR (Experimental Program to Stimulate Competitive Research) Meeting in Hattiesburg, MS

• Awarded GAANN Fellowship

2012

• Best Officer Award for the 2011-2012 Graduate Student Council Term

Position Held: Director of Graduate Affairs

• Placed 1st in Graduate Oral Presentation competition in the Chemistry and Chemical Engineering section at the Mississippi Academy of Sciences meeting in Hattiesburg, MS

• Placed 1st in Graduate Oral Presentation competition in the Graduate Student category at the Midsouth Computational Biology & Bioinformatics Society meeting in Oxford, MS

2011

• Placed 3rd in Graduate Biophysical Poster competition in the Biophysical Chemistry section at the NOBCChE (National Organization for the Professional Advancement of Black Chemists and Chemical Engineers) national meeting in Houston, TX

• Placed 2nd in Graduate poster competition in the Computational chemistry section at the Mississippi State EPSCoR (Experimental Program to Stimulate Competitive Research) Meeting in Starkville, MS

• Placed 1st in Graduate poster competition in the physical science section at the Graduate Student Council (GSC) 1st Annual Poster Symposium and Research Day, University of Mississippi

2010

• ***Selected as Young Researcher to attend the 60th Meeting of Nobel Laureates in Lindau Germany***

1 of 650 selected from a three round international competition. Over 40,000+ applicants reviewed

• Awarded the ESOF (European Open Science Forum) Fellowship to attend ESOF conference after 60th Meeting of Nobel Laureates

1 of 50 selected from the 650 accepted to attend the 60th Meeting of Nobel Laureates

2008

• Placed 1st in Graduate poster competition at the 4th Annual Research Symposium *Research in the Changing Times*, sponsored by the College of Juvenile Justice and Psychology at Prairie View A&M University

2004

• Who's Who Among American College Students

• National Deans list, Prairie View A&M University

• University Honors, Prairie View A&M University

2003

• Placed 2nd in undergraduate poster competition: University of Texas Medical Branch at Galveston; 17th Annual Undergraduate Research Symposium, in Galveston, TX

• University Honors, Prairie View A&M University

2002

• Beta Beta Beta National Biological Honor Society inductee

2001

• Kentucky Science Symposium – won all expense paid trip to the National Science Camp as state representative

• Kentucky Science Symposium – elected to attend the National Science Symposium in Orlando, FL

• Kentucky Science Symposium – elected as Kentucky State alternate for National Science Fair Competition

• Unsung Hero Award; awarded by Rotary Club of Louisville

• Papa John's Leadership Scholarship Award

2000

• National Student Leadership Scholar

• Kentucky Governor Scholar

Accomplishments:

• Chartered three organizations, one organization chapter, and one club

1. University of Mississippi Advocates for Students Disabilities Association (**2009**),
2. Prairie View A&M University Chess club (**2007**),
3. Prairie View A&M University Chemistry club (**2004**),
4. Prairie View A&M University chapter of National Council of Negro Women (**2002**)
5. Established and coordinated a nursing home visiting group (**1999**)

• Coordinated Pennies for Patients Drive fundraiser for Leukemia and Lymphoma Society for NOBCChE (**2013**)

• Directed grant awarding process for the University of Mississippi G01 graduate student grant (**2011**, **2012**)

• Coordinated Graduate Student Council Research Day Poster Session at the University of Mississippi

(**2012**)

• Served on the Hall of Fame selection committee to choose those students to be given the honor of induction into the Hall of Fame for the Class of 2011-2012 at the University of Mississippi (**2011**)

• Developed physician shadowing program in veterinary medicine, physical therapy, and dentistry (**2004**)

• Established and organized Annual Health Conference and College Admissions Workshop (**2003**)

• Coordinated Registration Process for Medical School Admission Workshop and Career Fair (**2002**)

• Coordinated College Admission Workshop for Oxford/Lafayette County (**2011, 2012**)

• Coordinated 30+ seminars (**2002-2012**)

Descriptions of selected seminars coordinated.

1. *College Admissions Workshop:* Seminar presented to inform parents and students in grades 8 to 12 about the college admission process, preparing for college during high school, and how to look for and obtain college scholarships. Educational Service Foundation, University of Mississippi personnel from the admissions office, and University of Mississippi graduate students were the speakers for this seminar.

2. *Post Doctoral Informational:* Seminar given to assist graduate students at the University of Mississippi on where to look for post doctoral opportunities. Cathy Fore from Oak Ridge Universities (ORAU) was the invited speaker.

3. *Grant Writing Workshop:* This workshop was held to assist University of Mississippi students in grant writing. Members from the Offices of Research and Sponsored Programs, and University of Mississippi professors presented the seminars

4. *Publishing Your Work Panel Discussion:* This panel discussion was held to inform University of Mississippi Student about the publishing process, and tips to maintain an active publishing career. Professors from the University of Mississippi having over 150+ publications each were panelist.

• Various Elected or Appointed Positions held;

1. Assistant Youth Director at Clear Creek Missionary Baptist Church (**2012, 2013**), *Responsibilities include* hosting events for the youth at Clear Creek Missionary Baptist Church.

Highlights: Developed a summer reading program to assist Oxford/Lafayette county youth in improving their reading skills. Initiated a Youth Talent Show, Youth Field day, and Youth Department Newsletter. Coordinated a Youth Lock-In and Christmas program. Assisted in organizing Easter Program and Mother's day program. Re-established a Youth Tutoring program.

2. Director of Graduate Affairs for Graduate Student Council **(2011-2012**), *Responsibilities included* overseeing the grant awarding process, organizing the GSC Research Day Poster Session, hosting seminars to address the needs of Graduate Students at the University of Mississippi.

3. Served on Lecture Series Committee (**2011-2013**), *Responsibilities include* reviewing applications for monetary assistance from individuals or organizations at the University of Mississippi who wish to invite speakers to present work at UM.

4. Hall of Fame selection committee (**2011**), *Responsibilities included* reviewing candidates for the University of Mississippi's Hall of Fame

5. President of Chemistry Club (**2004-2005**), *Responsibilities included* setting a vision, for the organization, overseeing the events, development and distribution of departmental newsletter and managing the organizations operations.

6. President of Minority Association of Pre-Health Students (**2003-2004**), *Responsibilities included* setting a vision, for the organization, overseeing the events, and managing the organizations operations.

7. 2nd Vice President of National Council of Negro Women PVAMU chapter (**2003-2004**), *Responsibilities included* overseeing all programs committees.

8. Treasurer of Chess Club (**2007-2008**), *Responsibilities included* accounting of monies for the organization

9. Secretary for Advocates for Students Disabilities Association (**2009**), *Responsibilities included* documenting minutes during ASDA meetings.

10. Parliamentarian/Chaplin for Beta Kappa Chi/National Institute of Science (**2002-2004**), *Responsibilities included* prayer for meetings, and ensuring meetings were conducted in accordance to Robert's Rules of Order

11. Community Service Chair for Minority Association of Pre-Health Students (MAPS) (**2002-2003**), *Responsibilities included* developing and implementing community service events for MAPS.

12. Community Service Co-Chair for National Council of Negro Women (NCNW) PVAMU Chapter (**2002-2003**), *Responsibilities included* developing and implementing community service events for NCNW.

13. Registration Committee Chair for Minority Association of Pre-Health Students (**2002-2003**), *Responsibilities included* overseeing the registration process for the Medical College Admission Conference and Career Fair

14. Black History Committee Chair for Minority Association of Pre-Health Students (**2001**). *Responsibilities included* designing and implementing programs for Black History Month for Campus students at PVAMU

Teaching Experience **from 2002 to 2013**

Classes Taught:

Biochemistry Lab (Reorganized Laboratory, helped to implement structure in class)

Forensic DNA Lab (Developed several DNA Laboratory experiments, student and TA lab manuals)

Chemistry Labs I and II for Chemistry majors

Organic Chemistry Labs I and II

General Chemistry Lab for Engineering majors, and Nursing majors

Substitute lecturer for Biophysical Chemistry

Substitute lecturer for General Chemistry

Subjects Tutored:

Medical College Admissions Test (MCAT) Chemistry,

Dental Admissions Test (DAT) Chemistry,

Biochemistry,

Organic Chemistry,

General Chemistry,

K-12 Mathematics,

K-12 Science,

K-7 History,

K-7 Language Arts,

K-7 Reading

Current Organizational Memberships:

• American Chemical Society: Graduate student member

• Biophysical Society: Graduate student member, subgroups – biological fluorescence and membrane structure and assembly

• National Organization for the Professional Advancement of Black Chemists and Chemical Engineers: member, University of Mississippi chapter

• Mississippi Academy of Sciences

• Midsouth Computational Biology & Bioinformatics Society

• Alpha Kappa Alpha Sorority Incorporated

Community Service:

• Forensic Science Exhibition for elementary and middle school youth.

(Hosted 3 groups; Middle school (**March 2013**), Oxford Middle School (**March 2013**), and Boys and Girls of Oxford/University Area (**April 2013**)

• Martin Luther King Day of Service (Help serve food to MLK Day activities attendants) (**2012**)

• 9/11 Day of Service (Help with packaging can goods, toiletries and personal items (for the Food Pantry, More Than a Meal and Boxes of Love) and participated in fixing community vegetable plots (CommunityHarvest) – Oxford, MS, (**2011**)

• Events hosted by Alpha Kappa Alpha Sorority Inc. (**2003-present**): Events including but not limited to health fairs, freshman move in, educational seminars, and serving food at cancer walks.

•Tutor for K-12 and college students (**1999-present**)